CHAPTER 18

Data Sheets

Introduction

1 The data sheets included as figures in this chapter are intended to assist in the calculations required in earlier chapters. They are based on work undertaken at research establishments, in particular the Defence Research Agency, Dunfermline, and are published in this book because they are not readily available elsewhere. The layout of the chapter consists of a short description of each set of data sheets and, where appropriate, how they should be used, followed by the data sheets themselves. A comprehensive description of the use of the data sheets is not generally included in this chapter, and for more details reference should be made to the appropriate chapter.

Stiffener Section Data

2 *Figure 18.1* contains the dimensions of the seven standard long stalk Tee bars used in most British warship structures. The data included is self explanatory and needs no enlargement, but it should be noted that the shape of the section drawn is idealised and should not be used for scaling.

3 *Figure 18.2* contains the dimensions of a number of British Standard offset bulb plates (OBPs or bulb flats). There are some 60 different shapes listed in BS4848 Part 5 so those included here can only be a representative selection over the range, for use as a guide. Although only one thickness of web has been shown for each section height, there are usually three thicknesses (and consequently weights and strengths) for each height. The first and last section height in *Figure 18.2* are the extreme sizes from BS4848 Part 5. Again the shape shown is an idealised one.

4 For flat bar stiffeners the properties may be derived from equations 18.1 and 18.2 below but simple elastic bending assumptions are only valid, that is tripping is unlikely, if the aspect ratio of the flat bar (d/t_s) is less than 10.

(18.1) $$d_{na} = (d^2 t_s + b t_p^2 + 2bdt_p)/\{2\,(dt_s + bt_p)\}$$

(18.2) $$I_{na} = d^3 t_s/3 + bdt_p\,(d + t_p) - d_{na}^2\,(dt_s + bt_p)$$

where d = height of flat bar stiffener
t_s = thickness of flat bar stiffener
b = breadth of plate acting with flat bar in bending
t_p = thickness of plate
d_{na} = distance of combined neutral axis from outer edge of flat bar
I_{na} = second moment of area about neutral axis.

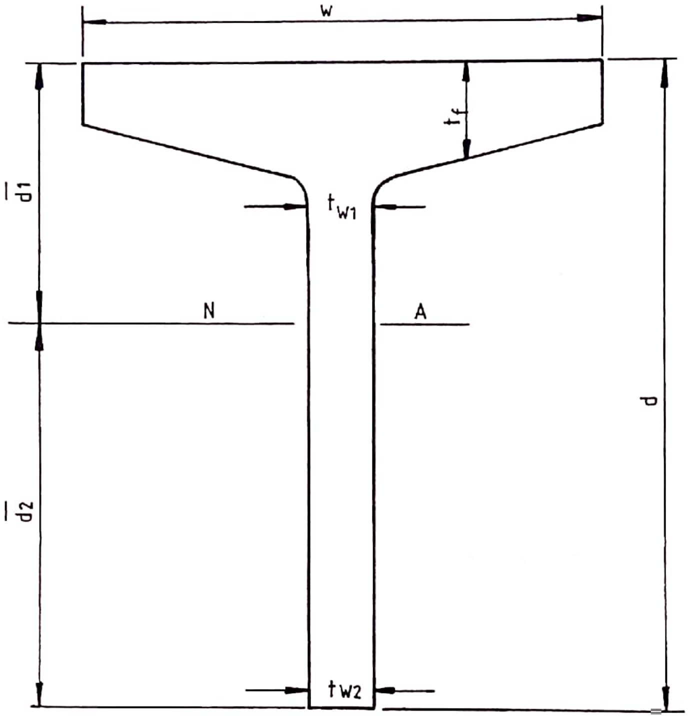

TYPE	SD No. 002558	SIZE w × d mm	THICKNESS mm			Wt/m kg	SECT AREA mm²	SECOND MOMENT ABOUT NA cm⁴	$\bar{d}_1$ mm	$\bar{d}_2$ mm
			t_f	t_{w1}	t_{w2}					
1	000	25.4 × 76.2	6.4	4.4	4.4	3.64	464	28	28.2	48.0
2	001	44.5 × 114.3	9.5	5.1	5.1	7.43	948	126	36.6	77.7
3	002	63.5 × 127.0	13.4	6.9	6.4	12.62	1613 ✓	248	37.6	89.4
4	003	76.2 × 152.4	14.2	7.4	6.9	16.29	2090	468	44.4	108.0
5	004	88.9 × 177.8	15.2	7.9	7.4	20.44	2606	805	51.8	126.0
6	005	101.6 × 203.2	16.3	8.4	7.9	25.01	3193	1289	58.4	144.8
7	006	127.0 × 254.0	18.3	9.4	8.9	35.40	4535	2811	69.3	184.7

Figure 18.1 Dimensions of MOD (PE) Standard Tee Bars

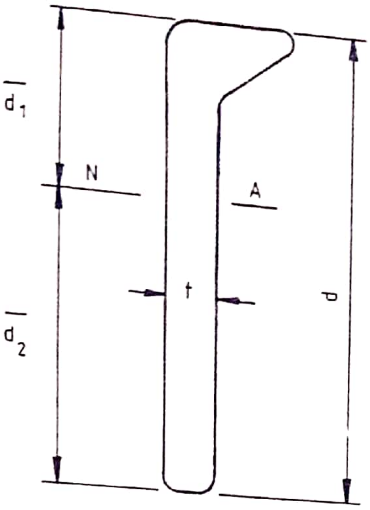

SIZE d × t (mm)	AREA (cm^2)	MASS PER UNIT LENGTH (kg/m)	$\bar{d}_1$ (mm)	$\bar{d}_2$ (mm)	SECOND MOMENT ABOUT NA (cm^4)
120 × 6	9.31	7.31	48.0	72.0	133
140 × 8	13.8	10.83	58.2	81.8	266
160 × 9	17.8	14.0	66.4	93.6	448
180 × 10	22.5	17.6	74.0	106.0	717
200 × 11	27.6	21.7	82.0	118.0	1090
240 × 12	37.3	29.3	96.0	144.0	2130
280 × 13	48.4	37.9	110.0	170.0	3760
320 × 13	57.4	45.0	121.0	199.0	5850
340 × 14	65.5	51.5	129.0	211.0	7540
370 × 15	77.0	60.5	140.0	230.0	10490
400 × 15	85.4	67.0	148.0	252.0	13580
430 × 20	115.0	90.8	167.0	263.0	21180

(Note: Properties are taken from BS4848 Part 5 out of a table of 60 sizes listed)

Figure 18.2 Properties of Typical Bulb Flats

Plate Strength Curves

5 The data sheets presented in *Figures 18.3* to *18.5* are taken from Smith et al (1988) and represent effective stress/strain curves for plates of different slenderness ratio β (=(b/t)$\sqrt{(\sigma_y/E)}$) with the load on the short edge, length b, of the plate. These types of curves are known as 'Load Shortening Curves'. For square plates and plates loaded along the long edge reference should be made to curves given in Smith et al (1988). The method of using these curves is explained in Chapter 7 but, in principle, they present the load carrying capability of plates within a normal grillage type structure and with small, average and large initial imperfections respectively. Unless there is reason to believe otherwise for a particular structure, the average imperfection curves should be used as it may be assumed that although there may be some severely distorted areas, these will be balanced by structure which is nearer to the ideal.

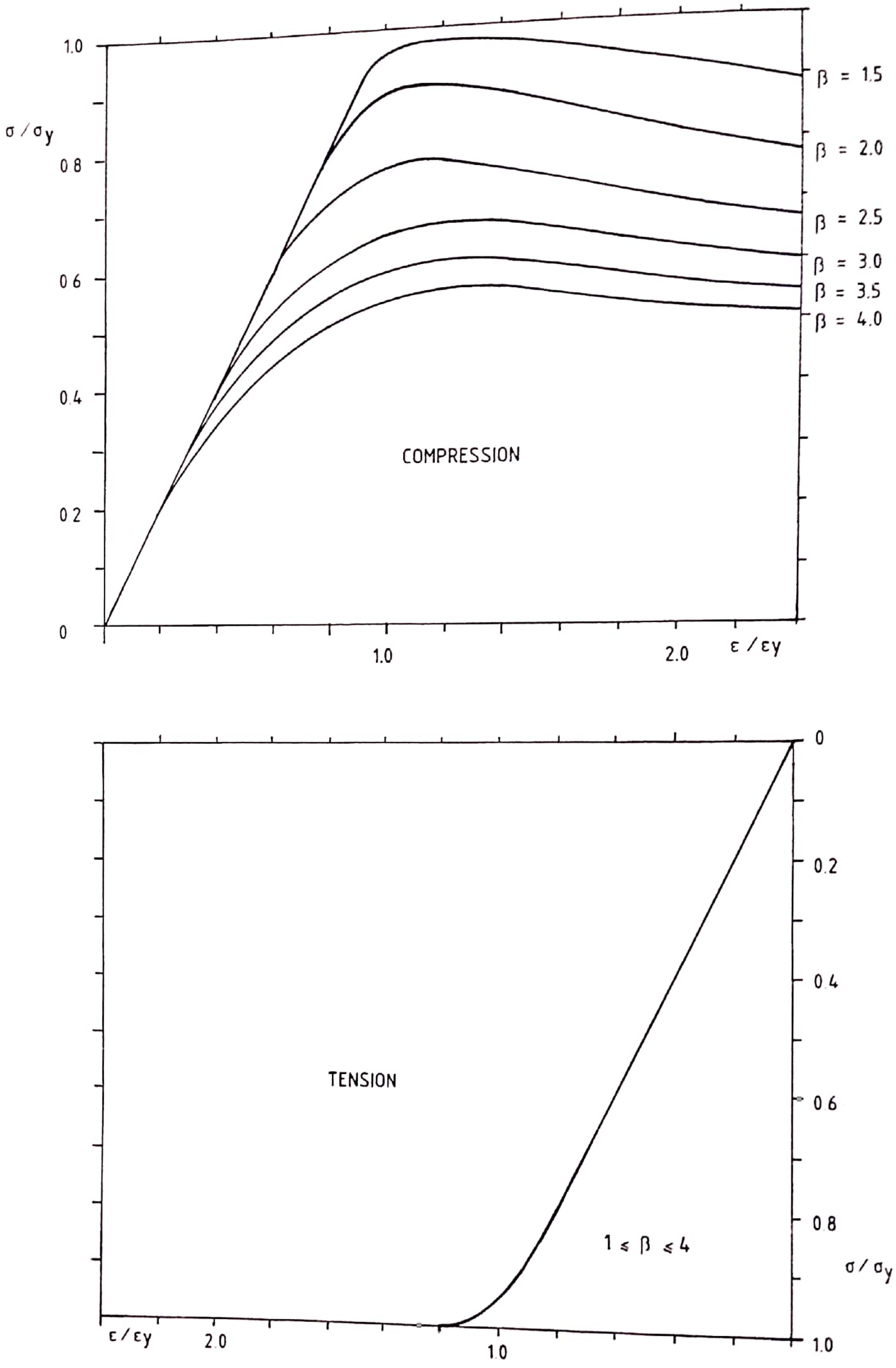

Figure 18.3 Plate Load - Shortening Curves - Small Imperfections

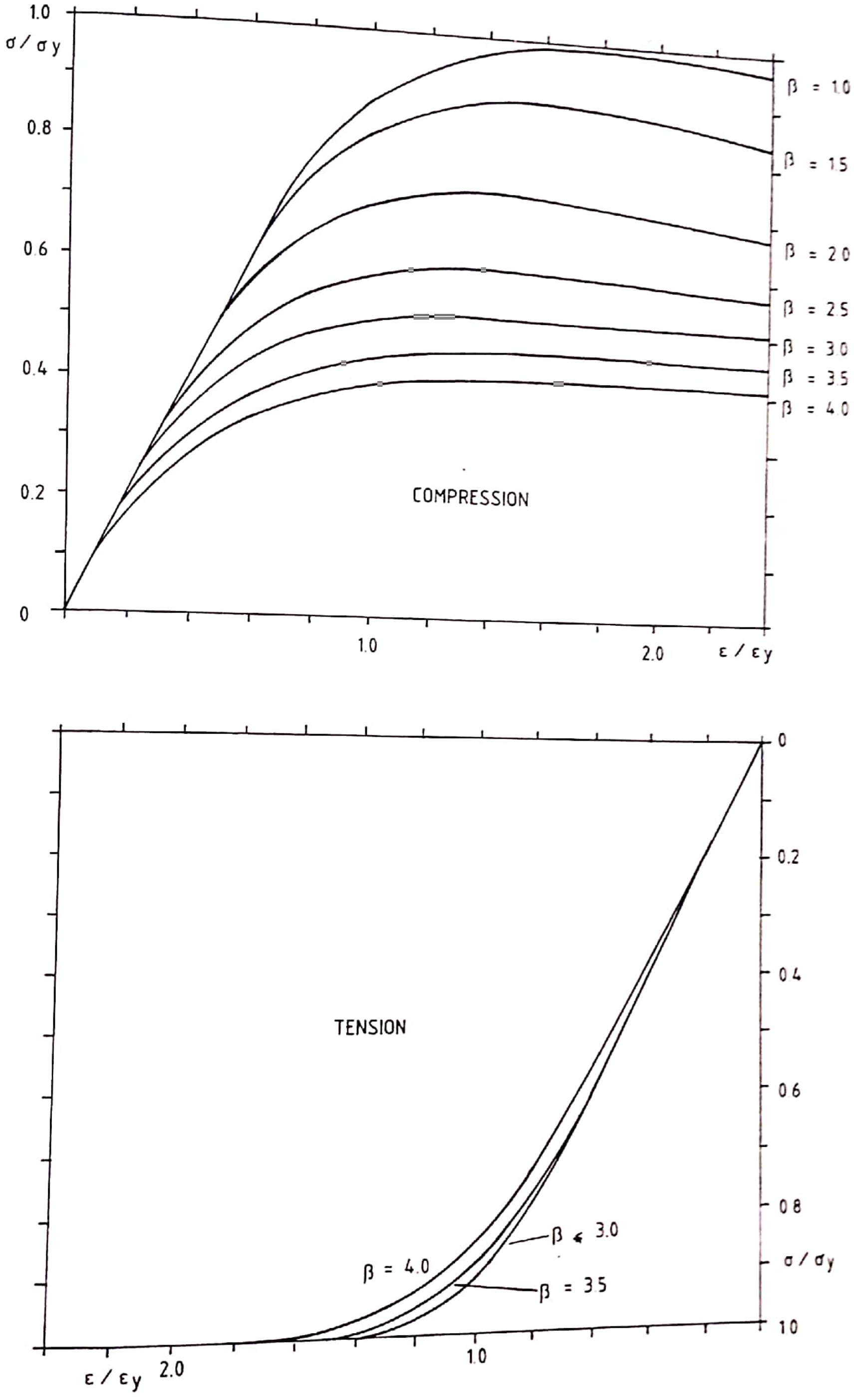

Figure 18.4 Plate Load - Shortening Curves - Average Imperfections

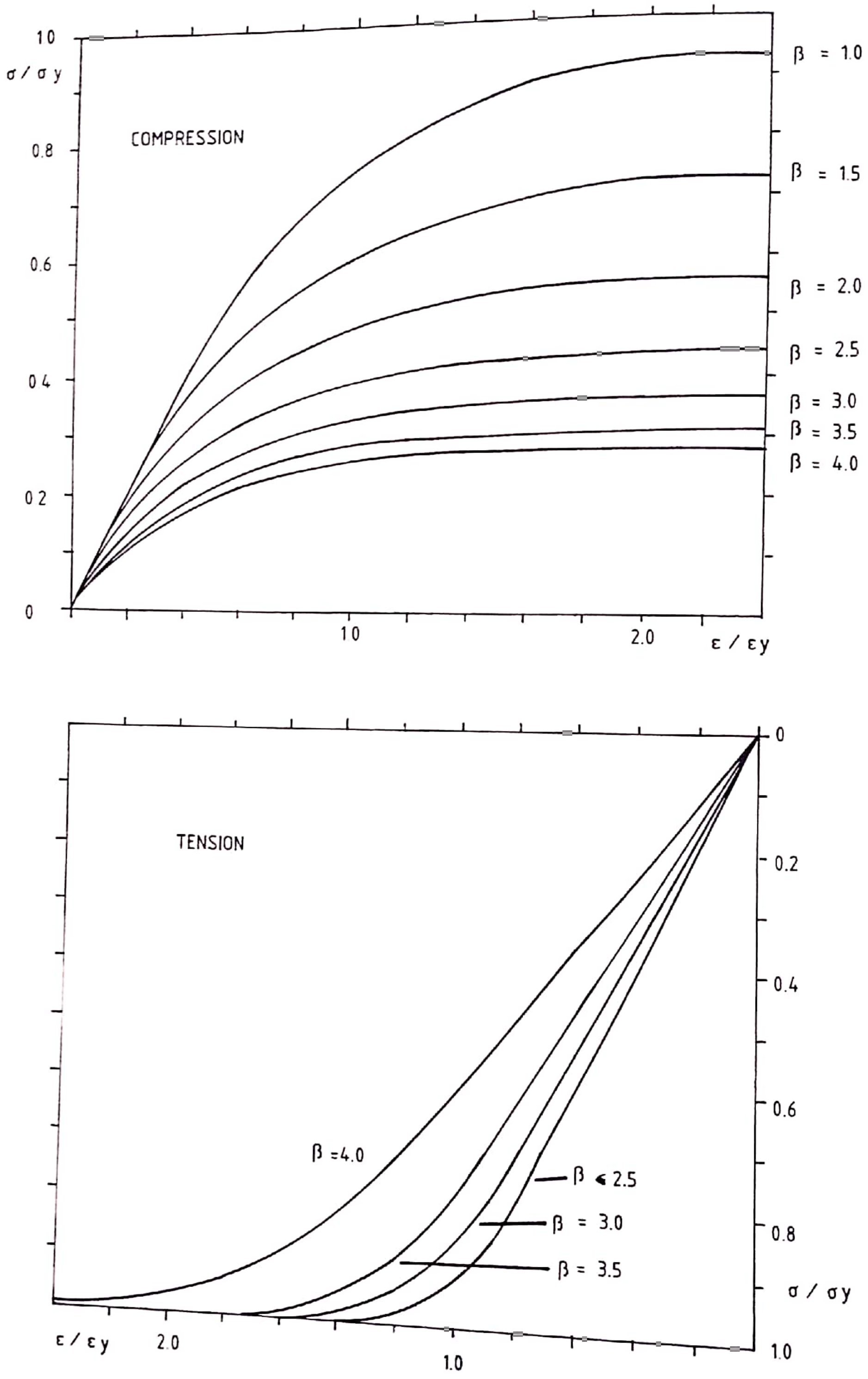

Figure 18.5 Plate Load - Shortening Curves - Large Imperfections

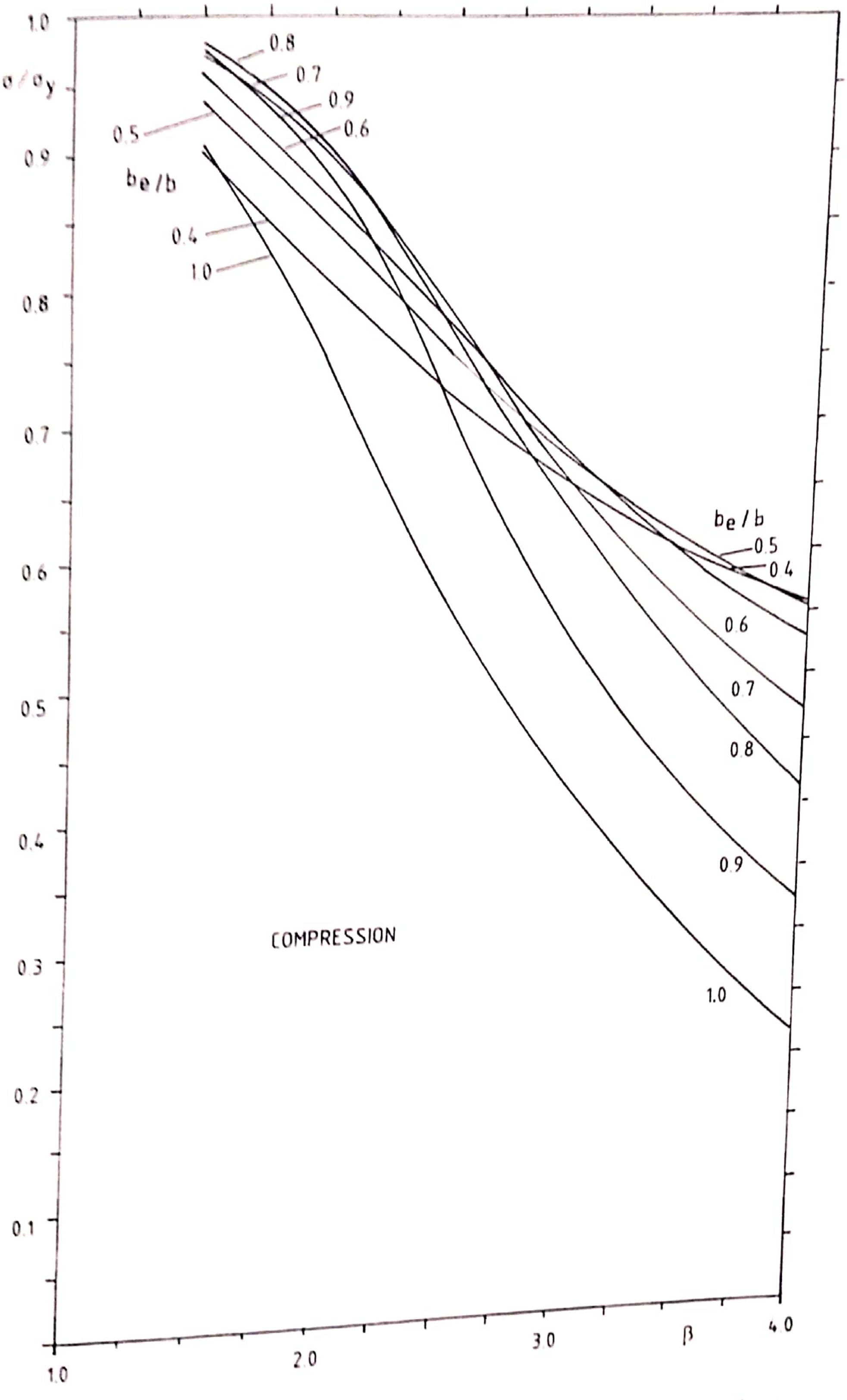

Figure 18.6 Effective Width Curves for Plate - Small Imperfections

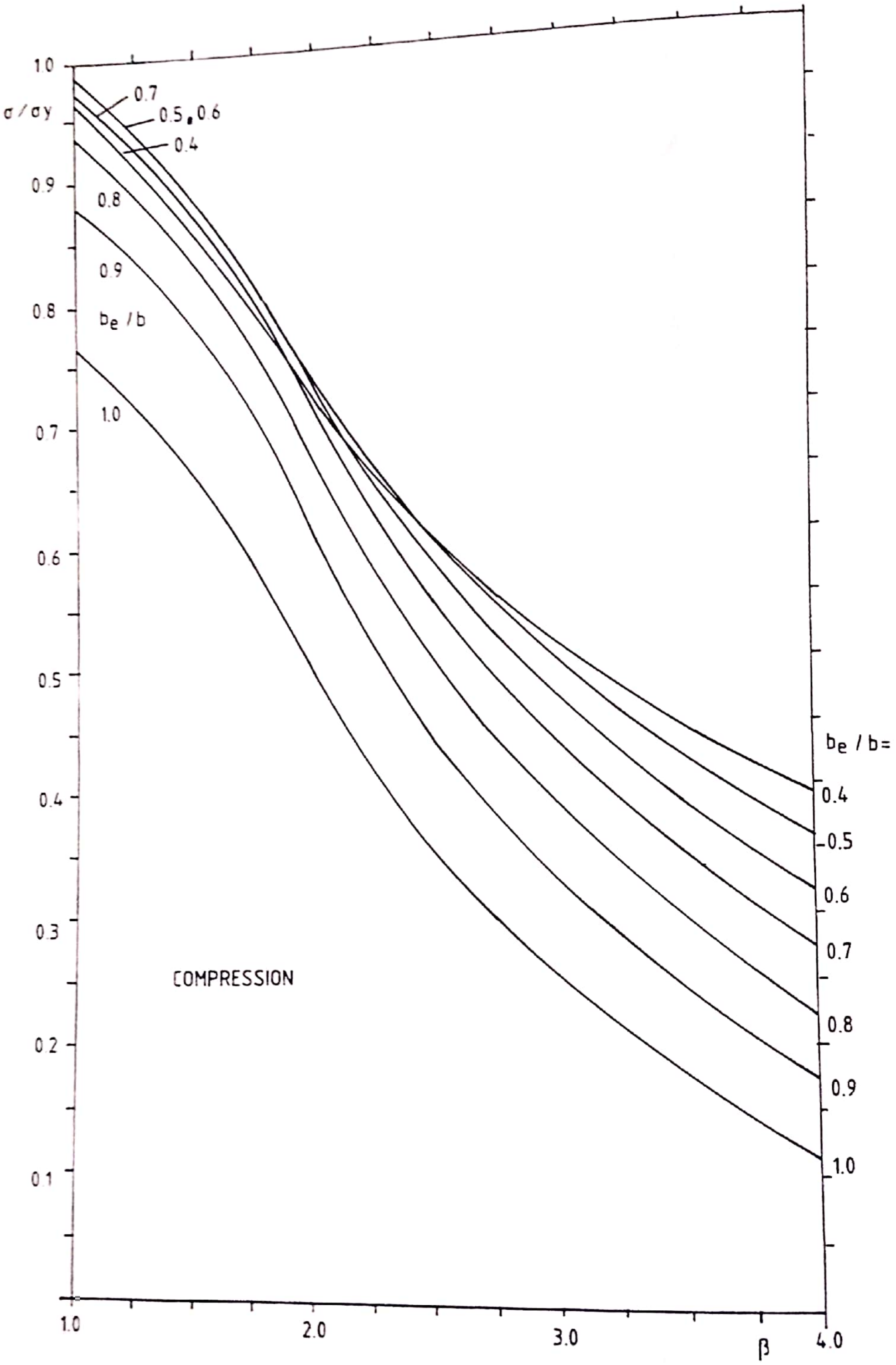

Figure 18.7 Effective Width Curves for Plate - Average Imperfections

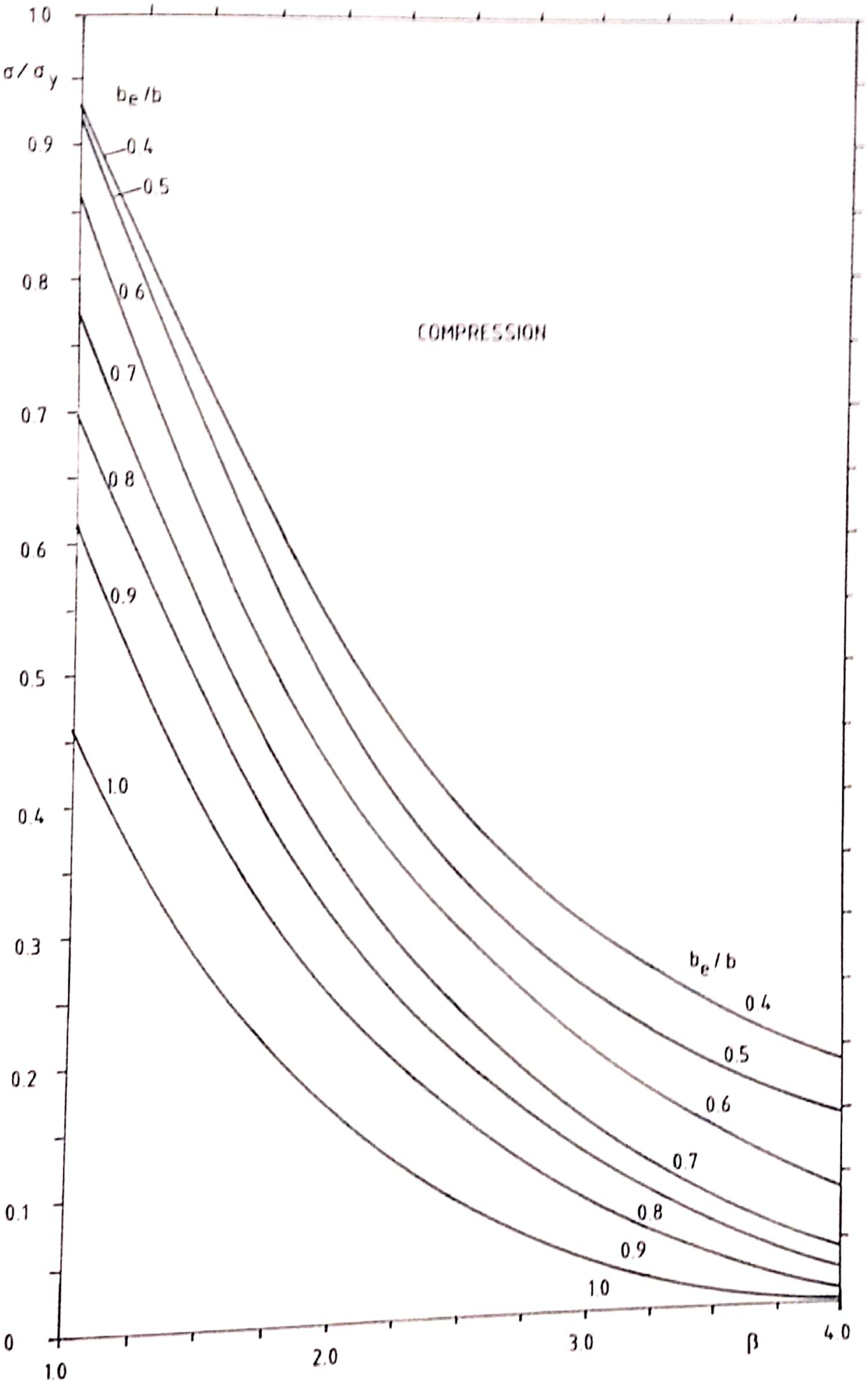

Figure 18.8 Effective Width Curves for Plate - Large Imperfections

6 It is possible to derive from the load-shortening curves the effective width of plate that would exist if that part of the plate was carrying all the load at constant stress. If b_e is the effective width, then the ratio b_e/b is equal to E_s/E, where E_s is the secant modulus and is equal to σ/ε for any point on a load-shortening curve. Consequently, any straight line through the origin of the load-shortening curves represents a constant value of b_e/b, and the curves in *Figures 18.6* to *18.8* are drawn on that basis for σ/σ_y against ß for different values of b_e/b. They therefore represent the effective width of plating carrying the stress σ for any value of ß.

7 The three figures again present results for small, average and large imperfections, and the average curves in *Figure 18.7* should be used for lack of any information to the contrary.

Column Strength Curves

8 The curves in these data sheets represent the strength of stiffener-plate combinations for small, average and large imperfections and have been calculated using finite element modelling and parametric studies. They are presented in a form similar to the load-shortening curves for plate but in *Figures 18.9* to *18.11* as σ_a/σ_y against the column slenderness λ $(=(a/\pi k)\sqrt{(\sigma_y/E)})$ for different values of plate slenderness ß, and in *Figures 18.12* to *18.14* as σ_a/σ_y against ß for different values of λ. σ_a is the average collapse stress of the plate stiffener combination and its use is described in Chapter 7.

9 Note that in calculating the value of radius of gyration k for input to λ the *full* width of plate b should be used, *not* the effective width.

10 Unless there is evidence that the accuracy of construction of the structure being designed is particularly better or worse than average, the average curves in *Figures 18.10* and *18.13* should be used.

Note: Figures 18.9 to *18.14* refer to tee bar stiffened panels with a standard value of $A_S/A = 0.2$.

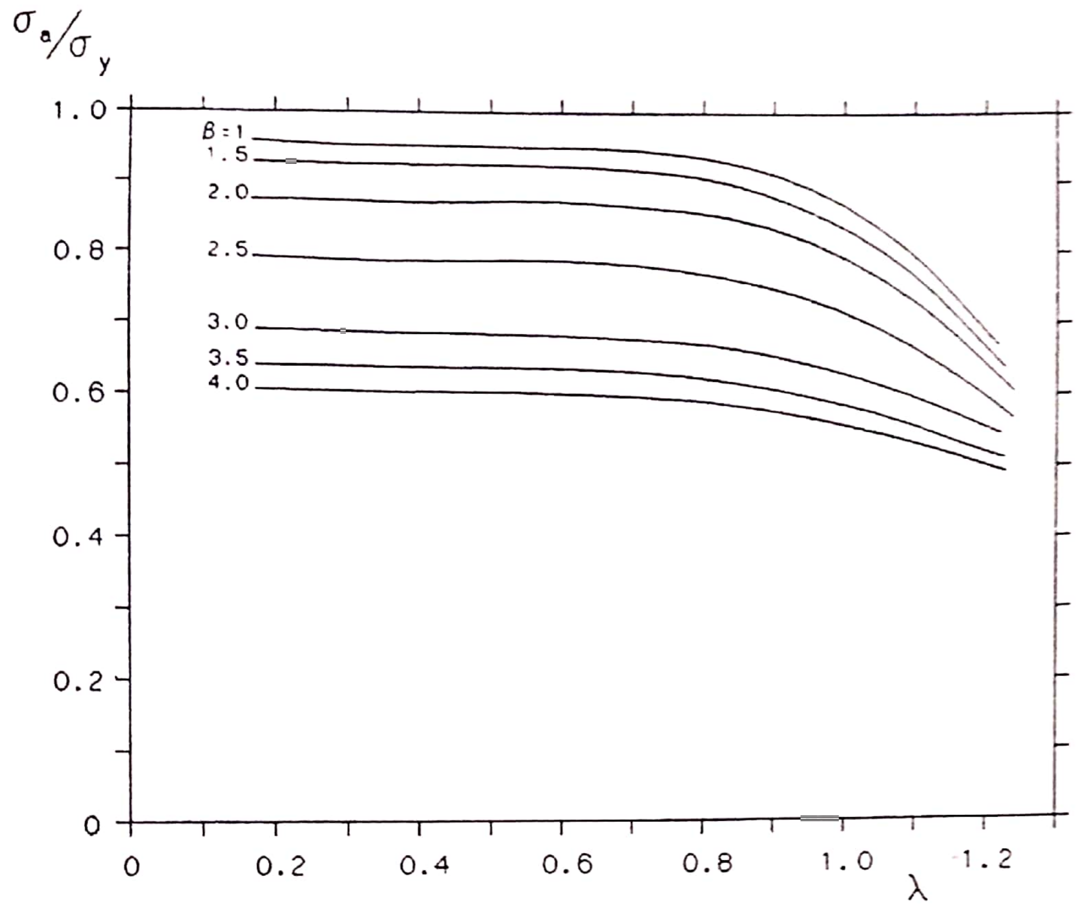

Figure 18.9 Column Strength Curves - Small Imperfections

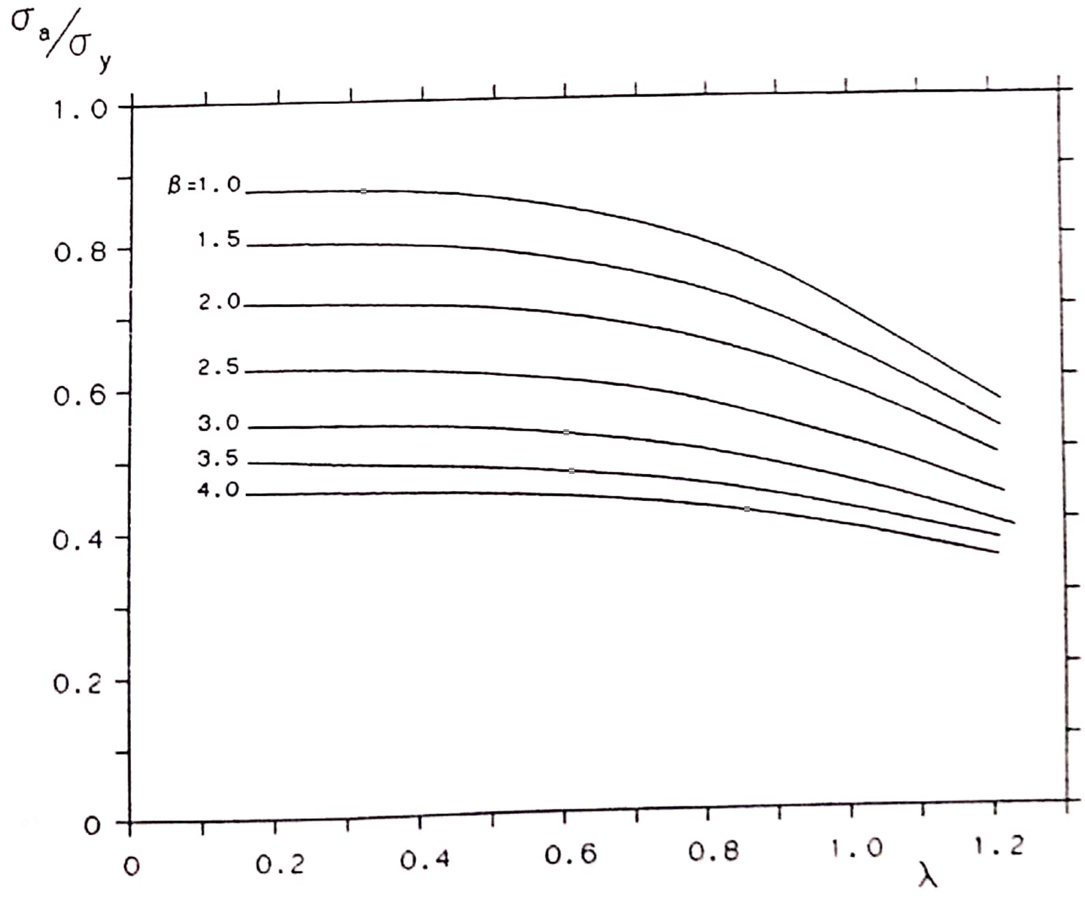

Figure 18.10 Column Strength Curves - Average Imperfections

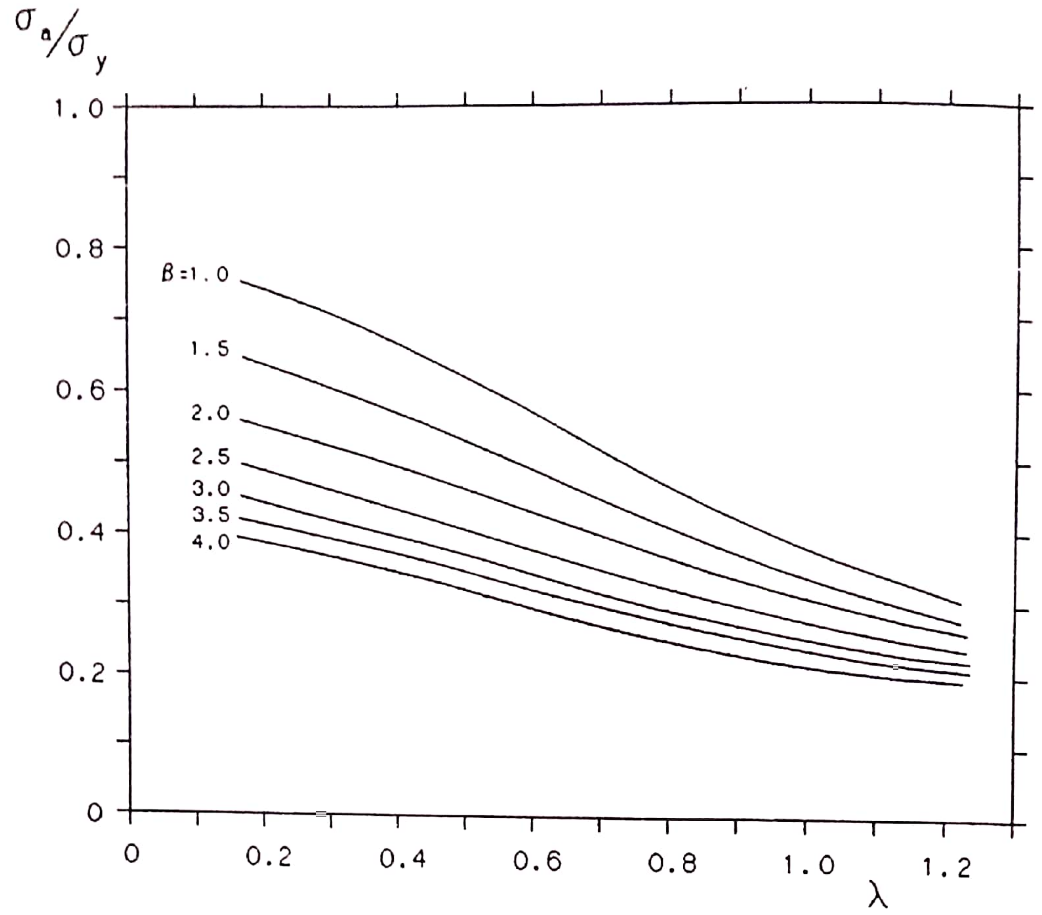

Figure 18.11 Column Strength Curves - Large Imperfections

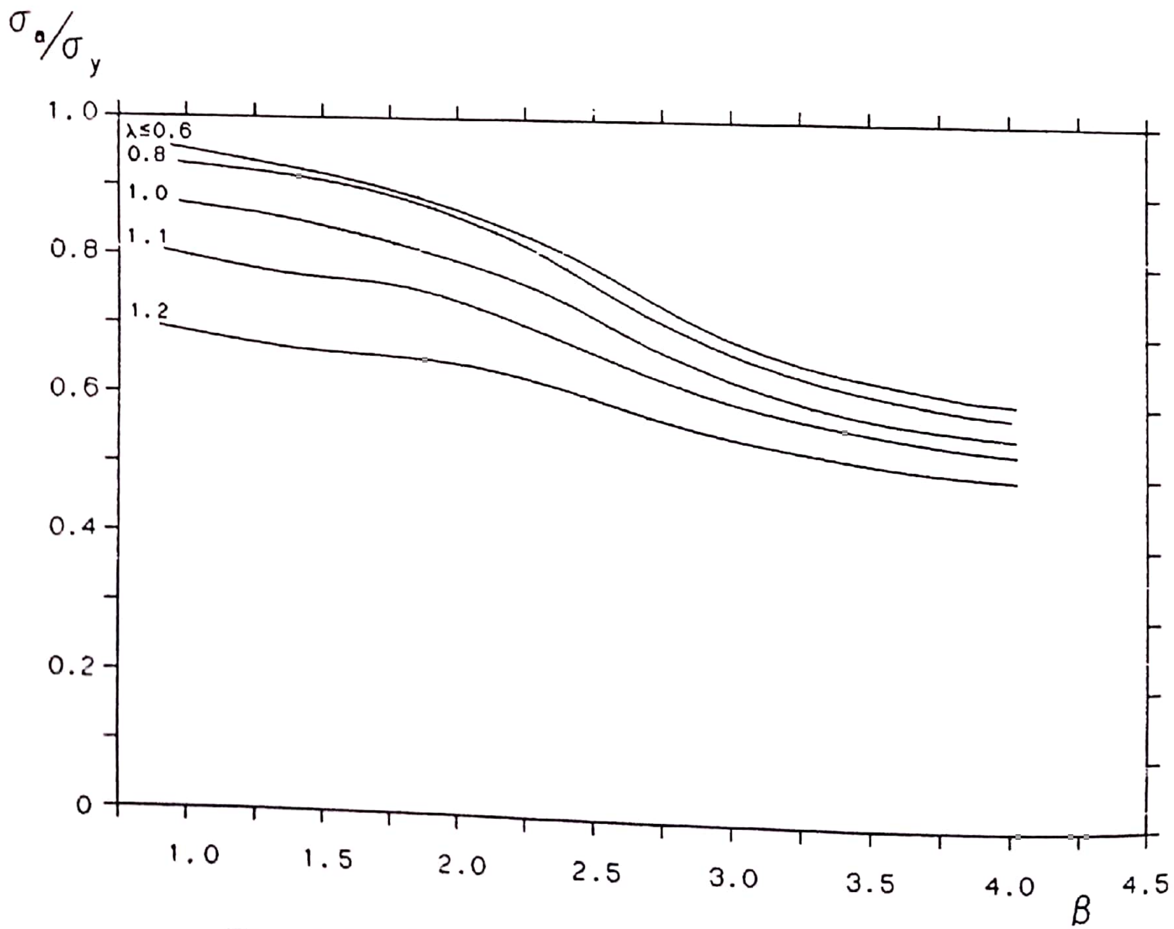

Figure 18.12 Column Strength Curves - Small Imperfections

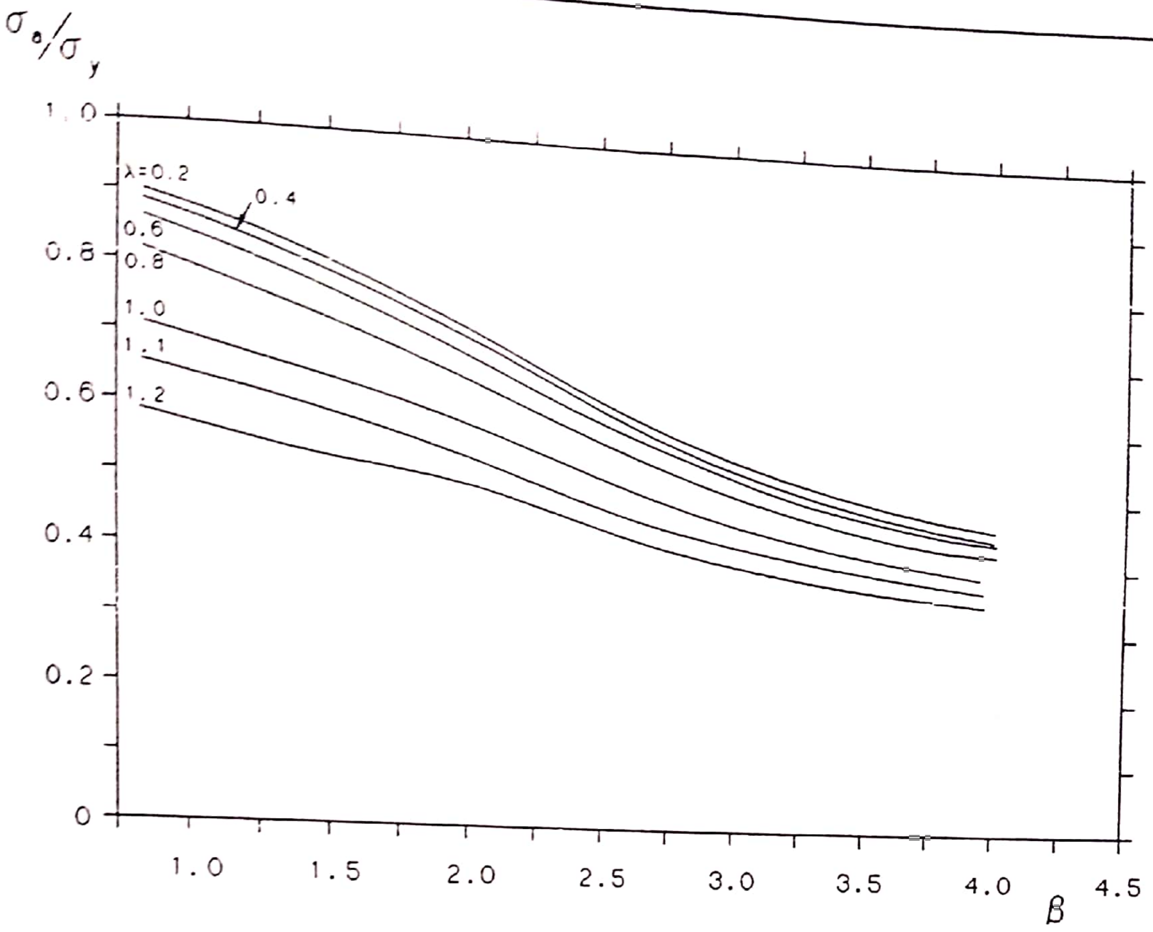

Figure 18.13 Column Strength Curves - Average Imperfections

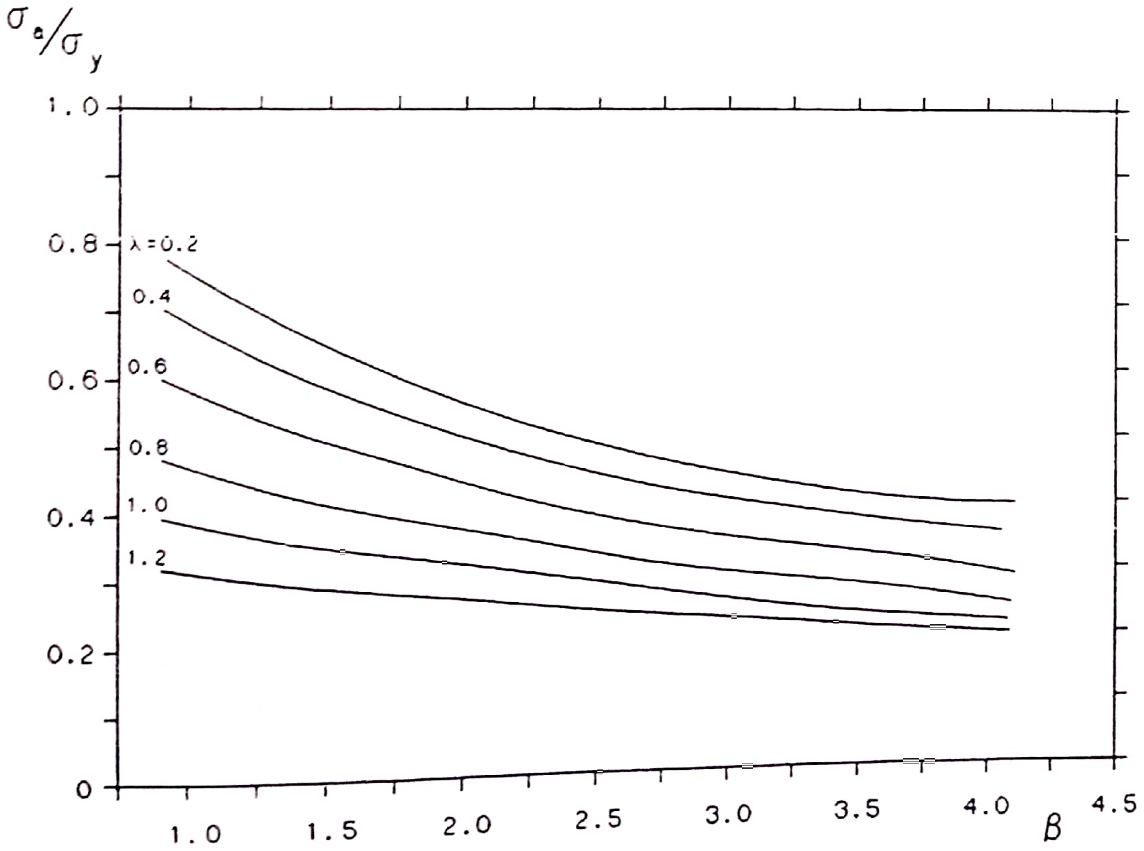

Figure 18.14 Column Strength Curves - Large Imperfections

Overall Collapse Curves for Grillages

11 The curves presented in this set are taken from Clarke (1977, 1979) and are based on theoretical work and parametric computer studies. The overall buckling behaviour of ship grillages is approximately determined by representing them as equivalent orthotropic plates. The accuracy of the calculated stresses and deflections increases with the number of stiffeners in each direction and is sufficient for most design purposes if the numbers *exceed three*. Since ship grillages always have some initial out-of-plane distortion, there is a progressive increase in bending stress as the in-plane load is increased and yielding at the outer fibres may occur before the elastic collapse load is reached. The curves therefore include a check on the possibility of yield induced collapse.

12 The edges and ends of the grillages are assumed to be *simply supported* as this is likely to be the most common case and will also be conservative if there is some edge constraint. Only bending and in-plane stresses are included, it being assumed that membrane and shear effects are negligible.

13 The nomenclature for the grillage is shown in *Figure 18.15* with the bending stiffness parameters for the orthotropic plate equation defined as:

(18.3a) $$D_x = EI_T\,(1/a - 1/A)$$

(18.3b) $$D_y = EI_L\,(1/b - 1/B)$$

I_T and I_L are the second moments of area of the transverse and longitudinal stiffeners respectively, *together with associated plating*. The effective breadth of plate in this instance should be taken as a half of the relevant stiffener spacing. The torsional stiffness parameter in the orthotropic plate equation is assumed to be zero as the torsional stiffness of open section stiffeners is very small.

14 Including those above there are some 19 parameters in the plate equation and these are reduced by judicious non-dimensionalising, to the following:

(18.4a) $$w^* = w/A$$

(18.4b) $$w_o^* = w_o/A$$

(18.4c) $$q^* = qB^4/AD_x$$

(18.4d) $$N_x^* = N_xB^2/D_x$$

(18.4e) $$N_y^* = N_yB^4/A^2D_x$$

(18.4f) $$M_x^* = M_xB^2/EI_TA$$

(18.4g) $$M_y^* = M_y A / EI_L$$

(18.4h) $$\mu = (A/B)^4 \, (D_x/D_y)$$

where	
w	is the out-of-plane deflection in the grillage produced by the load
w_o	is the initial out-of-plane deformation
q	is the lateral pressure applied to the grillage surface
N_x and N_y	are respectively the load per unit length and width applied to the grillage
M_x and M_y	are the bending moments per unit length in the transverse and longitudinal stiffeners respectively.

15 If a value of the maximum deflection δ (non-dimensionalised as $\delta^* = \delta/A$) is chosen then w^*, M_x^* and M_y^* can be expressed in terms of μ, N_x^*, N_y^* and q^*. The form of design curves presented is to plot w^*, M_x^* or M_y^* against μ for different values of N_y^* (since the load on the longitudinal stiffeners is usually dominant) at specific combinations of N_x^*/N_y^* and q^*.

16 The maximum deflection δ is always at the centre of the grillage, but the maximum moments move away from the centre for M_x^* at low values of μ and for M_y^* at high μ. This effect is illustrated in *Figure 18.16* as an example for uniform lateral pressure only.

17 *Figure 18.17* shows the variation of the maximum value of $w^* + w_o^*$ with μ and N_y^* for the common case of zero lateral pressure and no transverse load. The initial deflection is assumed as a single half wave along the grillage length with δ^* equal to the maximum recommended design value of 0.002 from Somerville et al (1977). For each value of N_y^*, w^* increases with μ until either elastic buckling occurs or a limiting deflection is reached. The corresponding values of M_x^* (greater than M_y^*) are shown in *Figure 18.18* and they exhibit similar behaviour.

18 The critical value of μ (μ_{cr}) corresponding to elastic buckling can be derived from equation 18.5.

(18.5) $$\mu_{cr} = m^4/(\{-N_x^* - m^2 N_y^*\}/\pi^2 - 1)$$

where m is the number of half waves longitudinally. For the case of end load only this simplifies to:

(18.5a) $$\mu_{cr} = 1/(-N_y^*/\pi^2 - 1)$$

19 For the single half wave case (m = 1) it can be seen that elastic buckling does not occur for N_y^* less than $-\pi^2$ for any value of stiffness ratio μ. However, as μ increases the higher order buckling modes predominate and lead to higher bending stresses as can be seen in *Figure 18.19*. The maximum bending moments, which in this case occur at the locations of maximum initial deflection, have been plotted. The bending moments for different m values have not been added since they occur at different locations and it would be too conservative to assume that the limiting values of all initial deflection modes could occur simultaneously.

20 *Figure 18.20* shows corresponding values of M_y^*. For m = 1 the values are nearly identical to M_x^* but the higher modes give higher values because the fraction of stiffener length over which bending occurs decreases, that is, the local curvature increases.

21 *Figures 18.21* to *18.24* give corresponding pairs of curves for N_x^*/N_y^* equal to 0.5 and 1.0. In order to reduce the number of figures w* has not been plotted in these cases as it is of little interest in design calculations. However, since the maximum deflection and stress occur at the same location w* can be approximated to using the expression $M_y^*/m^2\pi^2$.

22 The remaining figures show the effect of lateral pressure in addition to in-plane load. In order to limit the number of curves it is necessary to confine the cases covered to those with zero transverse load ($N_x = 0$). Also, only M_y^* has been plotted since stress in the transverse stiffeners is not likely to be limiting in this situation.

23 The values of q* of 0.05, 0.1, 0.2, 0.5 and 1.0 have been chosen to cover the probable range of interest, for example for q = 20 kPa and A = 10 m, B = 3 m and $D_x = 0.84$ MN.m then q* = 0.19. As q increases it can be seen that the m = 1 and m = 3 cases become more important than the m = 2 and m = 4 cases because they give maximum bending moments in the centre.

Application of the Design Curves

24 The curves in the data sheets are intended to enable the designer to make a rapid estimate of the outer fibre stress due to overall grillage bending. It must not be forgotten that the location of the maximum stress may not correspond to a stiffener position, so the curves may give an overestimate, but this effect will be small in grillages with a large number of stiffeners. It should also be noted that the curves do not take into account bending between stiffeners due to lateral pressure. If this is likely to be significant then a correction must be made as discussed for grillages under pressure alone (see paragraph 47).

25 Direct stresses also must be added to the bending stresses to give the total outer fibre stress. Assuming that the maximum overall bending and local bending occurs at the same location and are of the same sign as the direct stress (that is, compressive), the maximum outer fibre stress is given by:

$$\sigma_{of} = y_{of}\,(M_y^*\,E/A + 0.042qa^2b/I_L) + |N_y|\,b/A_L \tag{18.6}$$

where y_{of} is the distance between the neutral axis of the plate-stiffener combination and the outer fibre on the side of the grillage to which the pressure is applied, and A_L is the cross section area of the longitudinal plate-stiffener combination (in each case allowing for the effective width of plate).

26 Having established the maximum outer fibre stress it can be compared with an allowable fraction of the yield stress or, as suggested by Clarke (1977), a maximum of the direct stress plus 0.75 of the bending stress can be used for comparison with the yield stress. In either case allowance should be made for the presence of any compressive residual stresses.

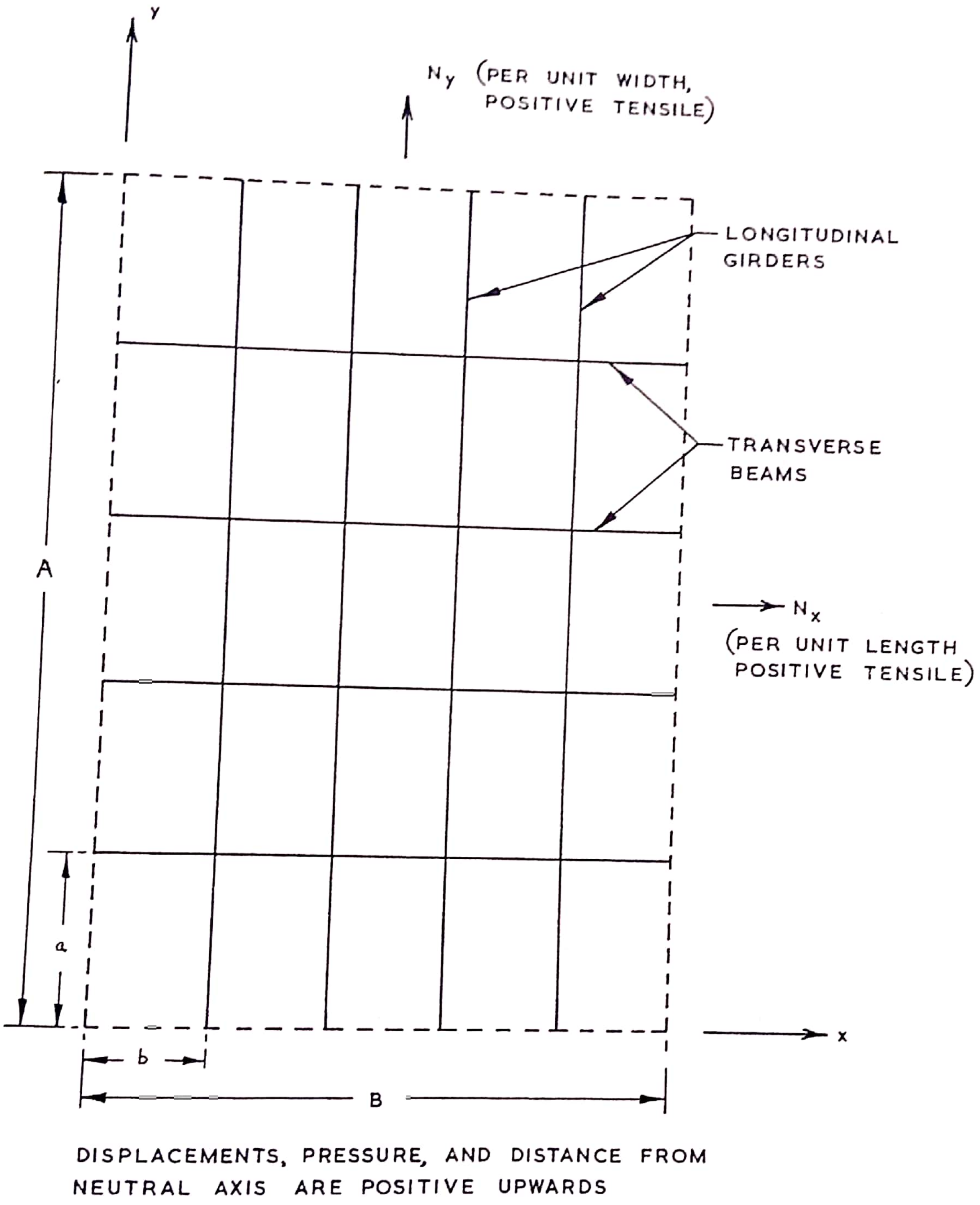
y
N_y (PER UNIT WIDTH, POSITIVE TENSILE)
LONGITUDINAL GIRDERS
TRANSVERSE BEAMS
A
N_x
(PER UNIT LENGTH POSITIVE TENSILE)
a
b
B
x
DISPLACEMENTS, PRESSURE, AND DISTANCE FROM NEUTRAL AXIS ARE POSITIVE UPWARDS

Figure 18.15 Grillage Nomenclature for Overall Buckling

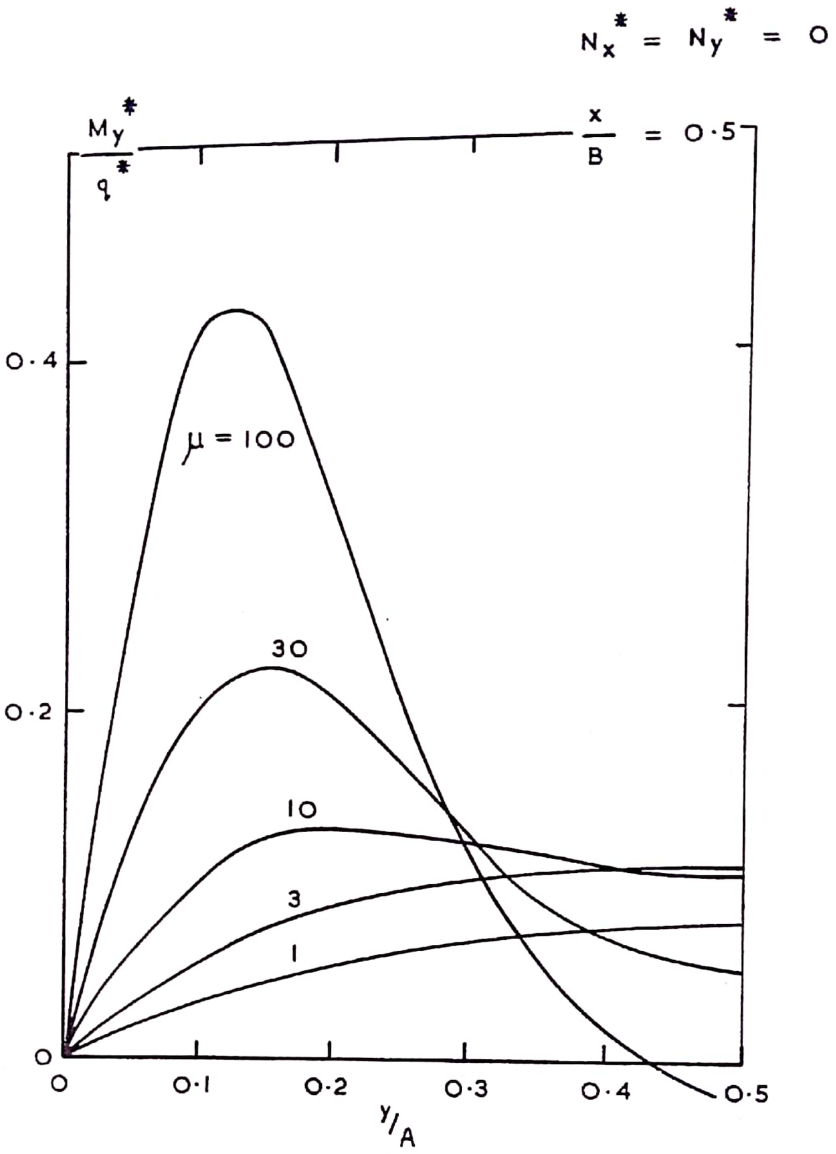

Figure 18.16 Effect of Flexibility on the Variation of Bending Moment with Length under Lateral Pressure

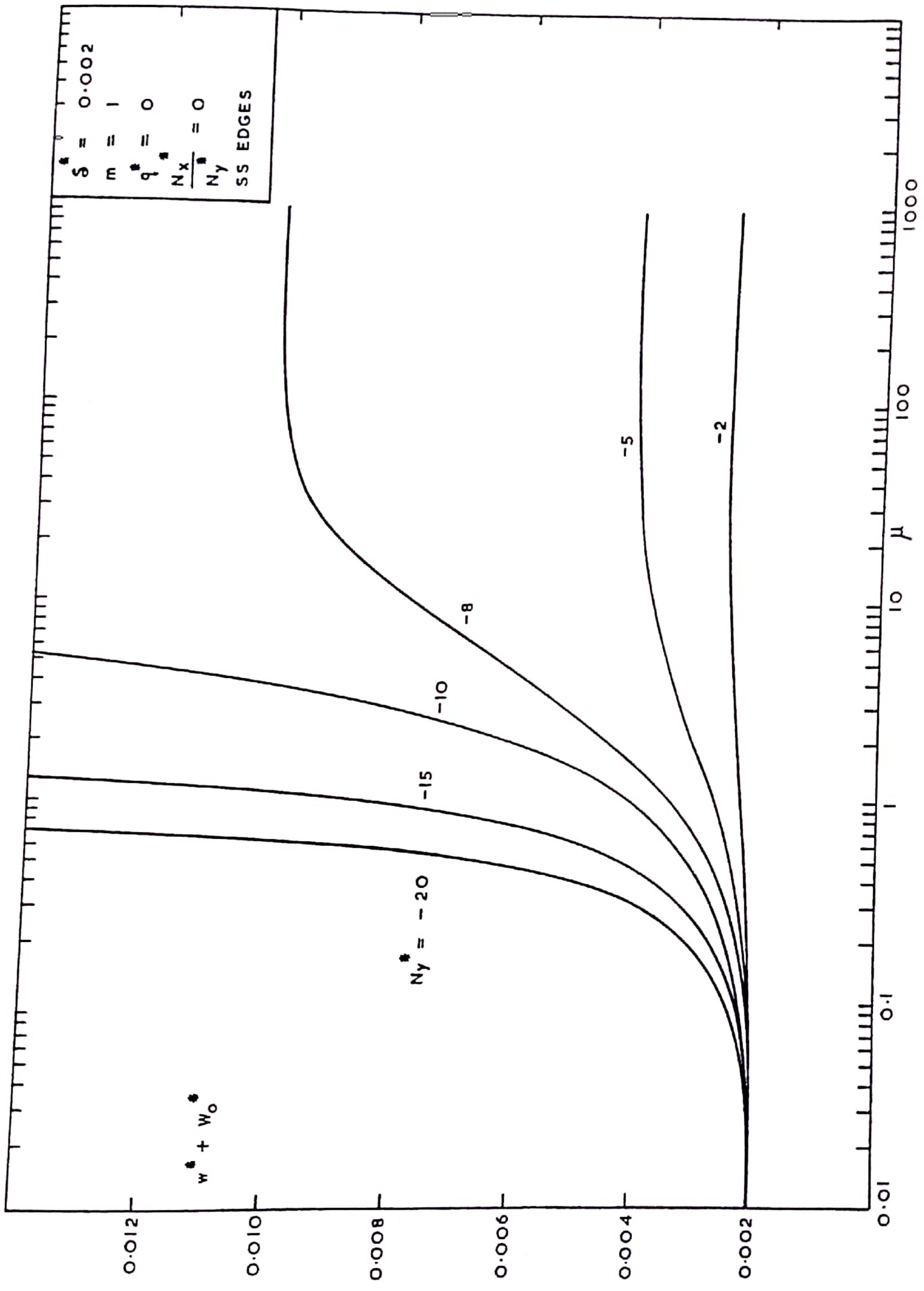

Figure 18.17 Maximum Total Deflection

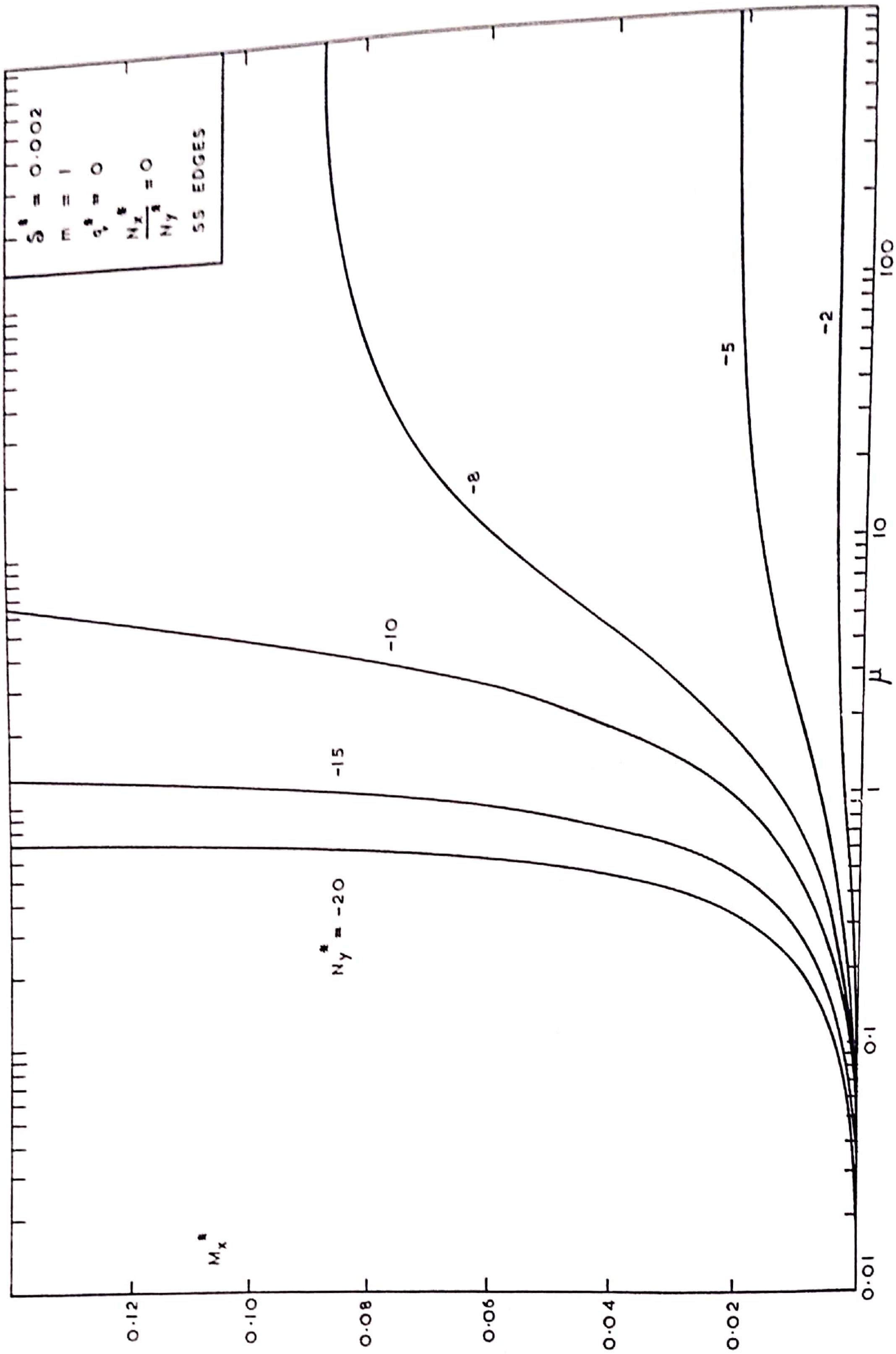

Figure 18.18 Variation of M_x^* with μ and N_y^* - Single Half Wave

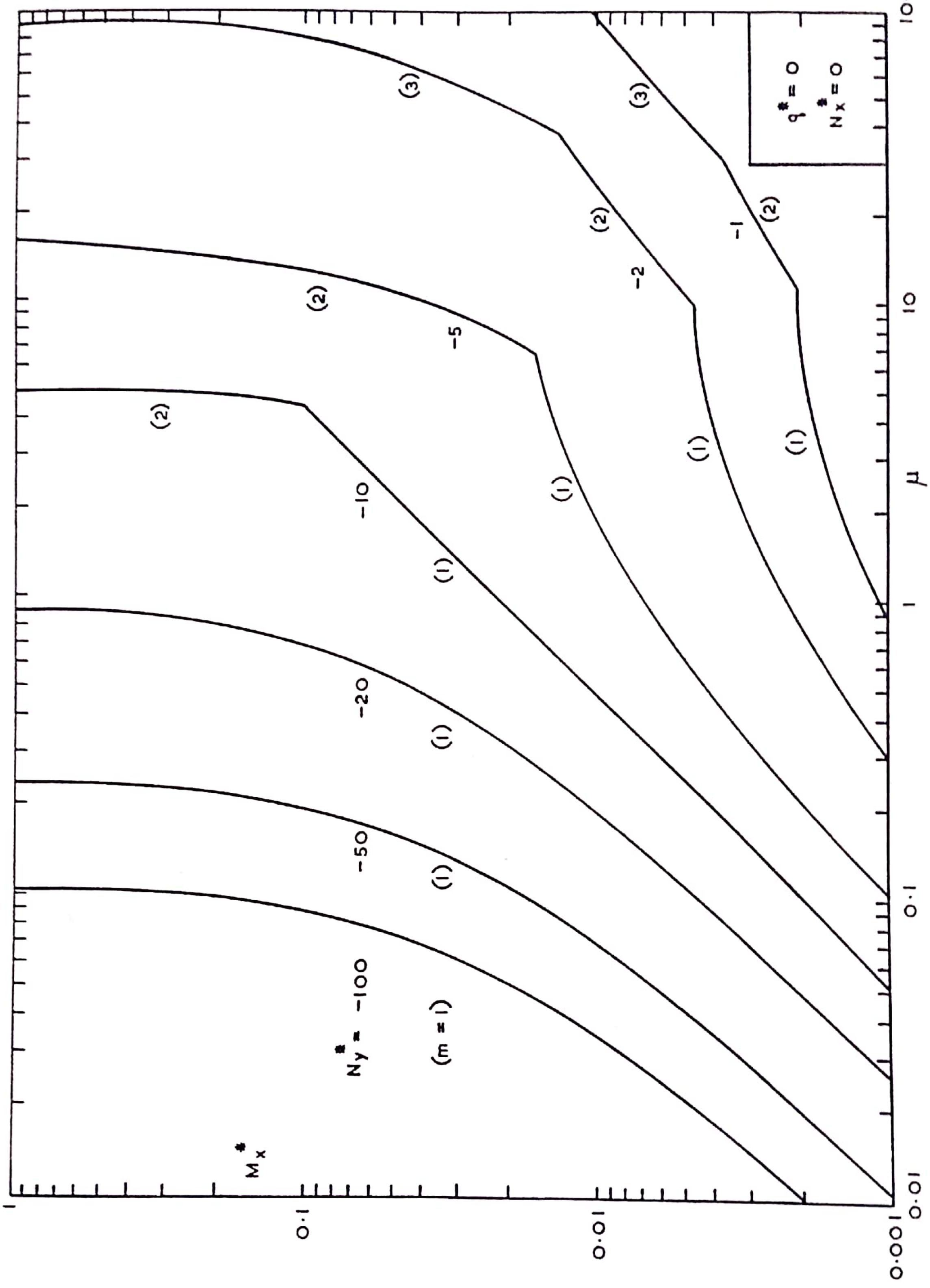

Figure 18.19 Variation of M_x^* with μ and N_y^* - Higher Order Modes

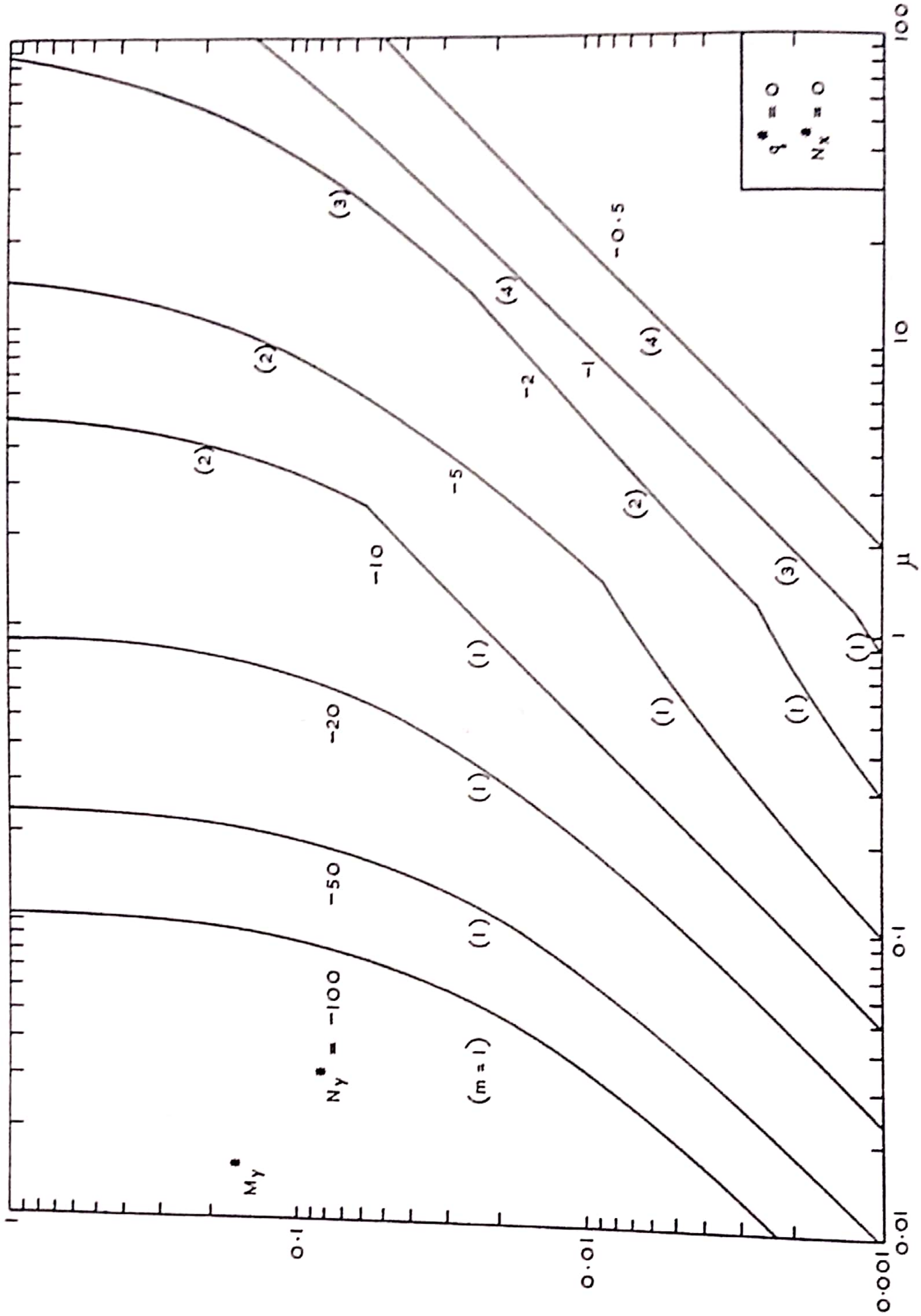

Figure 18.20 Variation of M_y^* with μ and N_y^*, $N_x^* = 0$

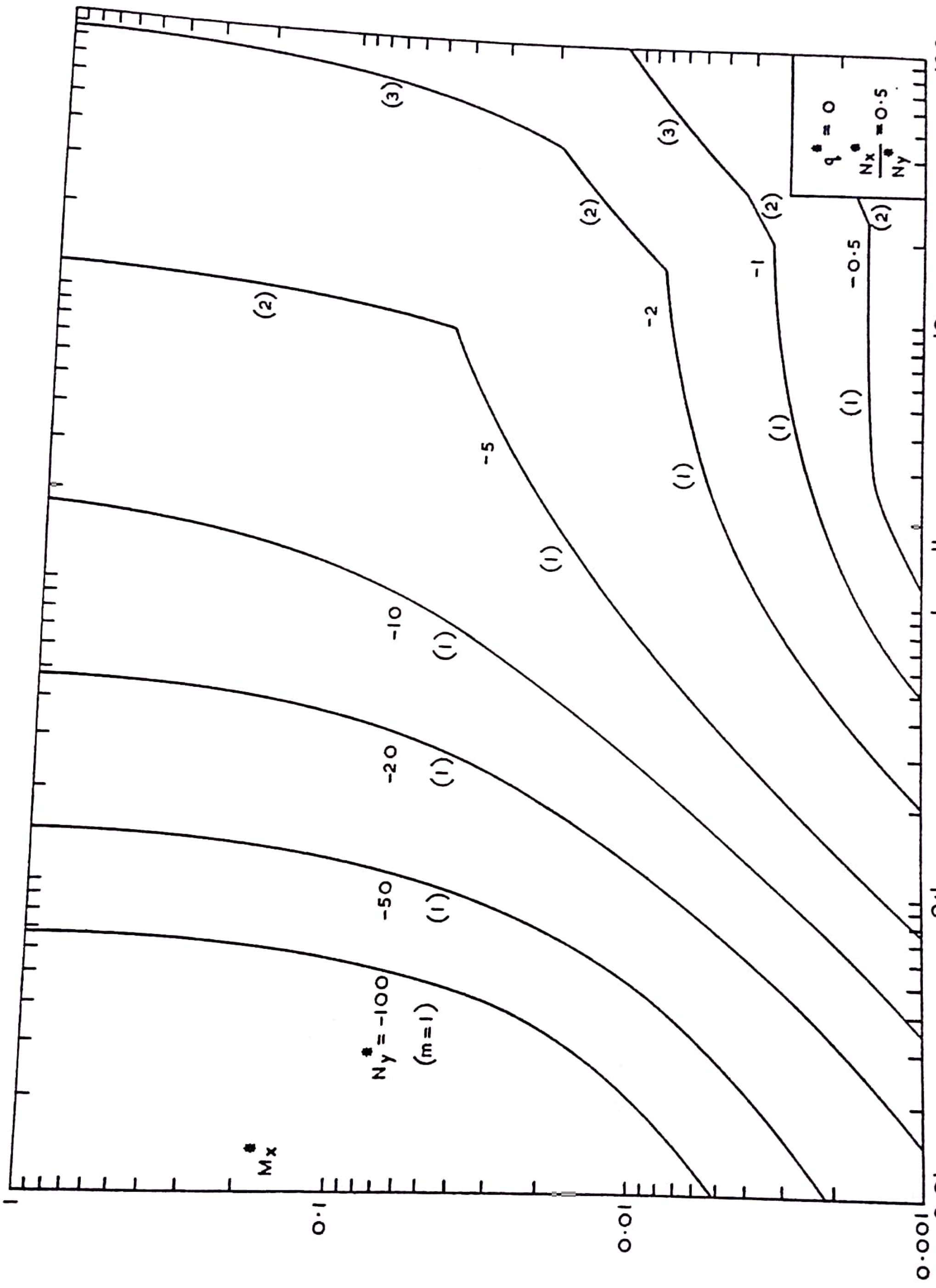

Figure 18.21 Variation of M_x^* with μ and N_y^*, $N_x^*/N_y^* = 0·5$

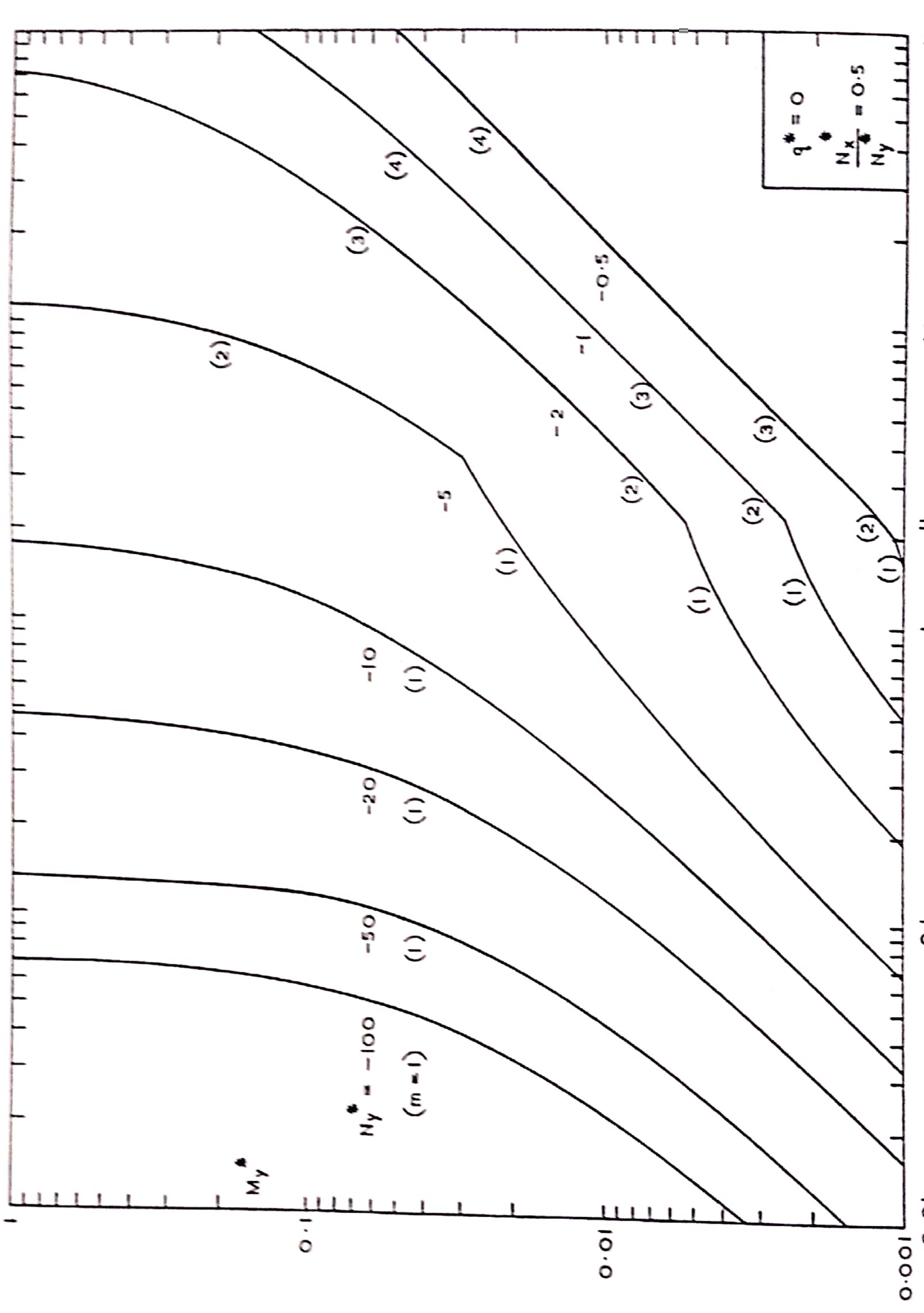

Figure 18.22 Variation of M_y^* with μ and N_y^*, $N_x^*/N_y^* = 0{\cdot}5$

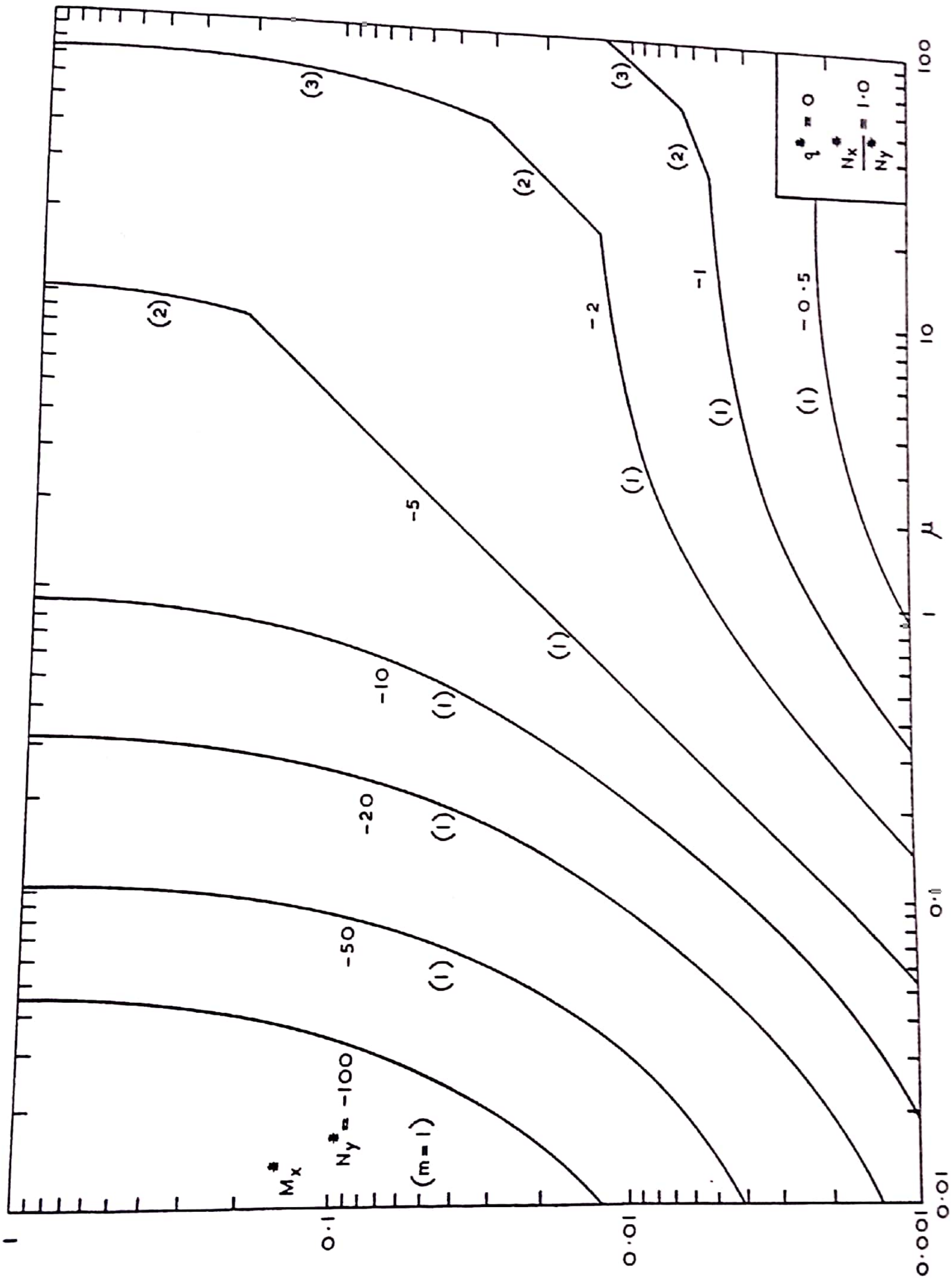

Figure 18.23 Variation of M_x^* with μ and N_y^*, $N_x^*/N_y^* = 1{\cdot}0$

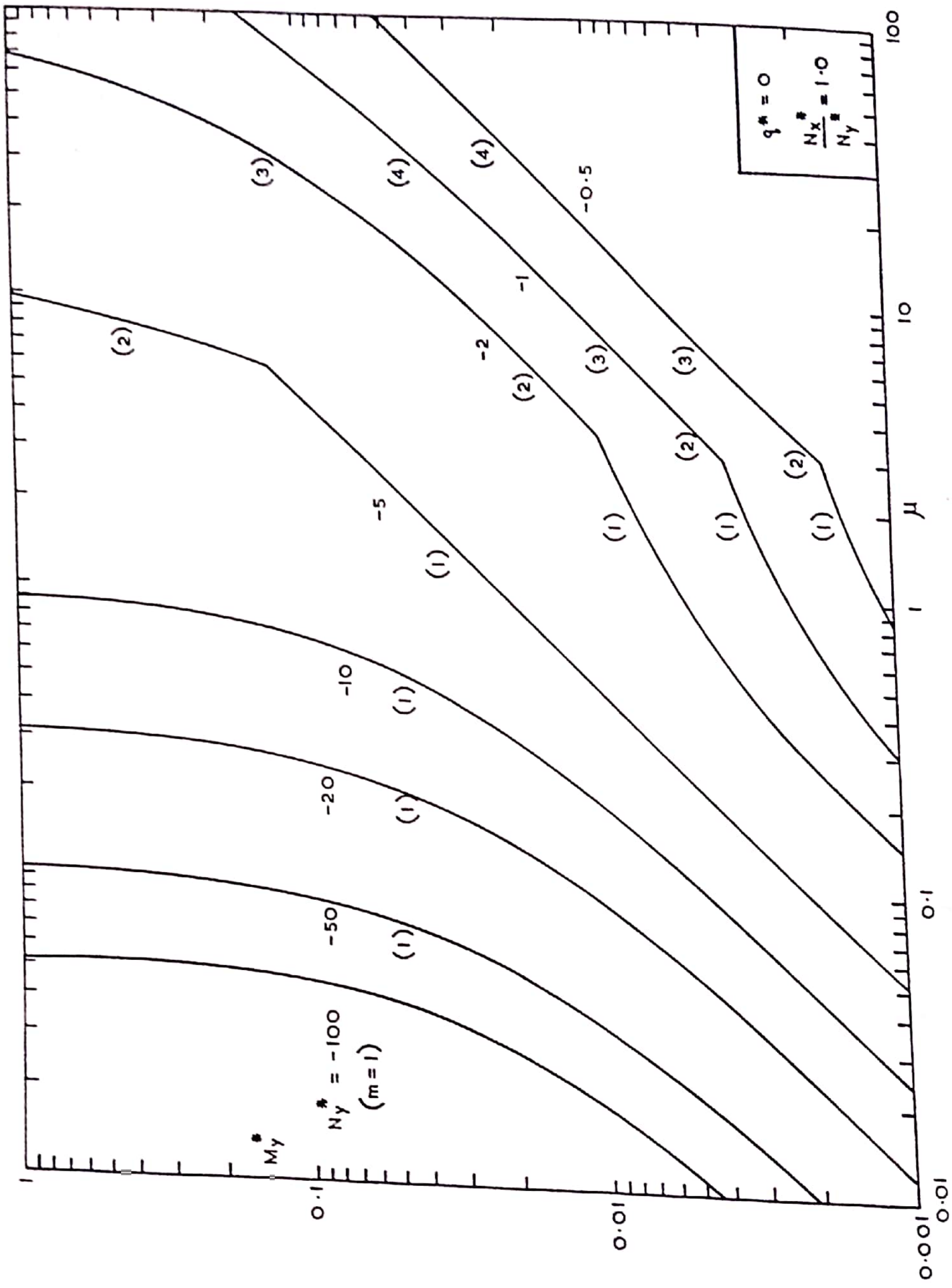

Figure 18.24 Variation of M_y^* with μ and N_y^*, $N_x^*/N_y^* = 1\cdot 0$

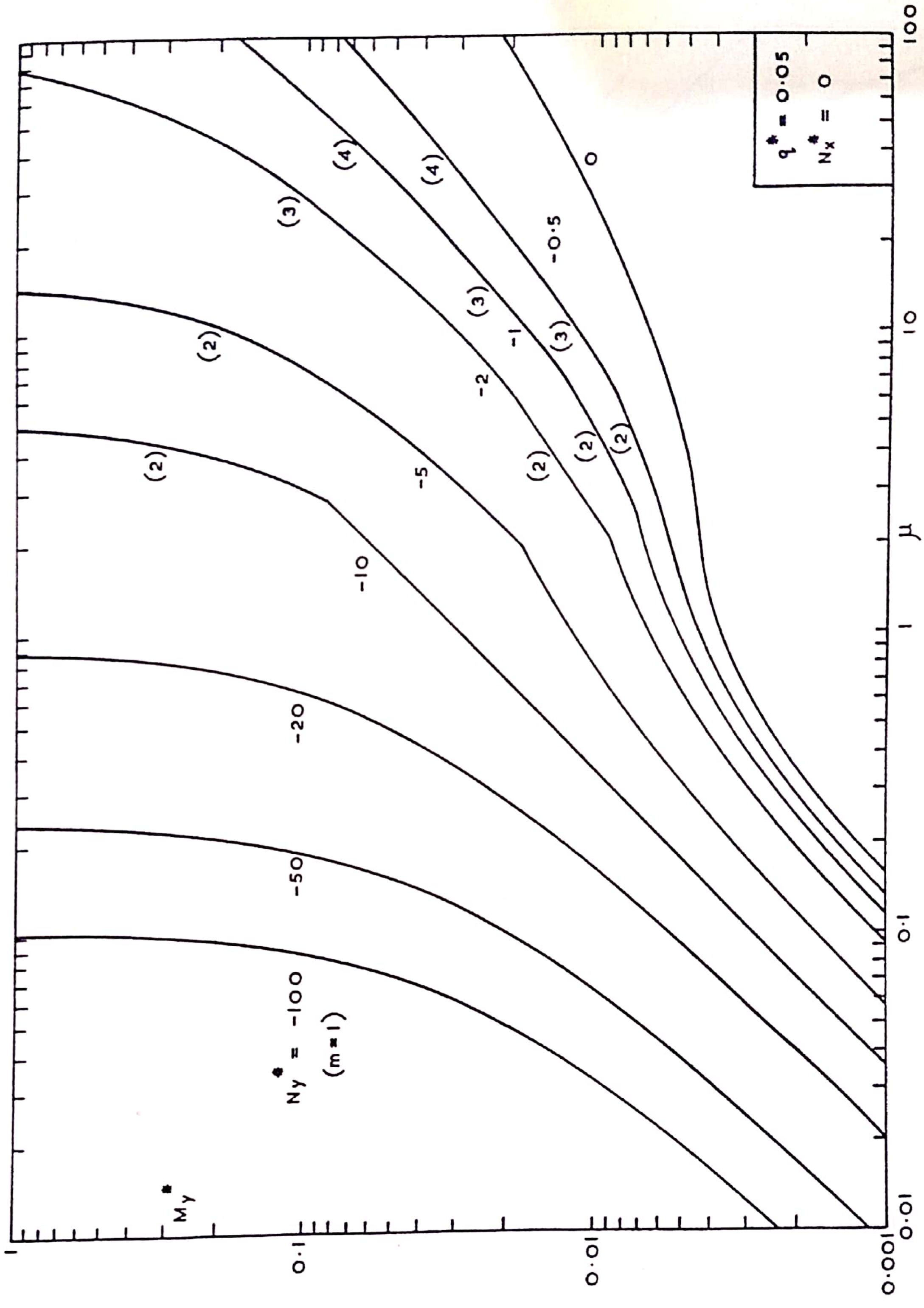

Figure 18.25 Variation of M_y^* with μ and N_y^*, $q^* = 0·05$

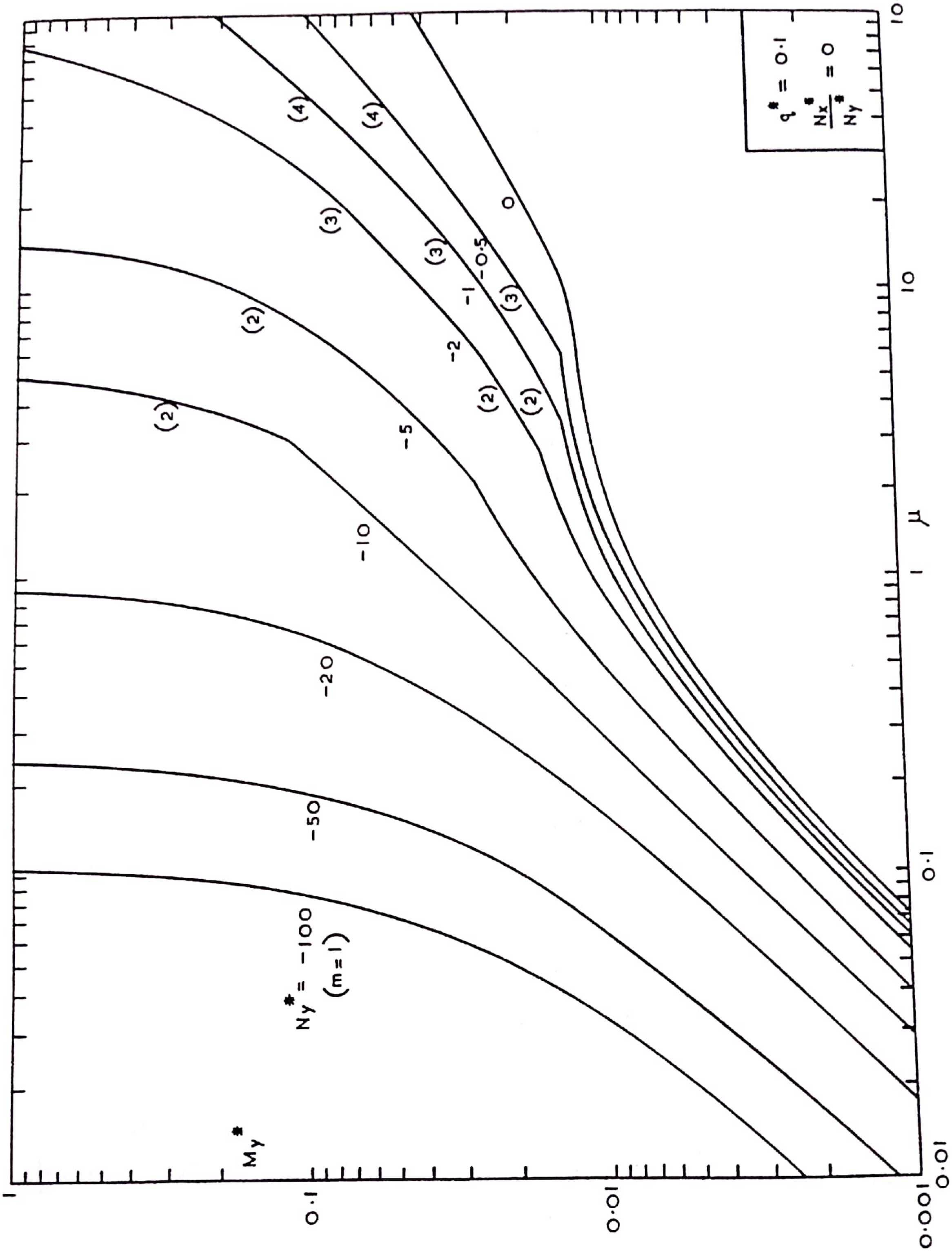

Figure 18.26 Variation of M_y^* with μ and N_y^*, $q^* = 0{\cdot}1$

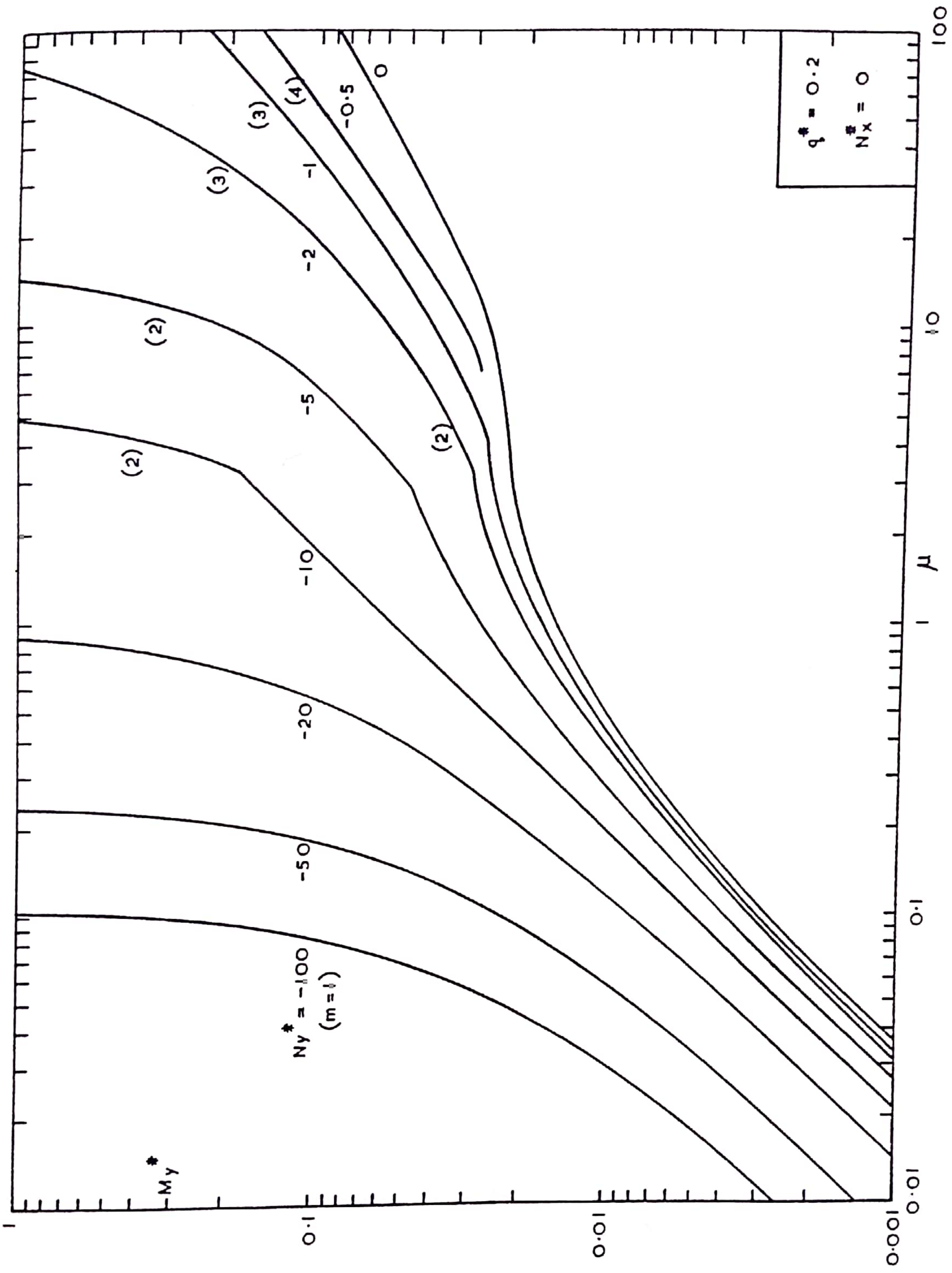

Figure 18.27 Variation of M_y^* with μ and N_y^*, $q^* = 0·2$

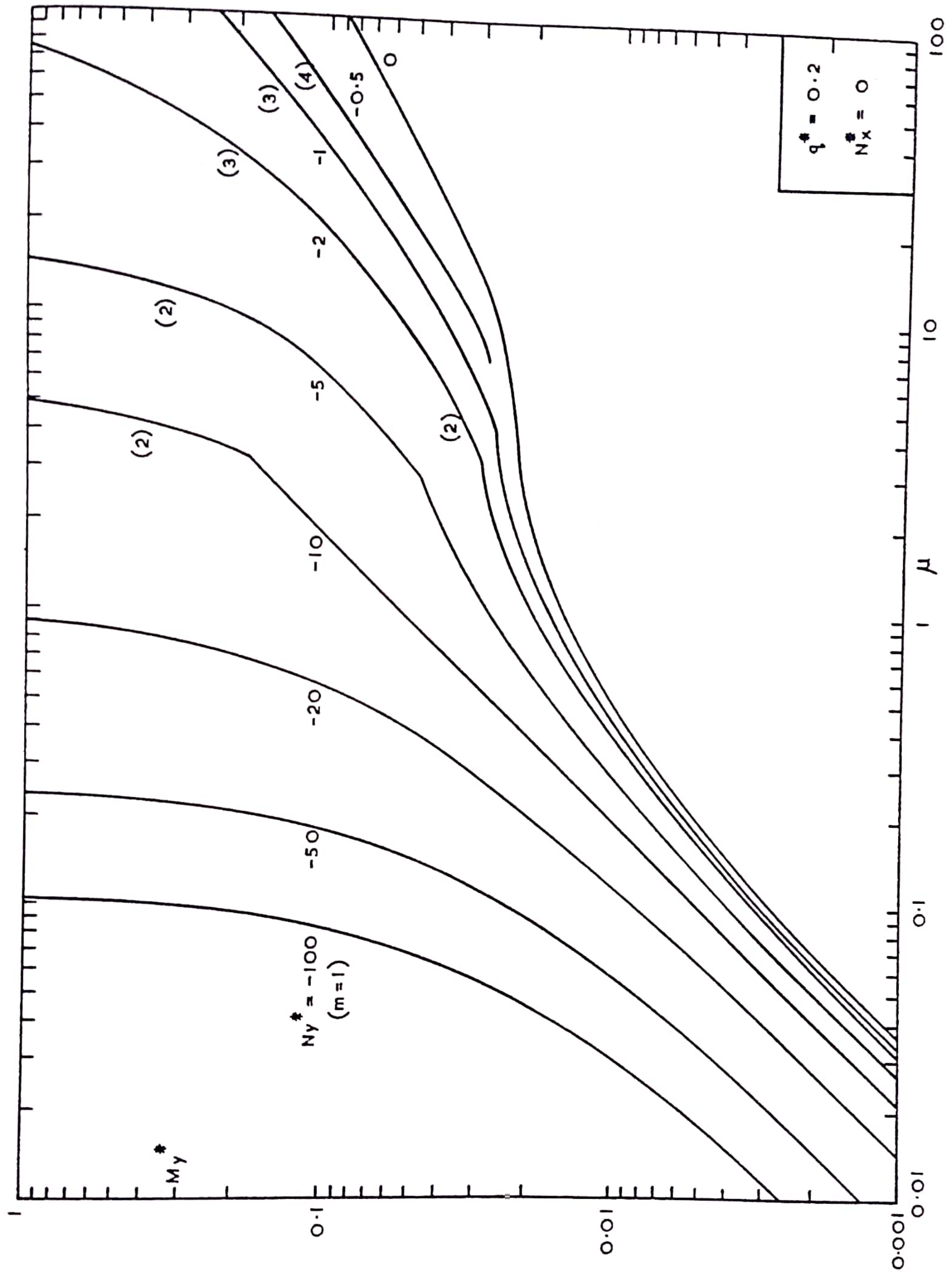

Figure 18.27 Variation of M_y^* with μ and N_y^*, $q^* = 0·2$

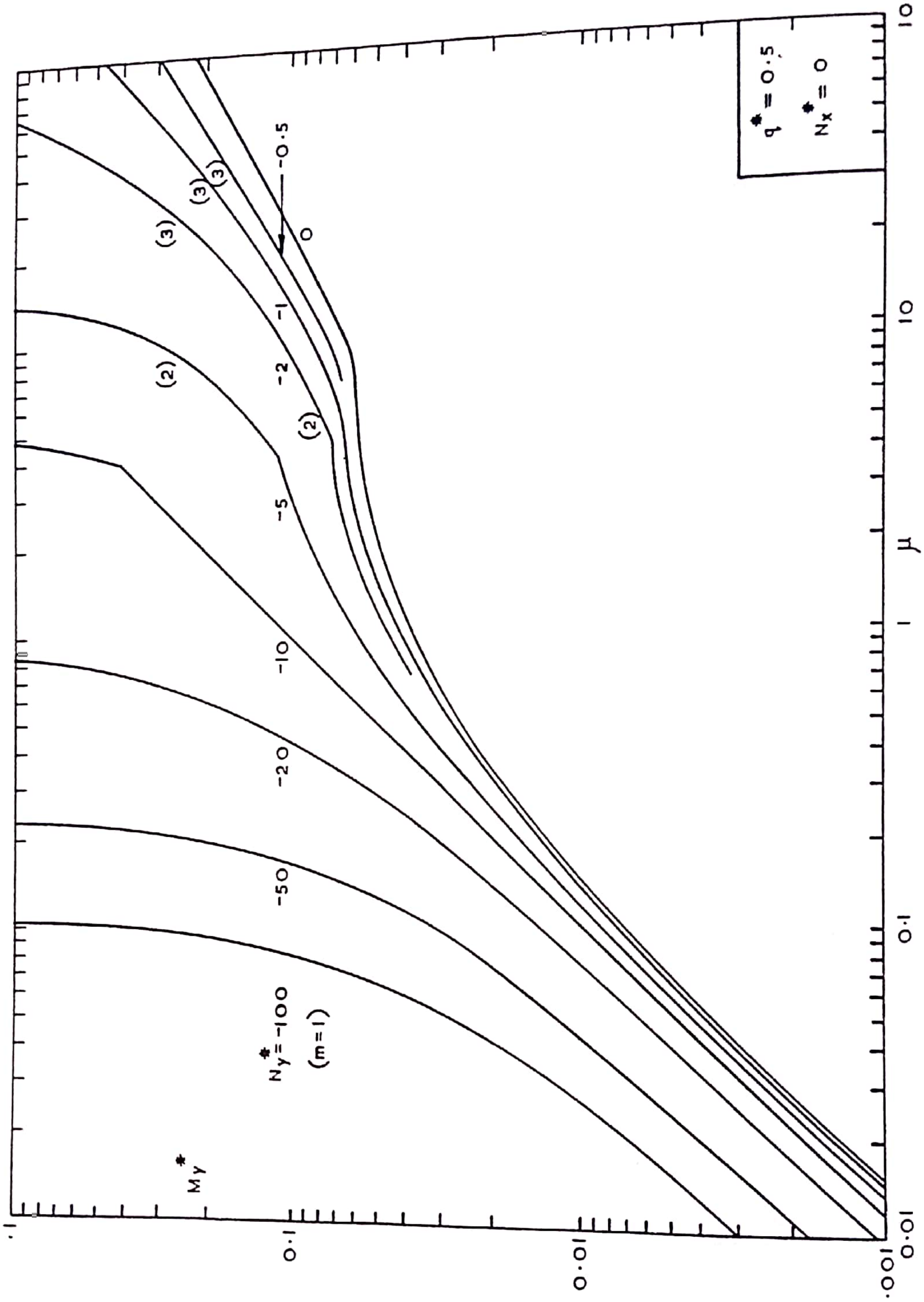

Figure 18.28 Variation of M_y^* with μ and N_y^*, $q^* = 0{\cdot}5$

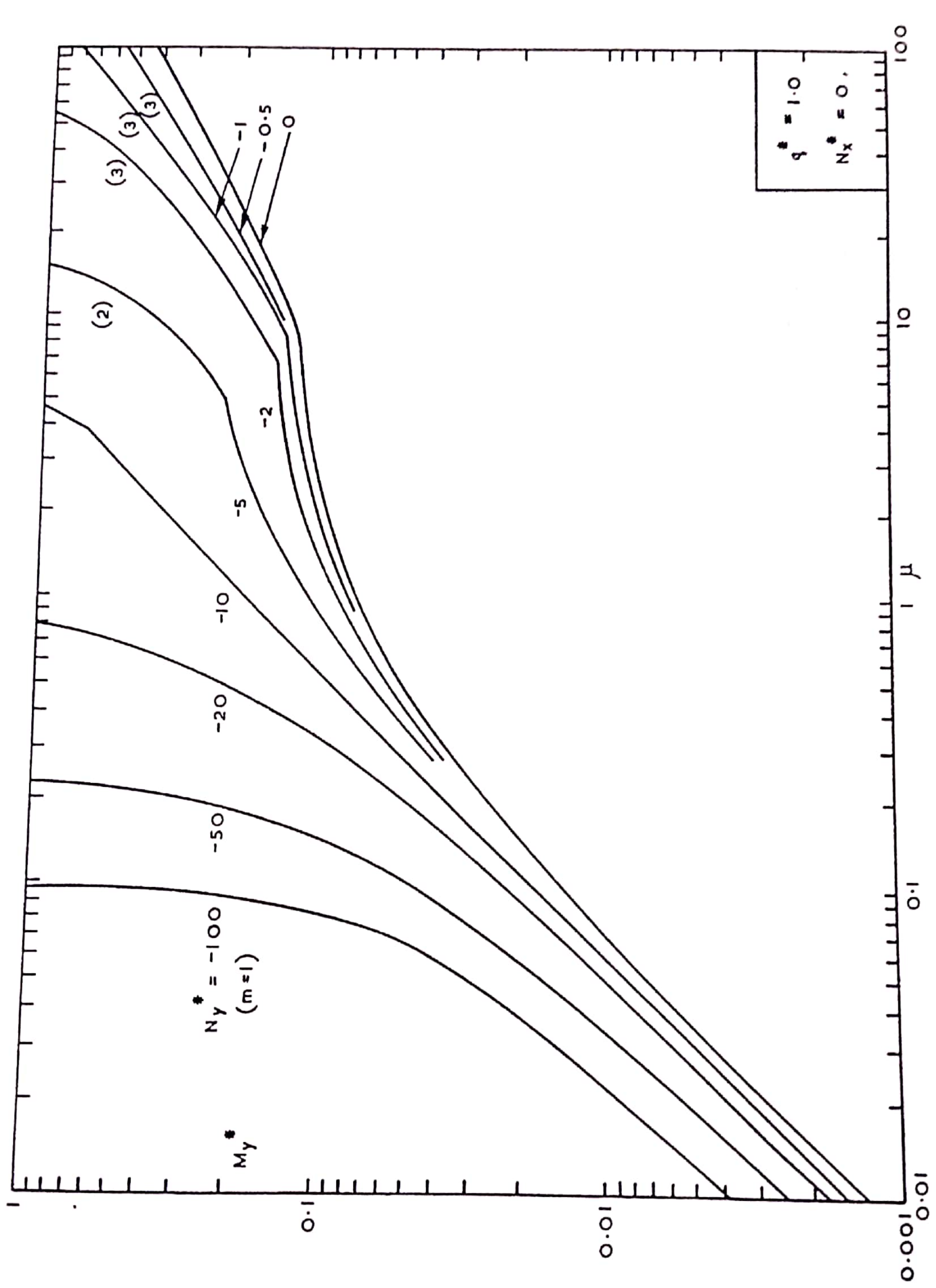

Figure 18.29 Variation of M_y^* with μ and N_y^*, $q^* = 1{\cdot}0$

Properties of Tee Bars and Associated Plate

27 *Figures 18.30* to *18.36* are generally self explanatory and provide values of second moment of area (I) and section modulus (Z) for the seven standard sizes of long-stalk Tee bar listed in *Figure 18.1* when attached to various thicknesses and widths of plate of the same material as the Tee bar. The calculation of the parameters is straightforward and the curves are included for convenience to enable a designer to get a rapid feel for the size of stiffener needed for a particular application. Note that to enable numbers of reasonable magnitude to be included in the curves, second moment is given in **cm³**; effective breadth in **metres** and thickness in **mm**.

28 The modulus given in the curves is the minimum one, that is the value at the outer fibre of the flange of the stiffener. The value at the plate surface, should it be required, can be found by deducing the position of the combined neutral axis from the ratio of second moment to modulus then, knowing the height of the stiffener from *Figure 18.1*, the distance of the plate surface from the neutral axis can be deduced and so the modulus at that surface may be calculated.

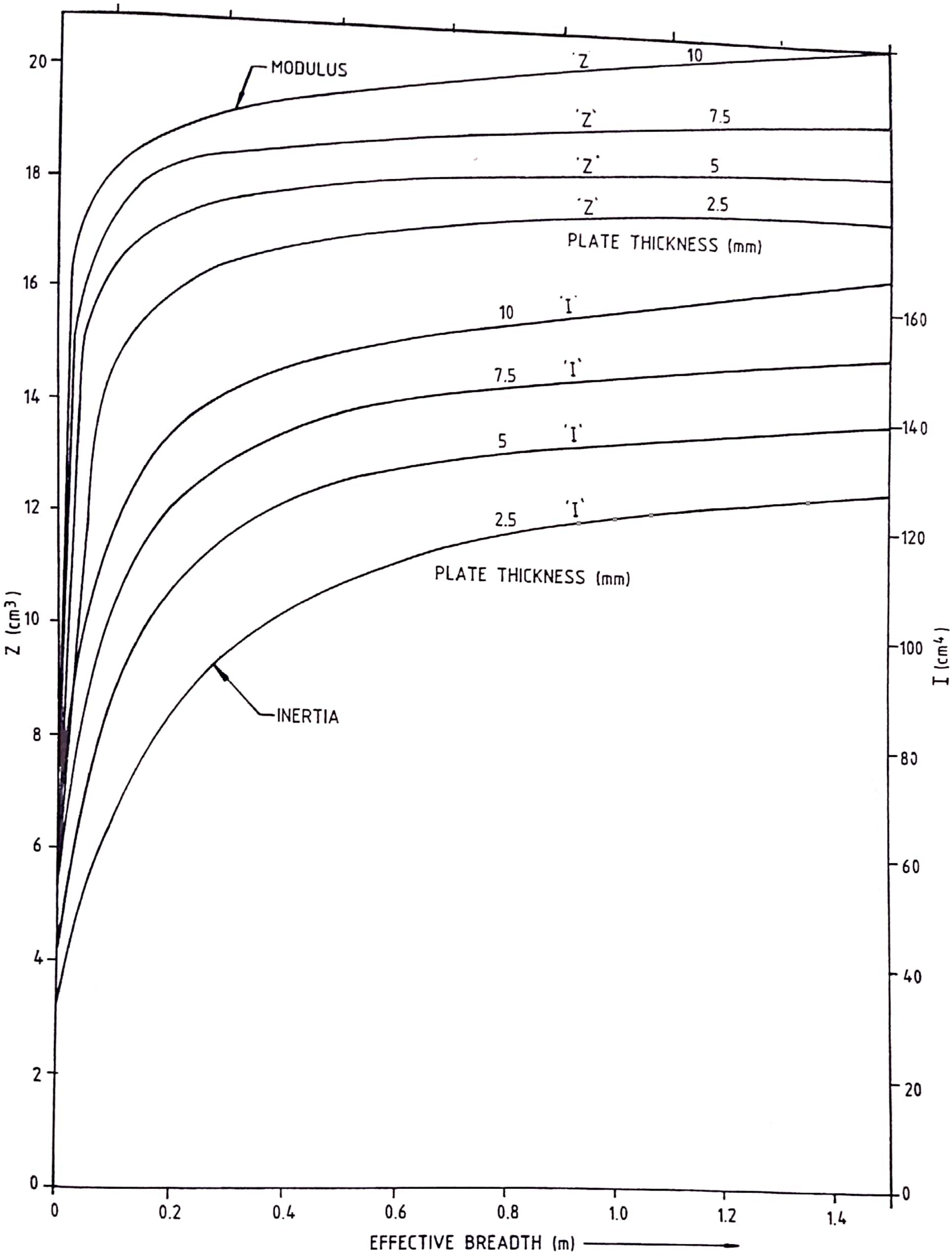

Figure 18.30 Properties of Tee Bar Stiffeners Type 1 (25.4 × 76.2mm)

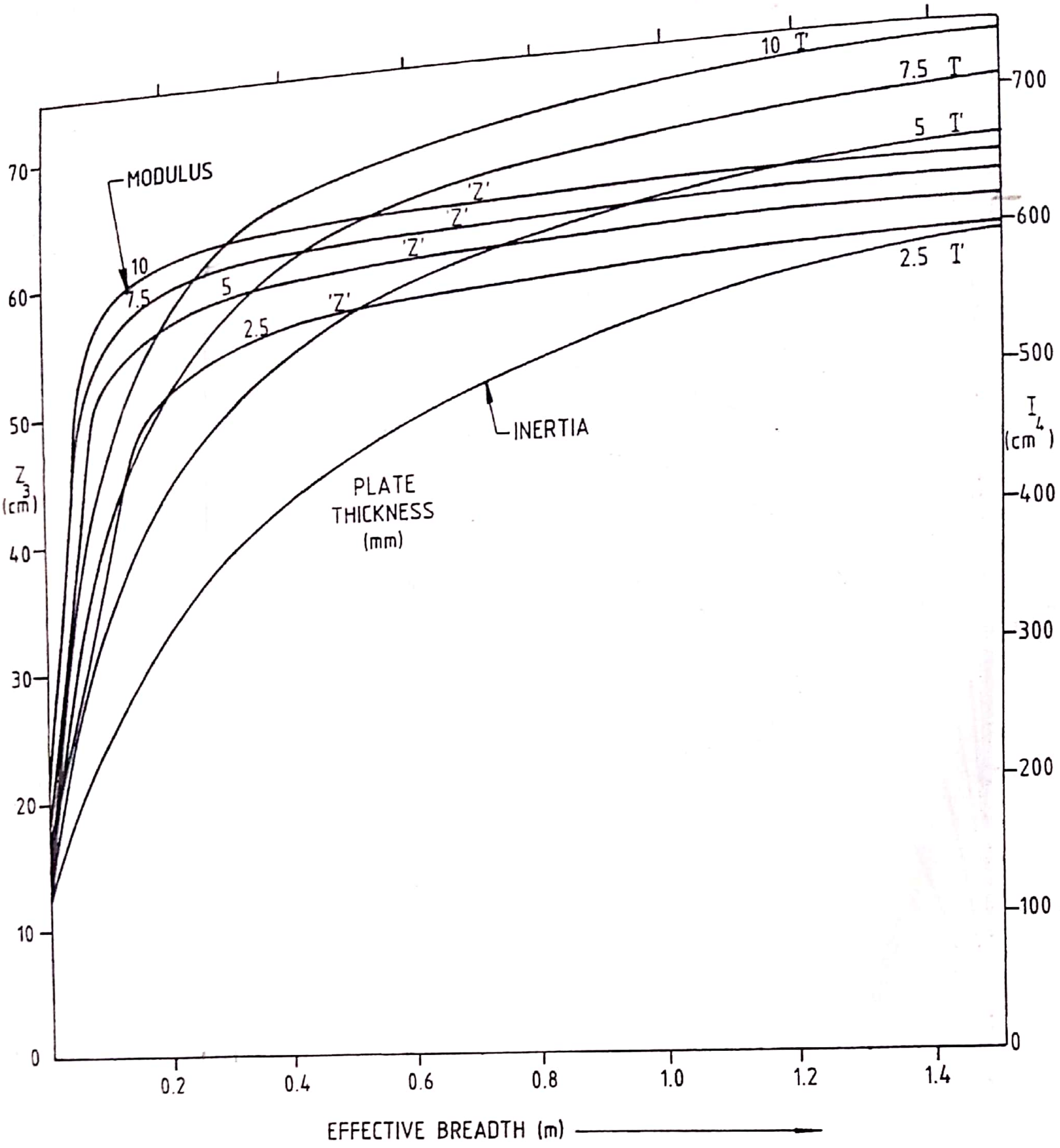

Figure 18.31 Properties of Tee Bar Stiffeners 44.5 × 114.3 (Type 2)

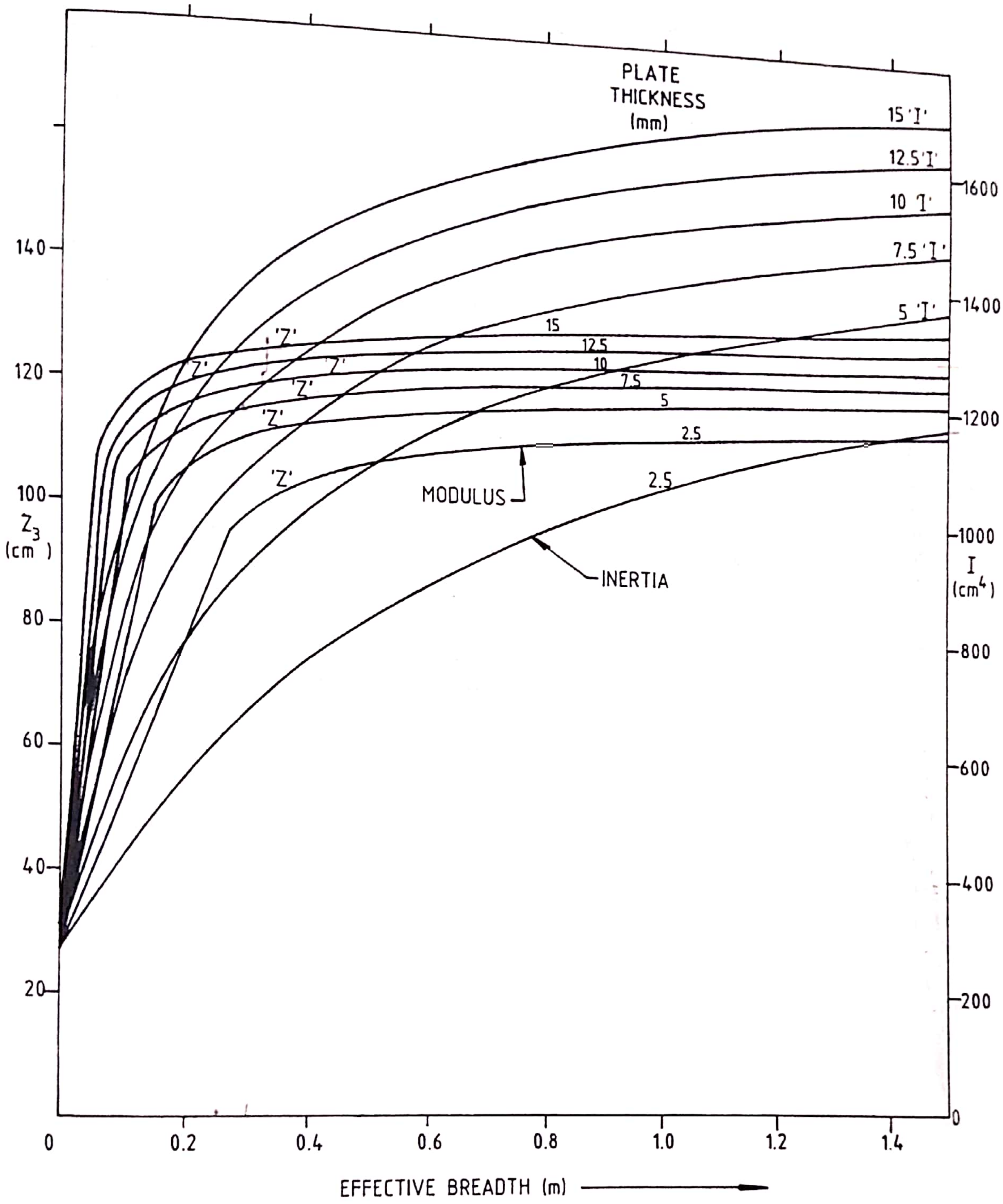

Figure 18.32 Properties of Tee Bar Stiffeners 63.5 × 127.0 (Type 3)

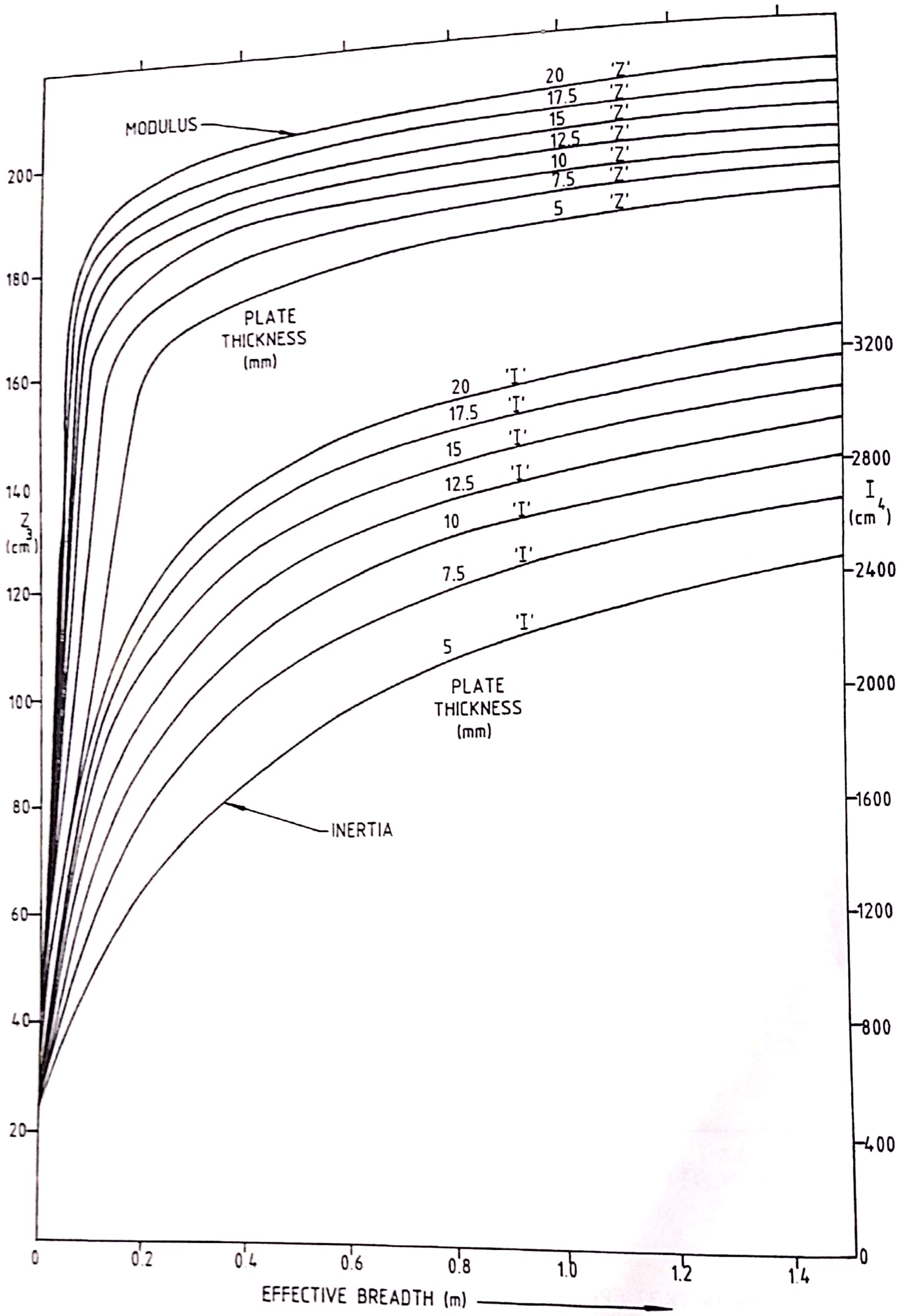

Figure 18.33 Properties of Tee Bar Stiffeners 76.2 × 152.4mm (Type 4)

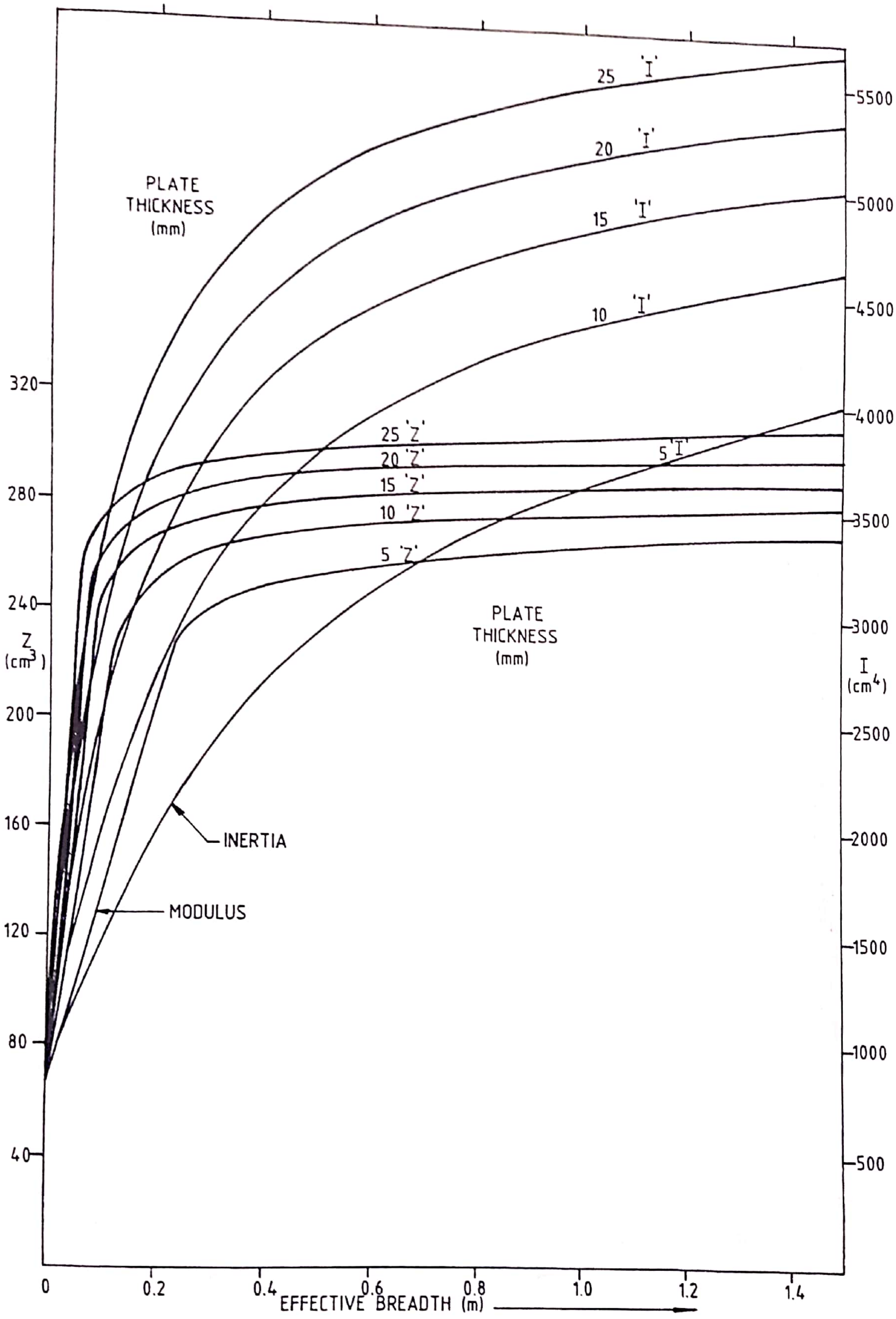

Figure 18.34 Properties of Tee Bar Stiffeners 88.9 × 177.8mm (Type 5)

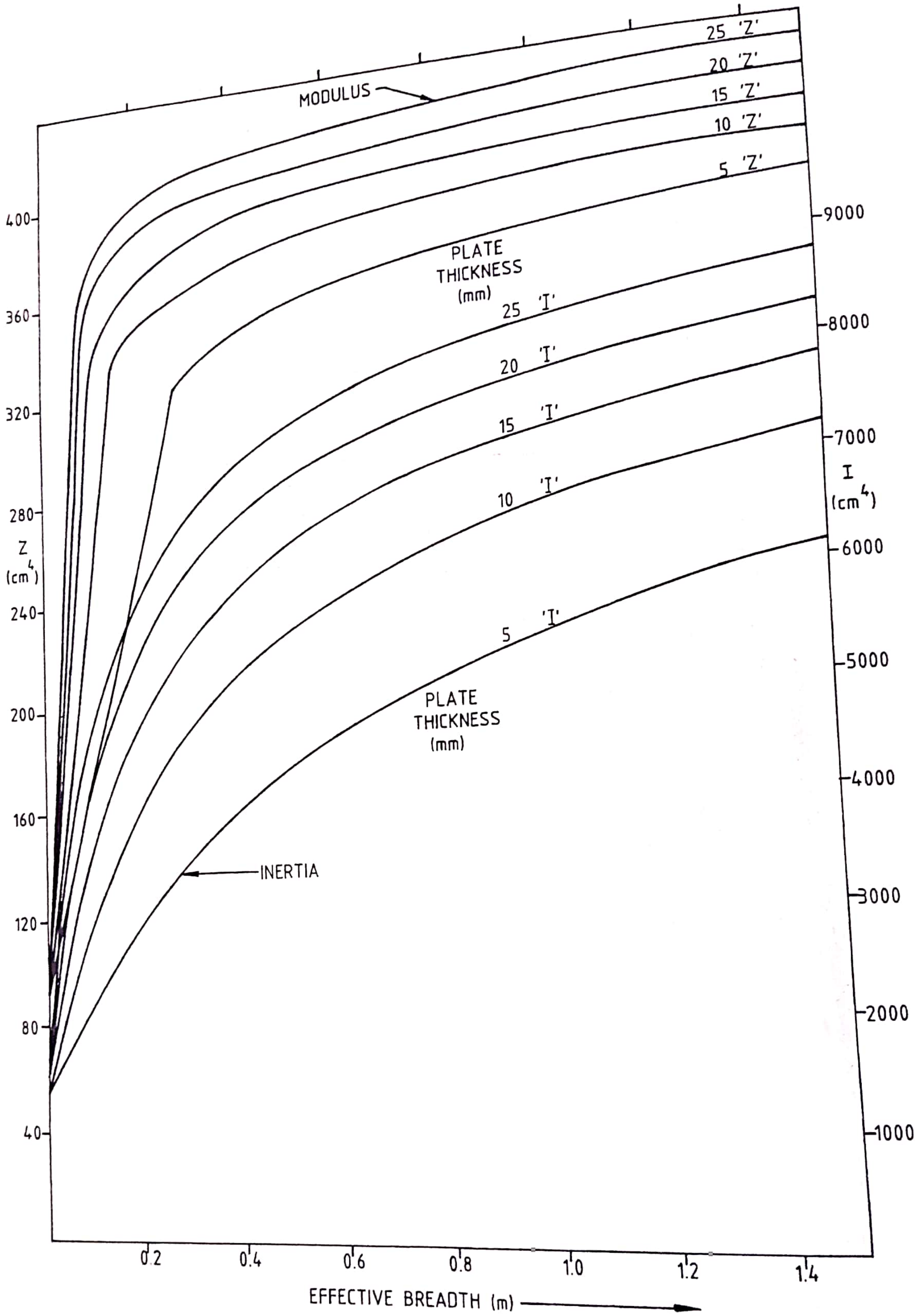

Figure 18.35 Properties of Tee Bar Stiffeners 101.6 × 203.2 (Type 6)

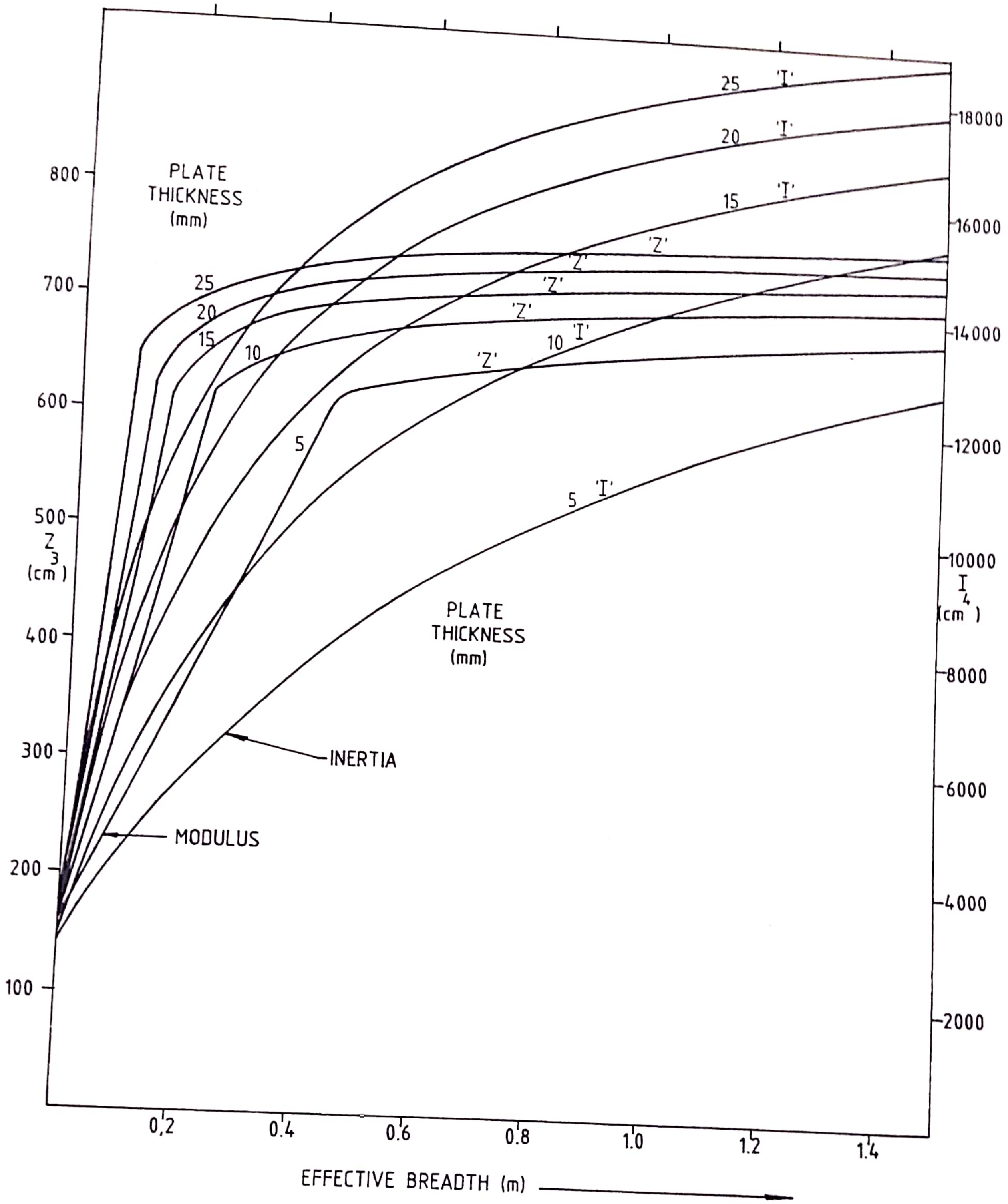

Figure 18.36 Properties of Tee Bar Stiffeners 127 × 254 (Type 7)

Buckling of Flat Plates in Shear

29 *Figures 18.37* and *18.38* are derived from ESDU data sheet 71005 (1976) with minor changes in nomenclature. *Figure 18.37* gives the critical shear buckling coefficient χ in equation 18.7 (which is the same as equation 7.11) for different boundary conditions and aspect ratios.

$$\tau_c = \chi E(t/b)^2 \qquad (18.7)$$

30 The critical buckling stress τ_c must, however, be reduced by a plasticity reduction factor to allow for the proximity of the critical stress to the yield stress. This factor (η_c) is given in *Figure 18.38* plotted against a ratio τ_c/σ_n for different values of m, where σ_n is the stress in the material at which the tangent modulus is a half of the Young's modulus, and m is a characteristic of the material. For all surface ship structural steels it may be assumed that σ_n is the same as σ_y and m is infinite. For structural aluminium referenced in Chapter 5, σ_n can be taken as 90% of the 0.2% proof stress with m = 15, and for ship structural fibre reinforced plastic (FRP) σ_n is equal to the tensile strength of the material with m again being infinite. For all other materials reference should be made to DEF STAN 00-932 and ESDU data sheet 76016 (1976).

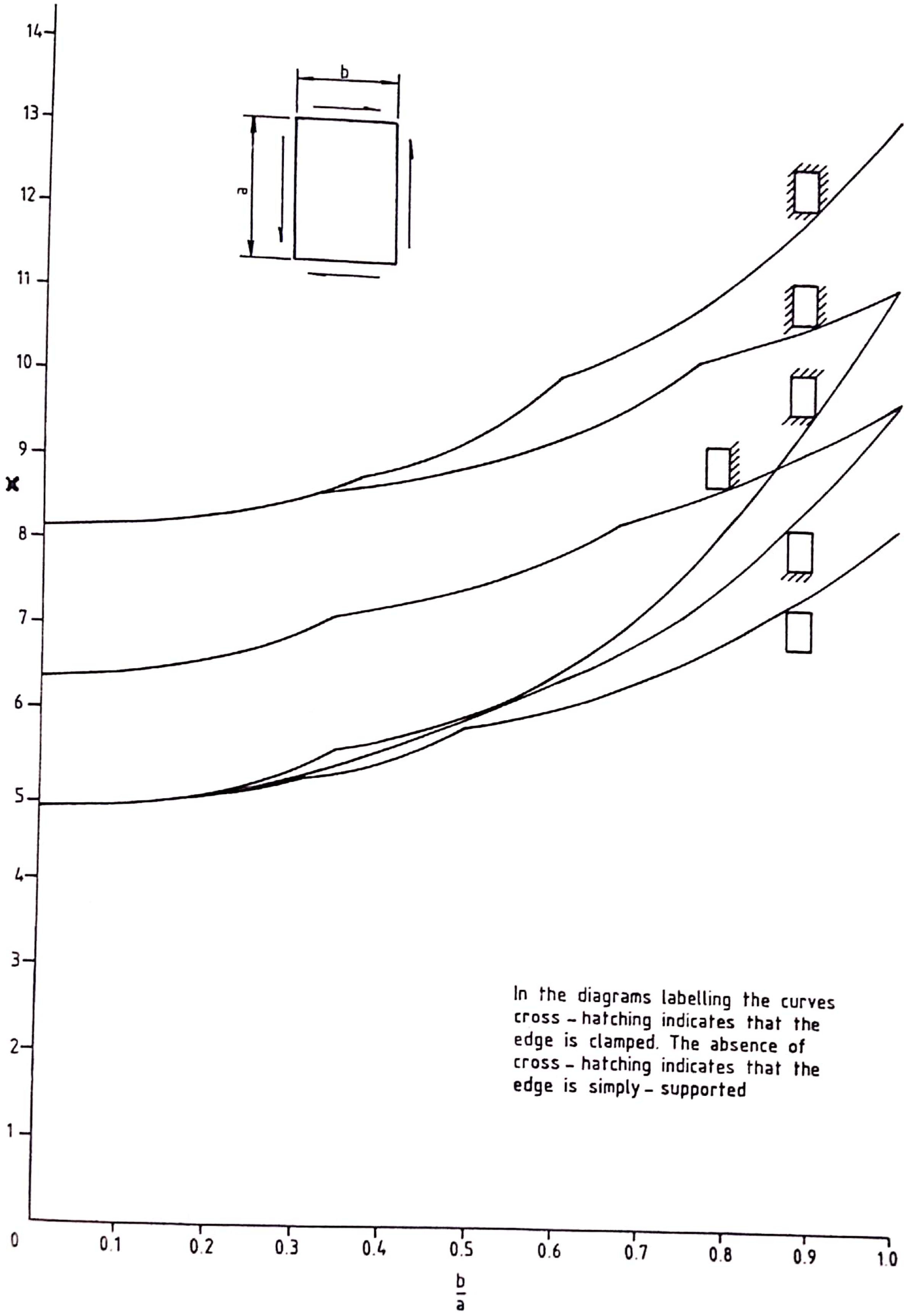

In the diagrams labelling the curves cross – hatching indicates that the edge is clamped. The absence of cross – hatching indicates that the edge is simply – supported

Figure 18.37 Critical Elastic Shear Buckling

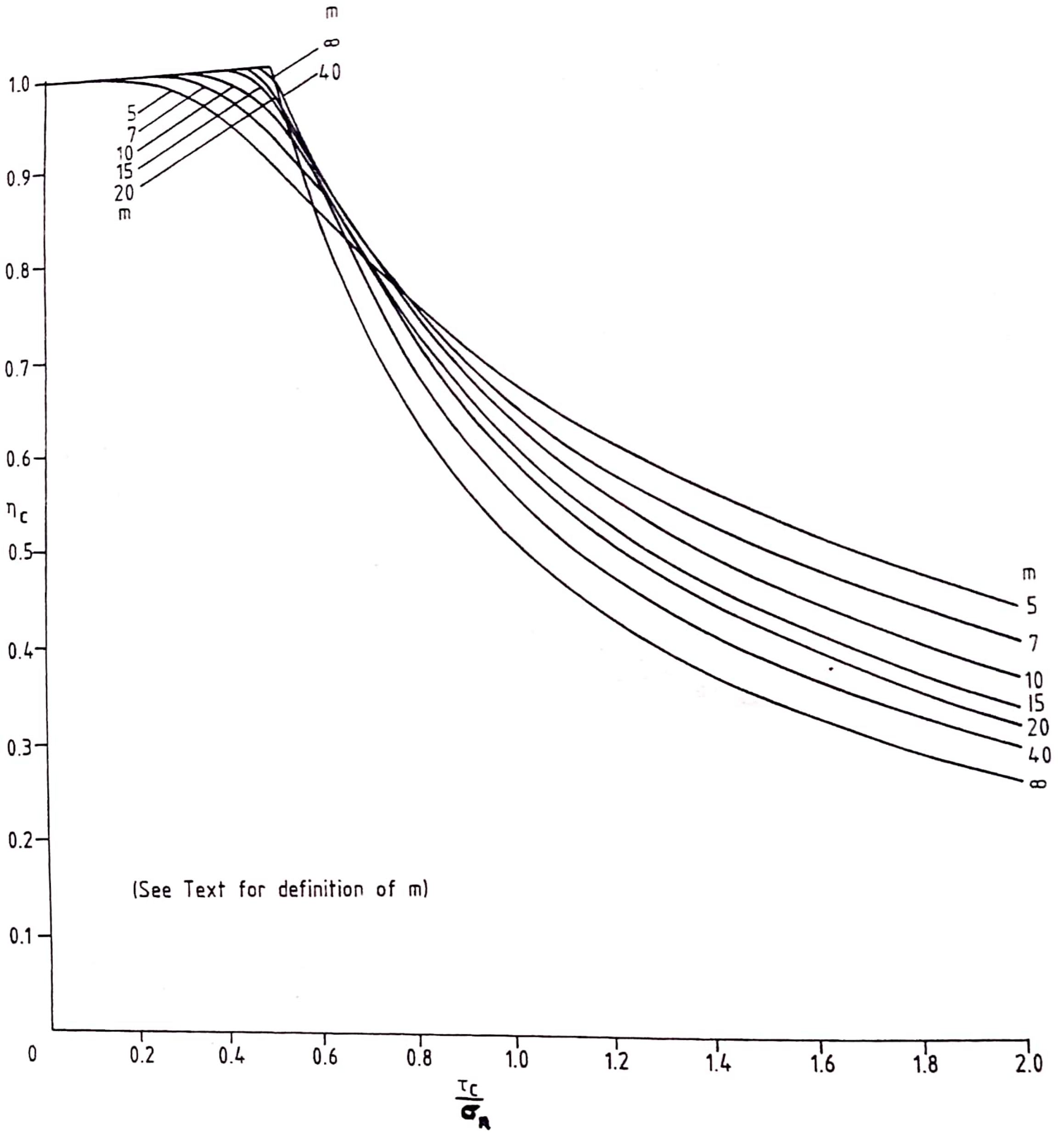

Figure 18.38 Plasticity Reduction Factor for Shear Buckling

Buckling in Shear of Long, Flat Panels with Transverse Stiffeners

31 *Figures 18.39* and *18.40* are derived from ESDU data sheet 02.03.02 (1983) with minor changes in nomenclature. They give the coefficient K for the critical shear buckling stress τ_{sc} in equation 18.8 (the same equation as 7.12) for long edges clamped and simply supported respectively against a stiffness parameter μ given by equation 18.8a, for different values of aspect ration a/b.

(18.8) $$\tau_{sc} = KE_p\,(t/b)^2$$

(18.8a) $$\mu = \sqrt{(E_{st}I_{st}b/E_p a^2 t^3)}$$

where a and b	are shown on the figures
t	is the plate thickness
E_p	is the Young's modulus of the plate
E_{st}	is the Young's modulus of the stiffeners
I_{st}	is the second moment of area of the stiffener about its point of attachment to the plate.

32 The value of μ_c shown on the curves as a dotted line is the point at which the stiffeners provide a pinned edge condition to the plate panel between stiffeners and beyond which K does not change. Note that the curves are drawn for a Poisson's ratio of 0.3 and for open section stiffeners with negligible torsional stiffness. For other stiffeners or conditions reference should be made to ESDU data sheet 02.03.02 (1983).

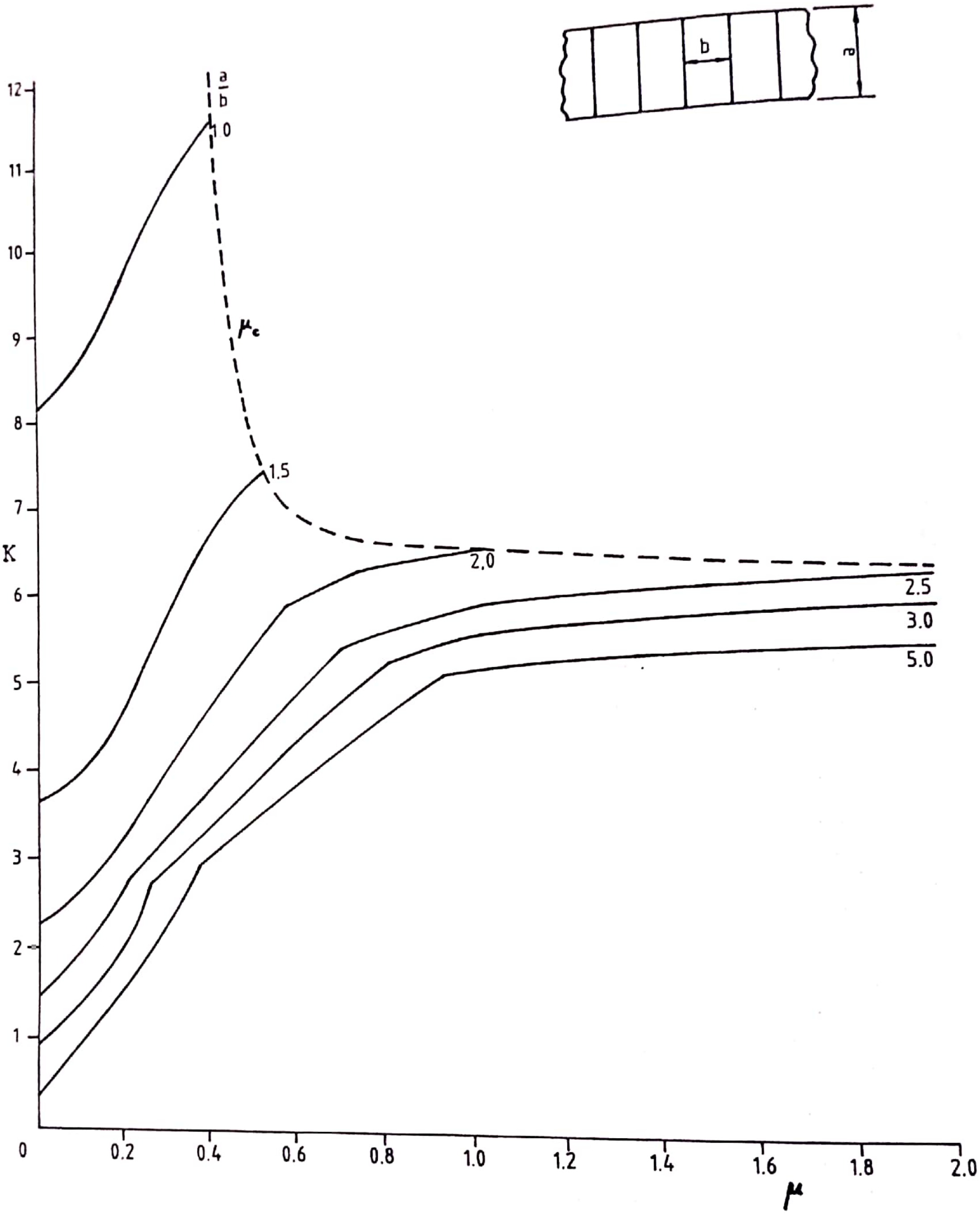

Figure 18.39 Longitudinal Edges Clamped No Torsional Stiffness

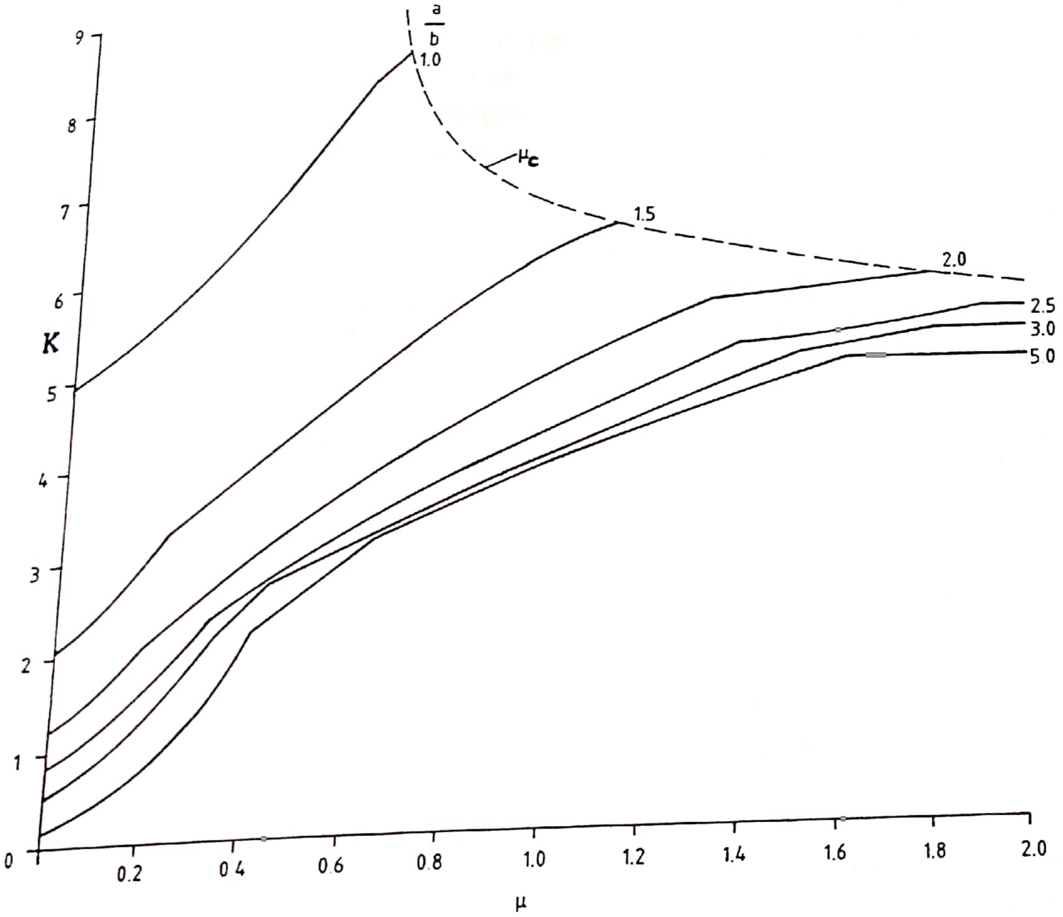

Figure 18.40 Longitudinal Edges Simply - Supported No Torsional Stiffness

Estimation of Superstructure Efficiency

33 *The following method for estimation of superstructure efficiency η_{ss} is based on the theory of Caldwell (1957) and as developed later by Lloyd's Register of Shipping but not now openly published. Nomenclature is as follows:*

d_{na} is the distance of the neutral axis of the superstructure material above the upper deck
D_{na} is the distance of the neutral axis of the hull structure (excluding the superstructure) below the upper deck

Note that both of these parameters are defined in *Figure 8.3*

A_s is the area of effective longitudinal material in the lowest tier of the superstructure
A_h is the area of effective longitudinal material in the hull at the same section
L_s is twice the distance from the section in question to the nearest end of the superstructure
B_s is the breadth of the superstructure
d_s is the height of the superstructure
t_s is the thickness of the superstructure side plating
E_{ss} is the Young's modulus of the superstructure material
E is the Young's modulus of the hull material.

34 The procedure starts with the calculation of the flexibility factor ψ from equation 8.4 or 18.9 which includes constants K and C depending respectively on the number of supporting bulkheads and the breadth of the superstructure in relation to the upper deck breadth. These constants are defined in Chapter 8, *Figure 8.4* and *Table 8.2*.

$$\psi = 1.2 \times 10^4 KC^2 (t_s E_{ss}/d_s E) \qquad (18.9)$$

Figure 18.41 is then entered with the value of ψ and the ratio L_s/d_s to obtain an initial estimate of efficiency η_{so} assuming standard values of the ratios B_s/d_s of 5.0, d_{na}/D_{na} of 0.35 and A_sE_{ss}/A_hE of 0.1.

35 *Figure 18.42* is then entered with $B_s/d_s = 5.0$ and the value of η_{so} from *Figure 18.41* and a line is followed parallel to the curves on the figure to a point where B_s/d_s is the true value; a new estimate of efficiency η_{s1} is then read off from that point. An example is shown on *Figure 18.42* for $B_s/d_s = 6.44$.

36 The same process is then followed on *Figure 18.43* using η_{s1} and $d_{na}/D_{na} = 0.35$ to obtain η_{s2} for the true value of d_{na}/D_{na}, and on *Figure 18.44* using η_{s2} and $A_sE_{ss}/A_hE = 0.1$ to obtain the final estimate of superstructure efficiency η_{ss} at the true value of A_sE_{ss}/A_hE. Examples are given on both these figures for $d_{na}/D_{na} = 0.338$ and for $A_sE_{ss}/A_hE = 0.203$ respectively.

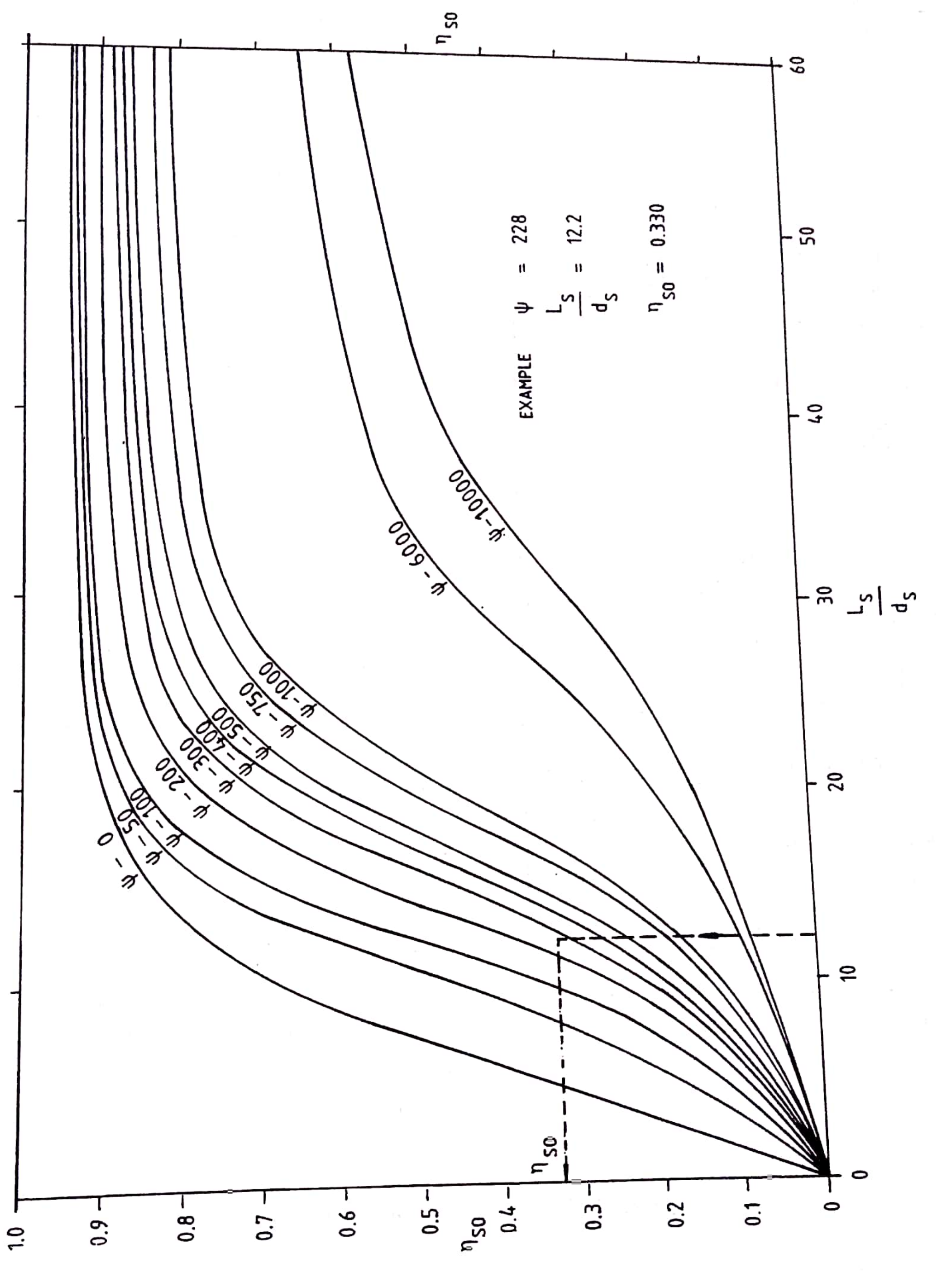

Figure 18.41 η_{SO} Value for L_S/d_S

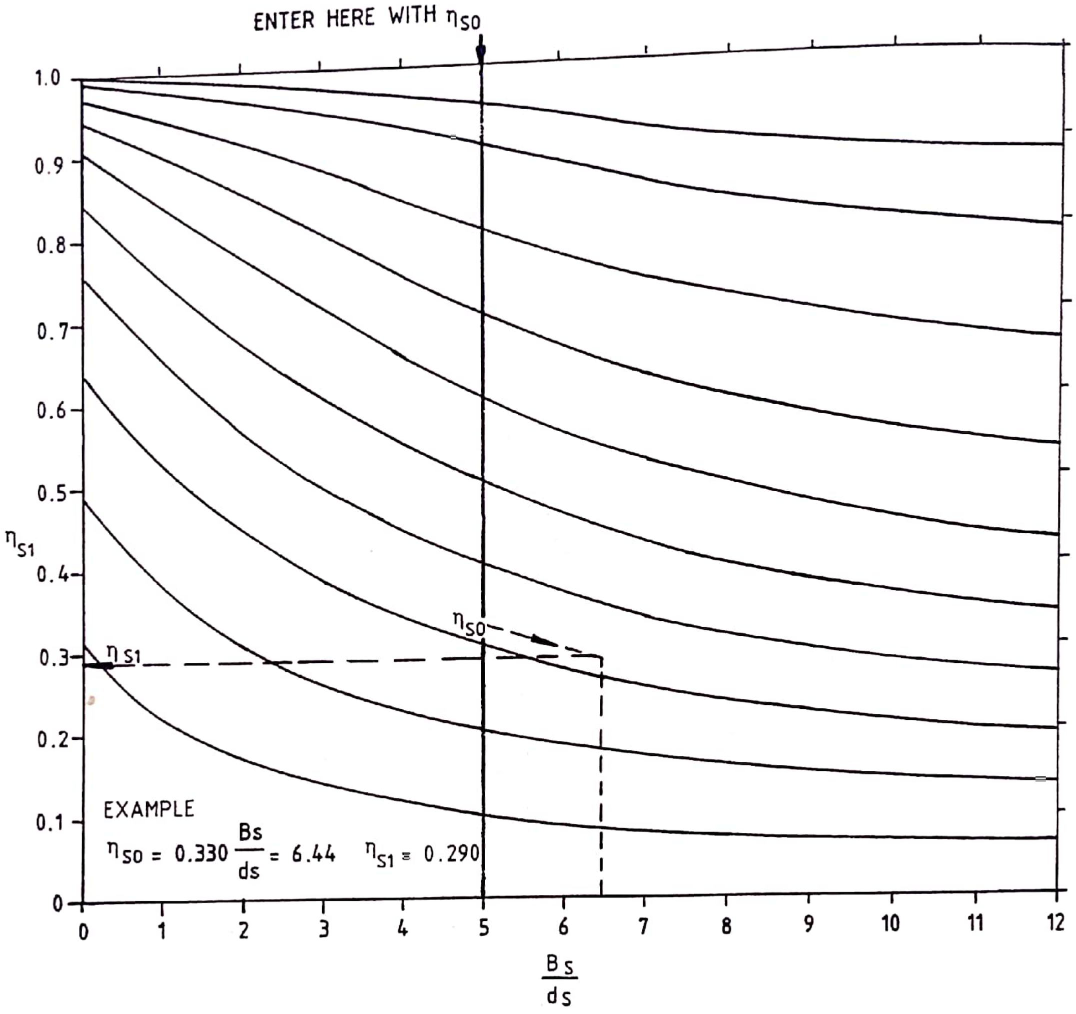

Figure 18.42 η_{S1} for Values of B_S/d_S

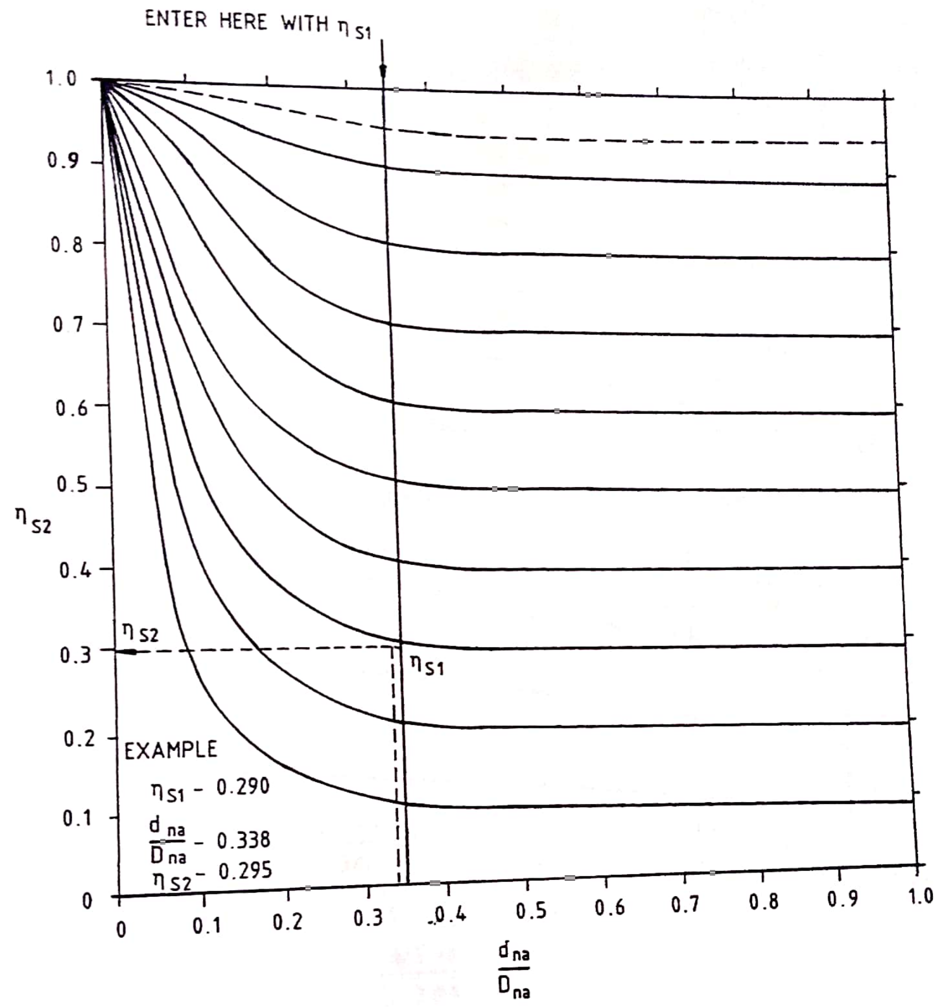

Figure 18.43 η_{S2} Values for d_{na}/D_{na}

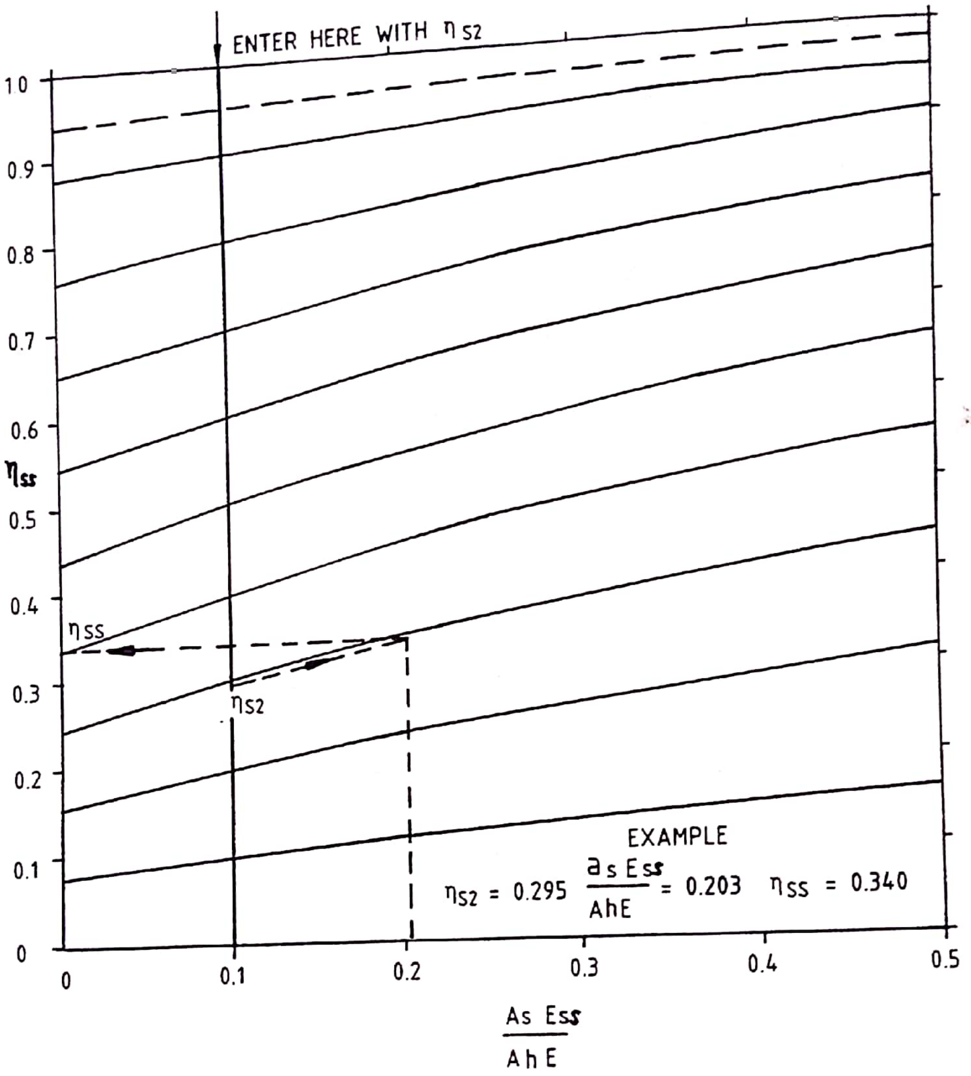

Figure 18.44 η_{ss} Values for As Ess/Ah E

Large Deflections of Rectangular Plates

37 These are four sets of curves providing estimates of large elastic and plastic deformations of rectangular plates and are mainly self explanatory. The first, *Figure 18.45*, provides stresses and deflections for large **elastic** deformations under lateral pressure with edges fully clamped: the nomenclature is given on the figure. The curves are derived from details in Timoshenko 'Theory of Plates and Shells' where information is given on how to compute equivalent values for plates with pinned edges or edges free to pull in, but the computations for these conditions are very complex.

38 *Figure 18.46* provides design pressures to cause particular values of **permanent central deflection** δ_p given by the deflection parameter of 0.1 or 0.2 equal to $(\delta_p/b)\sqrt{(E/\sigma_y)}$ for values of plate slenderness ratio ß $(=(b/t)\sqrt{(\sigma_y/E)})$. Also given are the values of pressure to cause initial yielding of the plate. The curves are valid for aspect ratios greater than 2.0 and for all edges clamped and are based on the theory of Clarkson (1956).

39 *Figure 18.47* is based on the same theory but provides the deflections under lateral pressure and consequent permanent set for clamped plates of different aspect ratios and plate slenderness. The governing criterion in this case is the pressure to cause a centre line plastic hinge for ß < 2.5 and membrane tension equal to $\frac{2}{3}\sigma_y$ for higher values of ß.

40 *Figure 18.48* is similar to *Figure 18.46* but allows **plate edges free to pull in** and is drawn for deflection parameter values of 0.2, 0.4 and 0.6. The curves are strictly for plates of aspect ratio 3.0 but in practice can be used for any long plate. These curves are based on the theory of Clarkson (1960).

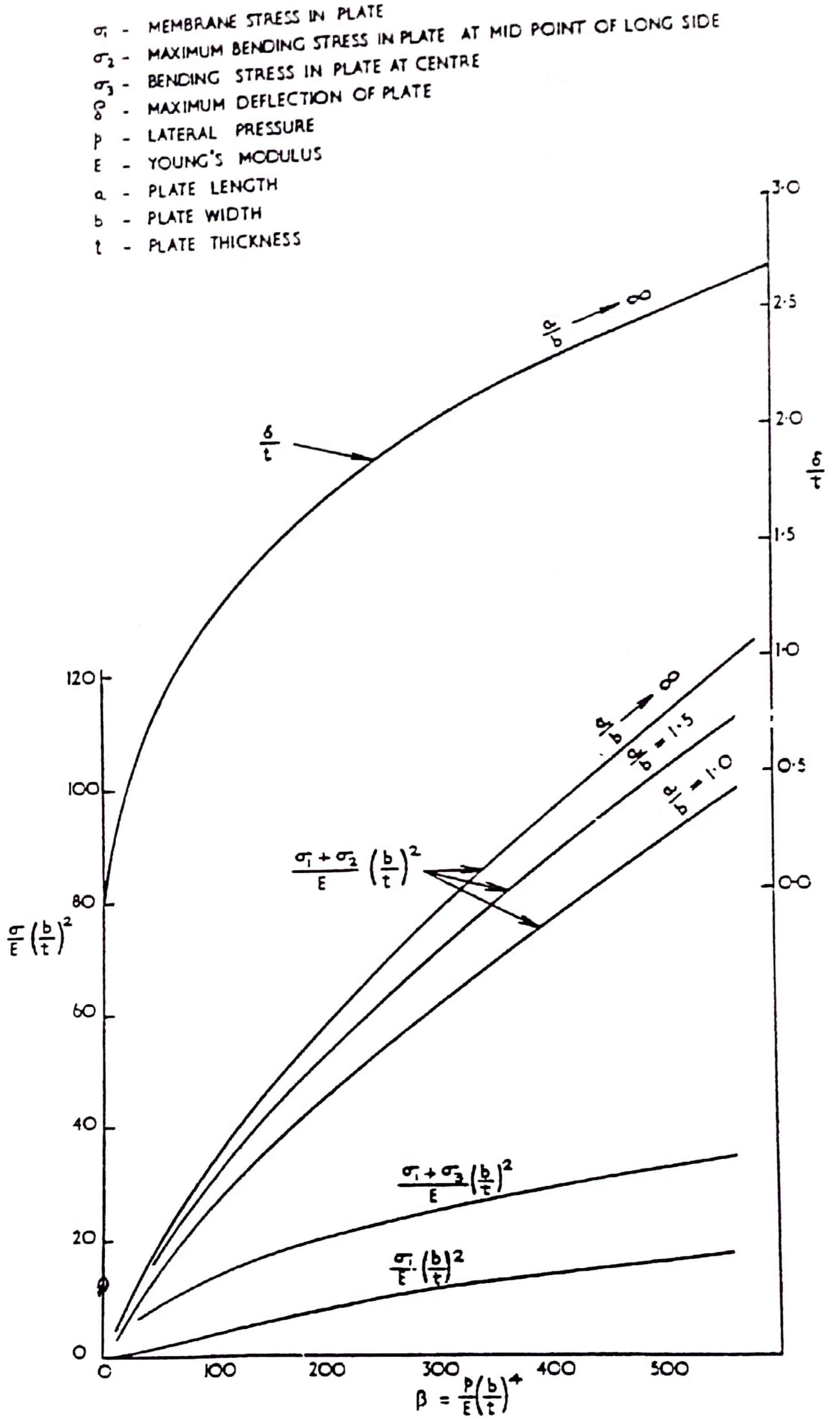

Figure 18.45 Bending of Rectangular Plates under Lateral Pressure Clamped Edges - Not Free to Approach

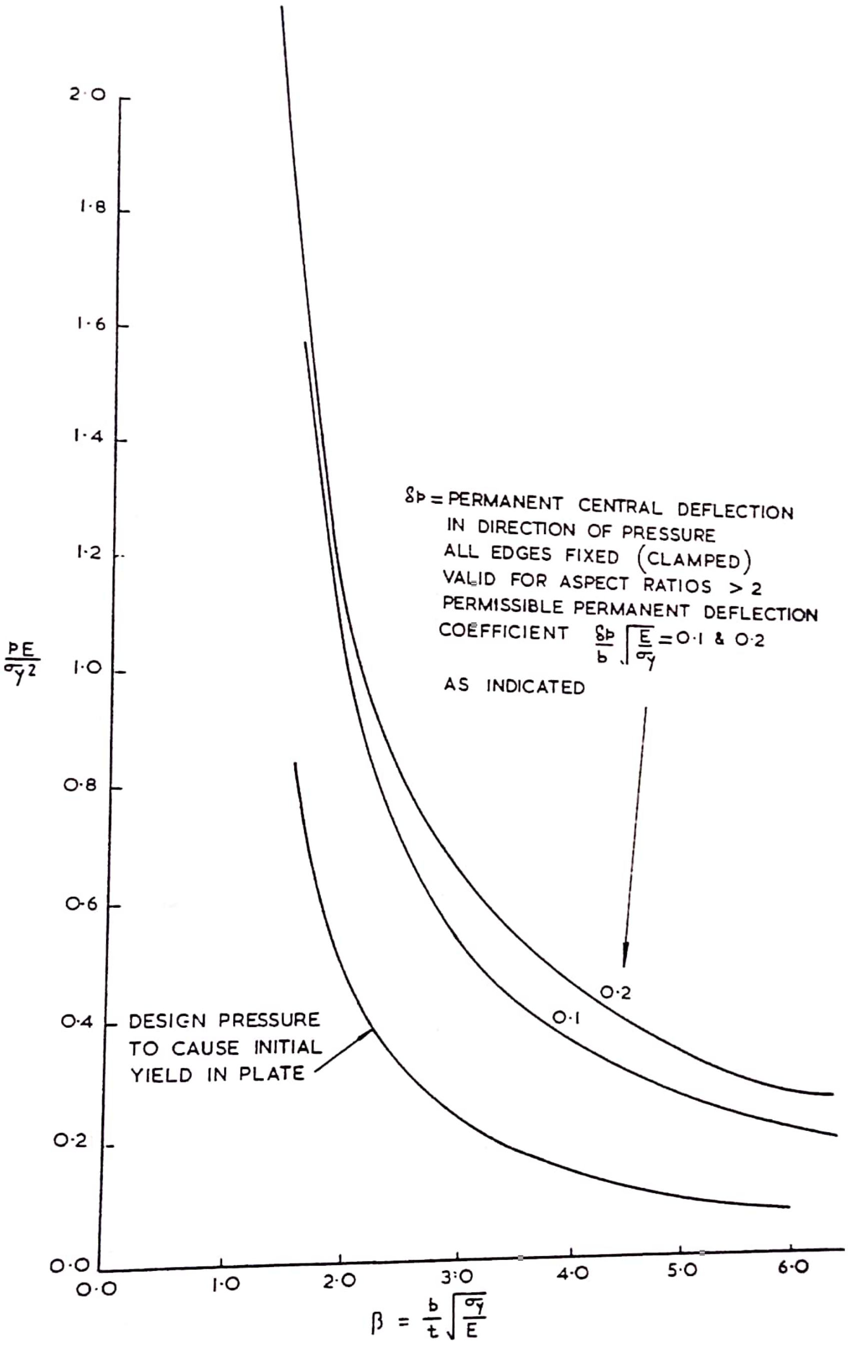

Figure 18.46 Design Pressures for Permanent Deflection Coefficient

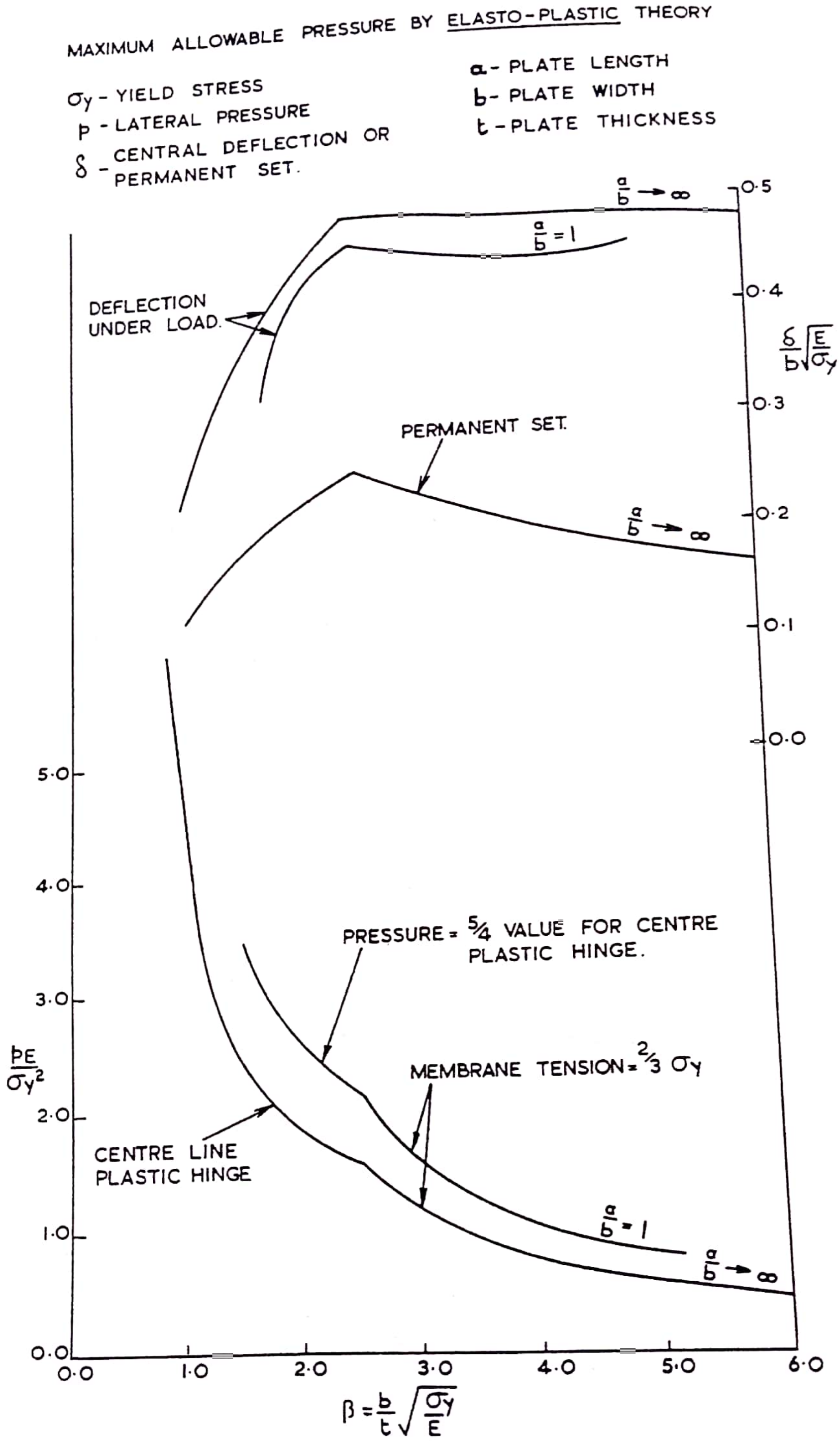

Figure 18.47 Bending of Rectangular Plates under Lateral Pressure with Clamped Edges

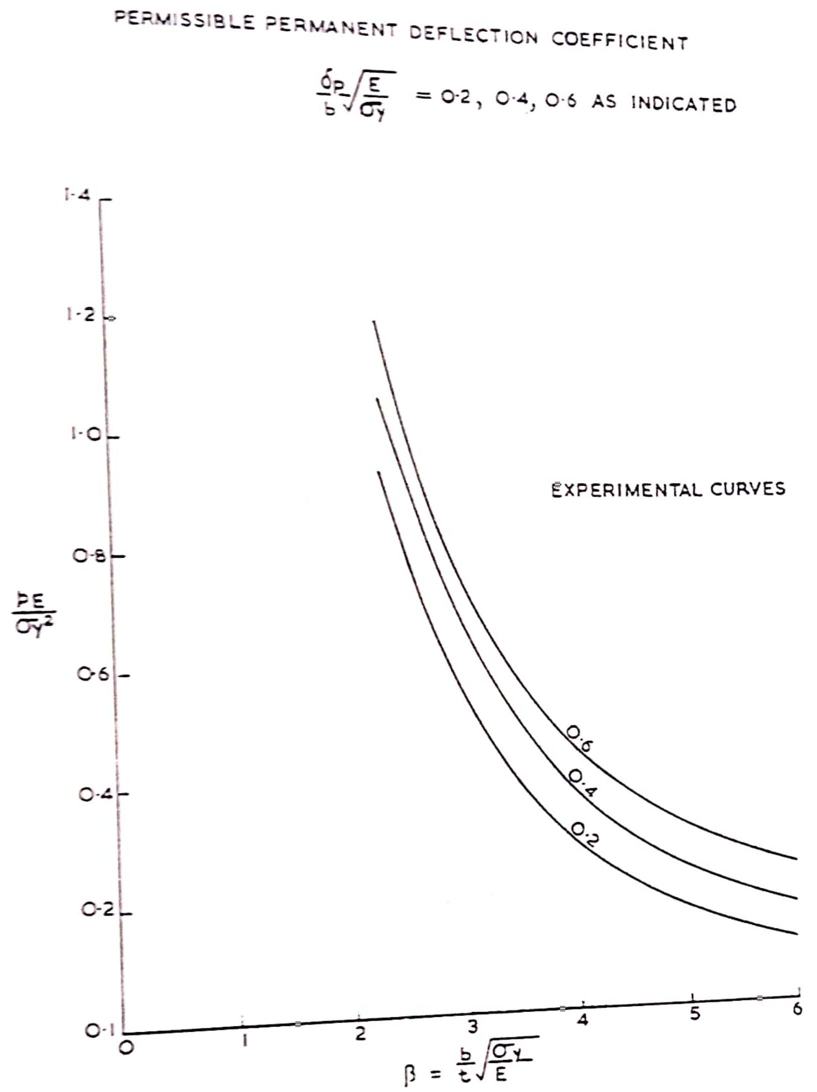

Figure 18.48 Design Curves for Flat Plates (Aspect Ratio 3·0) Edges Free to Pull-In

Effective Breadths of Plating

41 The three *Figures 18.49* to *18.51* are known as 'Schade's Curves' and are based on theory in Schade (1951 and 1953) and give effective breadth of plating acting with stiffeners under lateral loads of various types. They were originally defined for web stiffened structures such as may be found in merchant ships but are accurate enough for warship style structures. The curves are generally self explanatory, the first set giving effective breadth for a single stiffener, the second for a pair of stiffeners forming a box beam type of structure and the third is for multiple stiffeners. The nomenclature is given on the figures, but note that the parameter ß is *not* plate slenderness ratio but a parameter relating plate area to stiffener area. When using these curves the flange of a Tee bar or angle stiffener should be ignored.

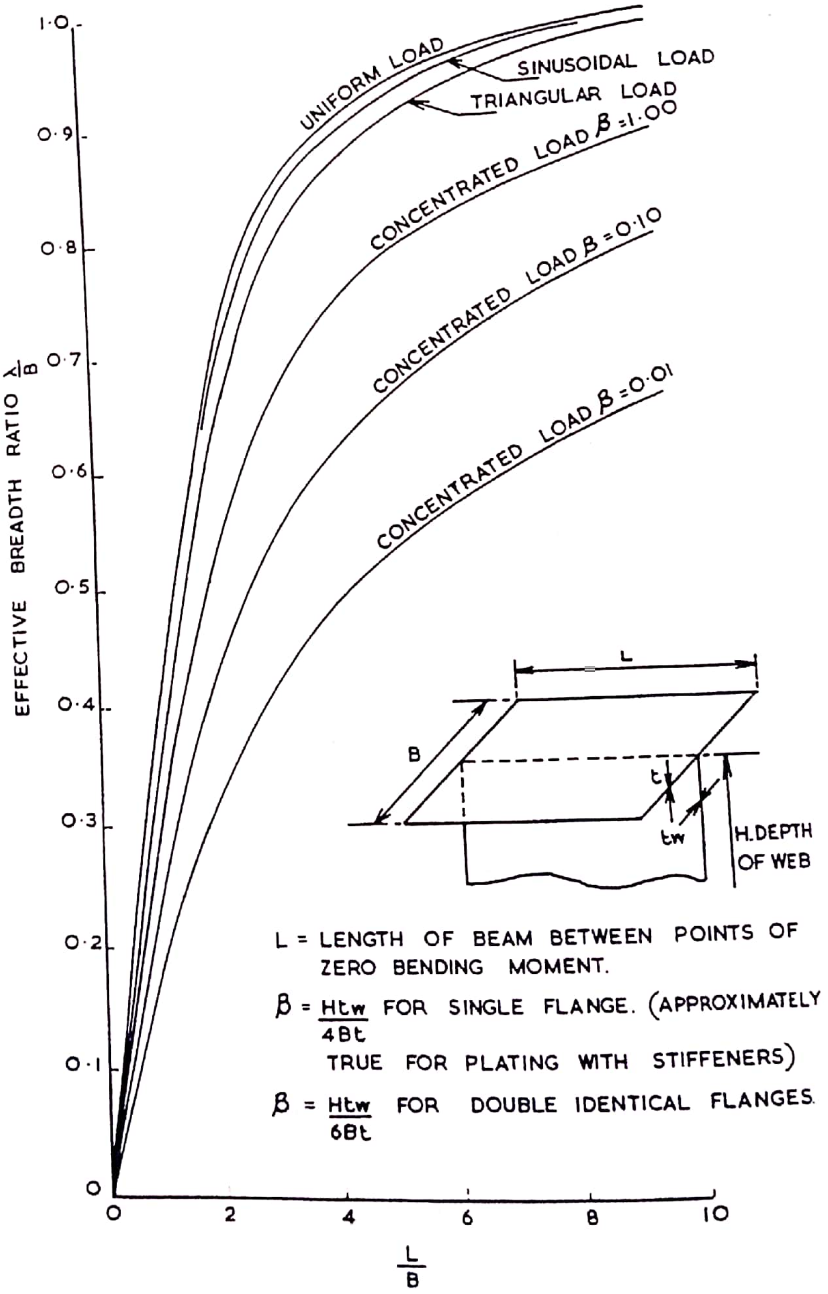

Figure 18.49 Effective Breadth of Plate - Single Web Symmetrical Flange Free Sides

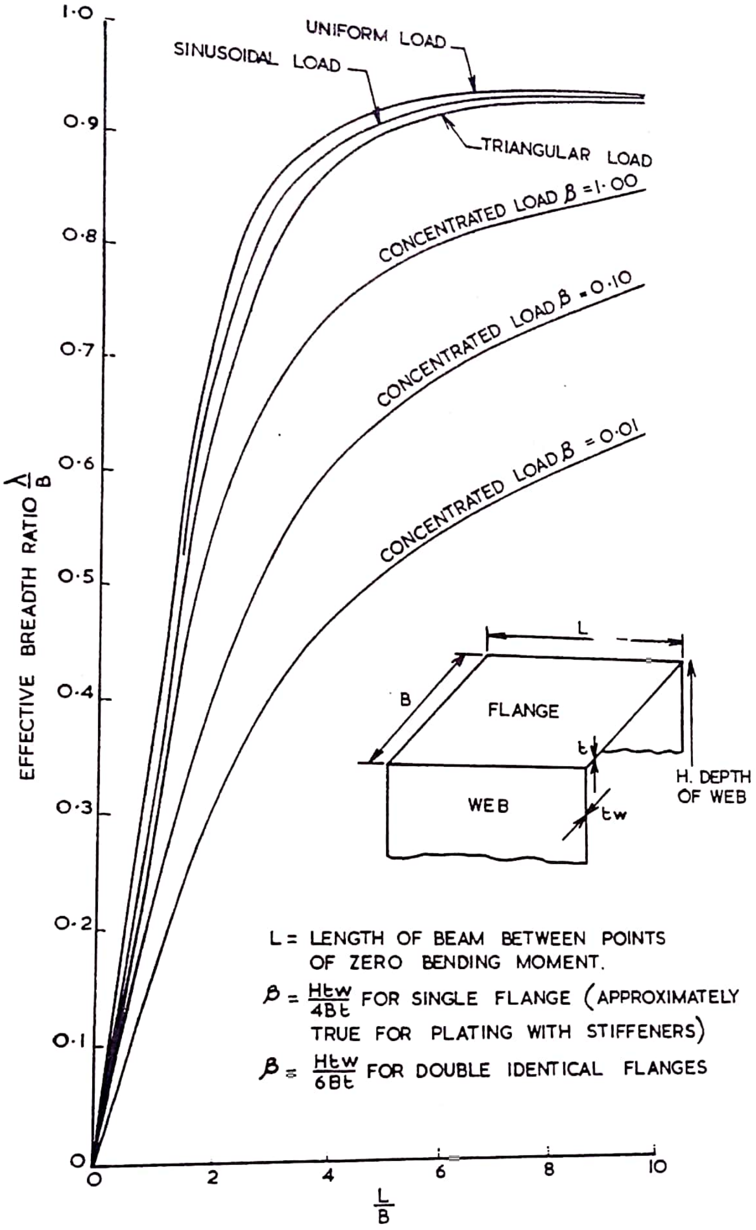

Figure 18.50 Effective Breadth of Plate Double Web, Flange Bonded by Webs

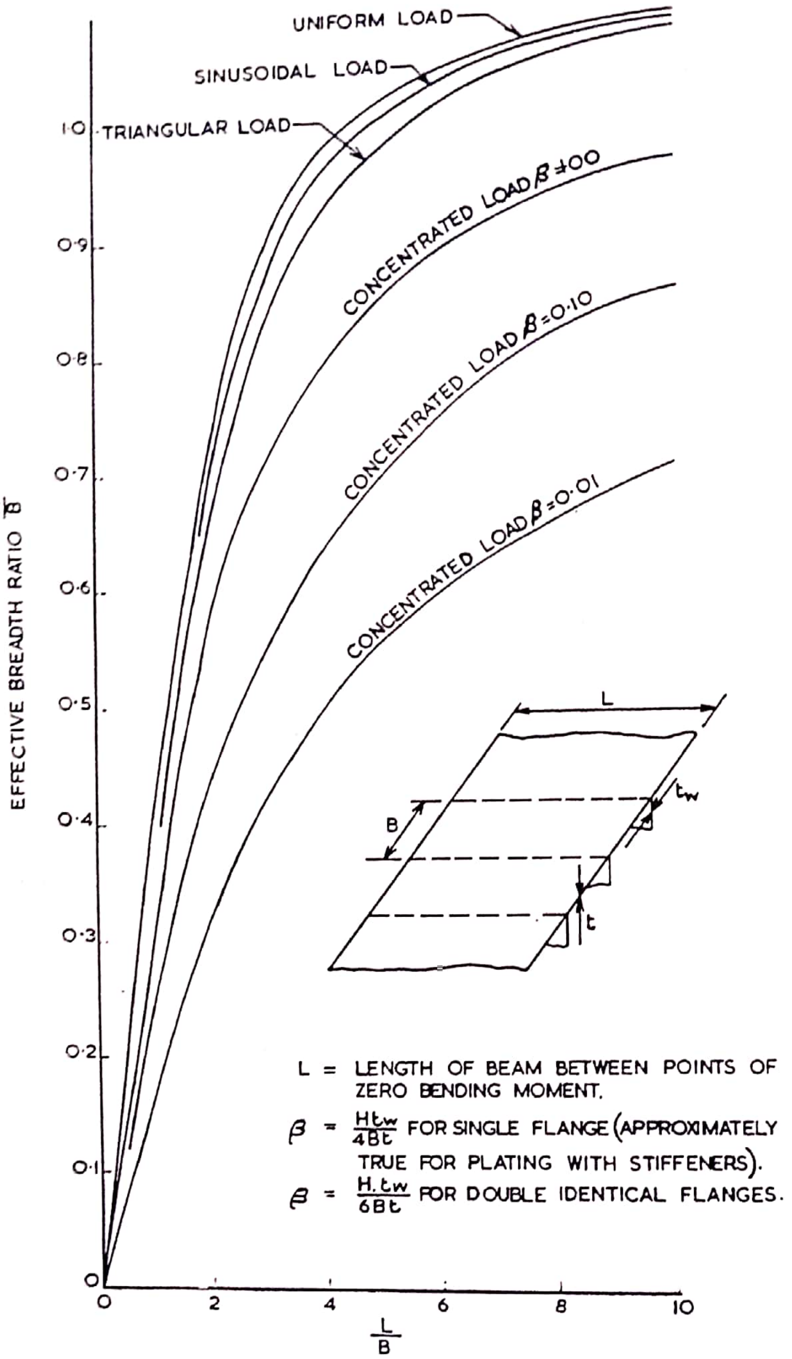

Figure 18.51 Effective Breadth of Plate Multiple Webs

Deflections and Bending Moments of Flat Grillages Under Uniform Pressure

42 These curves are taken from Clarkson (1965) with minor changes in nomenclature and they allow the estimation of deflections and bending moments in flat grillages for various edge conditions and different numbers of stiffeners in each direction. The geometry is given in *Figure 18.52* and the nomenclature is as follows:

A	is the breadth of the grillage across the ‘S’ stiffeners (that is the length of the ‘R’ stiffeners)
B	is the length of the grillage across the ‘R’ stiffeners (that is the length of the ‘S’ stiffeners)
r	is the number of R stiffeners of length A
s	is the number of S stiffeners of length B

Note that always $r \geq s$ and data is given specifically for odd values of r and s

i	is the position of stiffener intersections numbered from 0 inwards from the *edge* of the grillage (the first intersection is therefore at i - 1)
a	is the spacing of the S stiffeners = $A/(s + 1)$
b	is the spacing of the R stiffeners = $B/(r + 1)$
I_r	is the second moment of area of an R stiffener with effective breadth of plating equal to b/2
I_s	is the second moment of area of an S stiffener with effective breadth of plating a/2
K_a	is the edge clamping coefficient for the R stiffeners
K_b	is the edge clamping coefficient for the S stiffeners

Note that K = 0 indicates pinned edges and K = 1 indicates clamped edges

ζ	$= b^3I_r/a^3I_s$
ε	$= (r + 1)\zeta$
μ	$= \varepsilon/(s + 1)$
p	is the uniform pressure on the grillage
Q_r, Q_s	are the loads per unit length on the R and S stiffeners respectively arising from pressure on the adjacent plate
δ	is the central deflection
M_r, M_s	are the maximum bending moments in the R and S stiffeners respectively, for the loading considered as an equivalent point load at each stiffener intersection, that is, neglecting bending between intersections

Note that a positive bending moment indicates deflection *towards* the loaded side of the grillage.

43 The data in the figures are based on elastic analysis of unplated grillages under loads normal to the surface, and the effect of edge loads in the plane of the grillage is ignored. The results are applicable to single plated grillages provided that an effective breadth of plating equal to half the stiffener spacing is assumed to act with the stiffeners.

44 Data for calculating deflections and bending moments have been worked out for opposite pairs of edges either simply supported (K = 0) or clamped (K = 1). For grillages under uniform pressure which are continuous over bulkheads and joined to similar grillages, the edges should be assumed to be clamped due to the symmetry of loading. In other cases where the edge constraint arises from the rotational stiffness of adjoining structure, it is likely that simply supported edge conditions will be more appropriate. Where adequate information on edge restraint is available then interpolation between the two given conditions is permissible.

45 The stiffeners of each directional set are assumed to be of similar scantlings and evenly spaced, but they may differ in size, spacing and edge constraint from the other set. Stiffeners in the more numerous set are designated the R stiffeners and grillages with 1, 3, 5, 7, 9 and 15 stiffeners in either direction are specifically included. Results for other numbers of stiffeners may be found by careful interpolation ensuring that bending moments apply to equivalent places in the grillage.

Calculation of Maximum Deflections

46 The central deflection of grillages under uniform pressure may be found from *Figures 18.53* or *18.54*, whichever is appropriate for the edge conditions of the R stiffeners. In these figures the full line gives the central deflection for grillages with numerous stiffeners in each set; where there are only one or three S stiffeners the chain dotted lines apply and these are labelled with the appropriate stiffener configuration r × s. A correction has to be applied to r × 1 grillages with $K_a = 0$ by multiplying the calculated deflection by $\{1.25 - 0.125\ (b/a)\}$ if $a/b \geq 1$ and by $\{1.0 + 0.125\ (a/b)\}$ for $a/b \leq 1$. This correction allows for the additional effective loading which falls onto the central stiffener for this particular range of grillages. For all configurations it is possible that there may be a slightly larger deflection away from the centre due to deformation between stiffener intersections but this effect is not included.

Note that all the figures are plotted to a base of ε *or* μ *as indicates on the axes.*

Calculation of Maximum Bending Moments

47 The data curves have been calculated with the uniform pressure load considered as an equivalent concentrated load of magnitude (p.a.b) applied at each stiffener intersection, and this is usually sufficiently accurate for design purposes. An exception arises when the two sets of stiffeners have markedly different stiffnesses, in which case the bending moments in the less stiff set of stiffeners may be significantly affected by local bending between the comparatively rigid support from the stiffer members at the intersections, and it is necessary to calculate a term additional to the result from the data sheet. The local bending term is usually important for the R stiffeners where ζ is less than 0.2 and for the S stiffeners when ζ is greater than 5.0, but it may be wise to check the magnitude of the correction even when the value of ζ is outside those ranges.

48 The additional term is calculated by considering the pressure on each panel to be divided between the four portions of the bounding stiffeners and the following empirical rule gives the loading per unit length:

(18.10a) For $a/b \geq 1.5$ $\quad Q_r = pb$

(18.10b) For $1.5 > a/b \geq 1.0$ $\quad Q_r = pb\ \{0.625 + 0.75\ (a/b - 1)\}$

(18.10c) For $a/b < 1.0$ $\quad Q_r = 0.625\ pa$

(18.11a)	For $a/b \geq 1.0$	$Q_s = 0.625\ pb$
(18.11b)	For $1.0 > a/b \geq 0.667$	$Q_s = pa\ \{0.625 + 0.75\ (a/b - 1)\}$
(18.11c)	For $a/b < 0.667$	$Q_s = pa$

The bending moment in the individual stiffener is calculated for the appropriate loading from equations 18.10 or 18.11 assuming that the intersections do not deflect. The local bending moment diagrams for simply supported edges and for clamped edges are given in *Figure 18.55(b)* and *18.56(b)* respectively. This local bending moment is then added to the data sheet value (*Figures 18.55(a)* and *18.56(a)*) to give the total bending moment on the stiffener (*Figures 18.55(c)* and *18.56(c)*).

Bending Moments in Simply Supported Stiffeners

49 For the case of the R stiffeners simply supported ($K_a = 0$) the maximum bending moment M_r in the R stiffeners is found from *Figures 18.57, 18.61, 18.65* or *18.69* depending on the number of the S stiffeners. In these figures the full line gives the maximum grillage bending moment except where both sets contain three stiffeners or less in which case the chain dotted line gives the maximum grillage bending moment.

50 The figures also include dashed lines marked ‘C’ over the range where local bending of the R stiffeners between intersections may affect the maximum bending moment. The lines marked ‘C’ give the maximum bending moment occurring in the R stiffeners at the first intersection ($i = 1$) with an S stiffener. Where curve C coincides with the full or chain dotted lines the maximum bending moment occurs at $i = 1$ and its value is given by the full or chain dotted lines. Where no curve C is given, the grillage bending moment at $i = 1$ is given by the full or chain dotted lines throughout.

51 Towards the right hand end of the curves (ε or μ large) the R stiffeners are the stiffer set and the maximum bending moment in the R stiffeners is given directly by the appropriate full or chain dotted line. It occurs at the mid-length of a stiffener but not necessarily at the central one; as the number of R and S stiffeners and their stiffnesses become more unequal, the position of the maximum bending moment moves away from the central stiffener.

52 Towards the left hand end of the curves (ε or μ small) the R stiffeners are the less stiff set and local bending moments have to be added to the values obtained. The largest total bending moment may arise in one of the following three ways with the value of Q_r being obtained from equation 18.10:

a. At an intersection adjacent to the edge of the grillage ($i = 1$). The maximum grillage bending moment at $i = 1$ is obtained as described in paragraph 50. This bending moment, which is negative, is reduced in absolute magnitude by the effect of line distributed loading, hence the local bending moment of $+0.106\ Q_r a^2$ as shown in *Figure 18.55(b)* is to be added to give the total bending moment at $i = 1$.

b. At a position midway between the edges of the grillage and the first intersection ($i = ½$). The maximum grillage bending moment is equal to half the value at $i = 1$ given by

(a) and it is increased by the effect of the line distributed loading. The local bending moment $-0.072\ Q_ra^2$ is to be added as shown in *Figure 18.55(b)*.

c. At a stiffener intersection other than $i = 1$. The maximum grillage bending moment in the R stiffeners at any intersection other an $i = 1$ is given with sufficient accuracy by the appropriate full or chain dotted line as described in paragraph 50, but the moment thus obtained is to be reduced by the local bending term $+0.081\ Q_ra^2$ as shown in *Figure 18.55(b)*.

53 The largest total arising from a, b or c above is to be used for design calculations and the procedure is illustrated in *Figure 18.55 (a→b→c)*.

54 For grillages having simply supported R stiffeners of only two spans ($r \times 1$ with $K_a = 0$) regardless of the other boundary conditions the bending moments have to be multiplied by the same factors that are applied to deflections in paragraph 46.

55 The procedure for calculating the maximum bending moment in the S stiffeners when they are simply supported mirrors that described in paragraphs 49 to 53 except that *Figures 18.58, 18.62, 18.66* or *18.70* are used and the chain dotted lines generally apply for five or less stiffeners. The corrections discussed in paragraph 52 are the same except that the term Q_sb^2 must be substituted for Q_ra^2, with Q_s being obtained from equation 18.11.

Bending Moments in Clamped Stiffeners

56 For calculating the maximum bending moment in stiffeners with clamped ends *Figures 18.59, 18.63, 18.67* or *18.71* are used for the R stiffeners and *Figures 18.60, 18.64, 18.68* or *18.72* are used for the S stiffeners. The maximum bending moment is obtained from the appropriate full or chain dotted line depending on the configuration of stiffeners; it always occurs at the edge of the grillage but not necessarily in the central stiffener. As the number and stiffnesses of the two sets of stiffeners becomes more unequal the position of the maximum bending moment in the stiffer set moves away from the central member.

57 The effect of local bending due to the loading described in equations 18.10 and 18.11 is allowed for by adding the local term $Q_ra^2/12$ to the moments in the R stiffeners or $Q_sb^2/12$ to the moments in the S stiffeners. The procedure is illustrated in *Figure 18.56 (a→b→c)*.

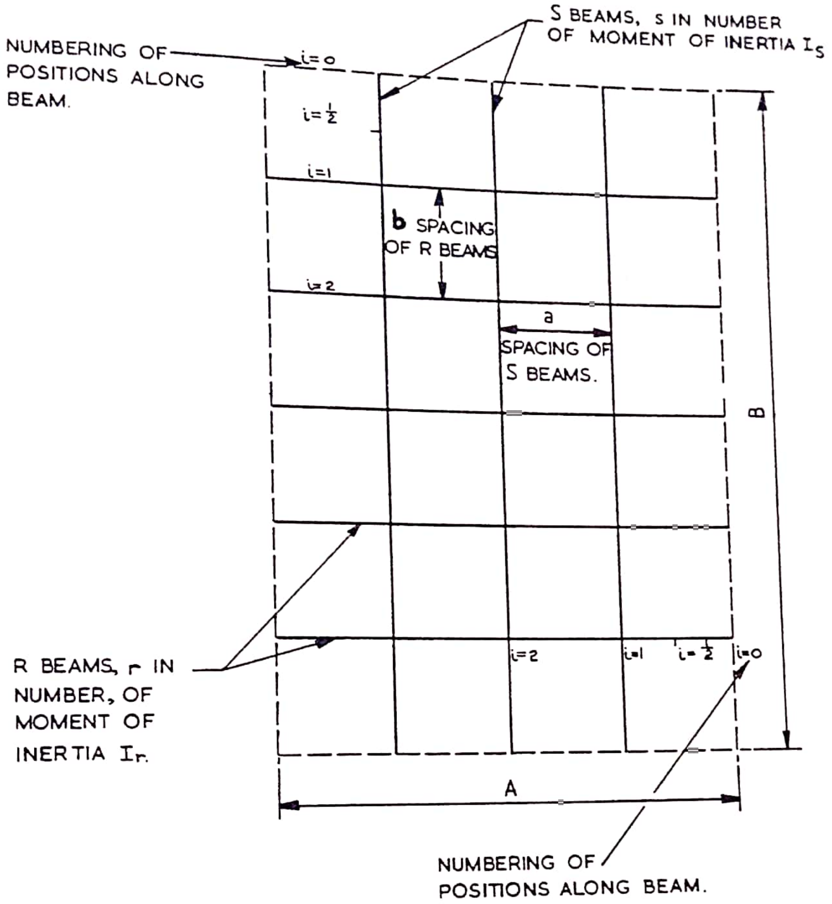
S BEAMS, s IN NUMBER OF MOMENT OF INERTIA I_S
NUMBERING OF POSITIONS ALONG BEAM.
i=0
i=½
i=1
b SPACING OF R BEAMS
i=2
a
SPACING OF S BEAMS.
B
R BEAMS, r IN NUMBER, OF MOMENT OF INERTIA I_r.
i=2
i=1
i=½
i=0
A
NUMBERING OF POSITIONS ALONG BEAM.

NOTE. R BEAMS ARE THE MORE NUMEROUS SET I.E. $r \leqslant s$

Figure 18.52 Grillage Notation

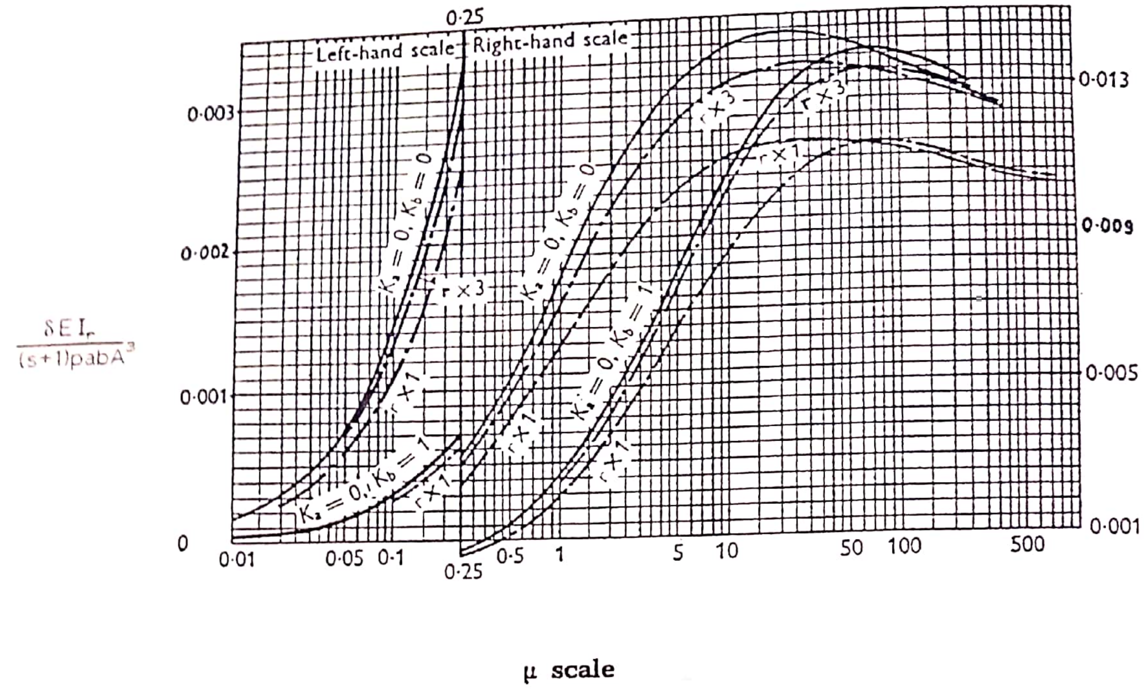

Figure 18.53 Central Deflection for $K_a = 0$

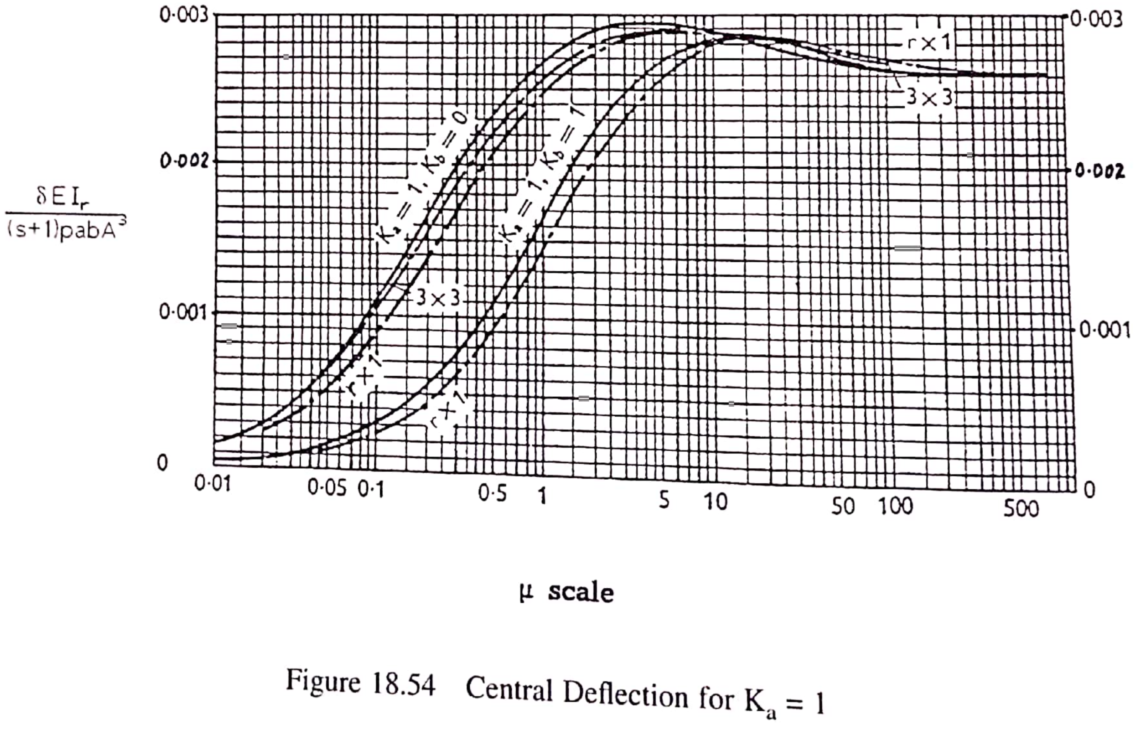

Figure 18.54 Central Deflection for $K_a = 1$

(a) B. M. DUE TO LOADS AT INTERSECTION.

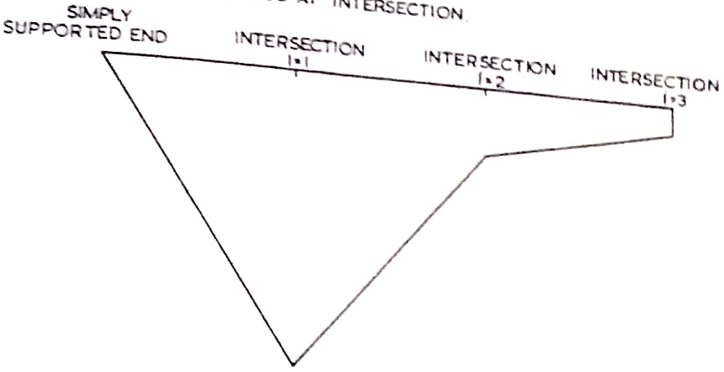

(b) B.M. DUE TO LOCAL BENDING
ORDINATES SHOW APPROXIMATE VALUES OF $B.M./Q_T a^2$ OR $BM/Q_S b^2$

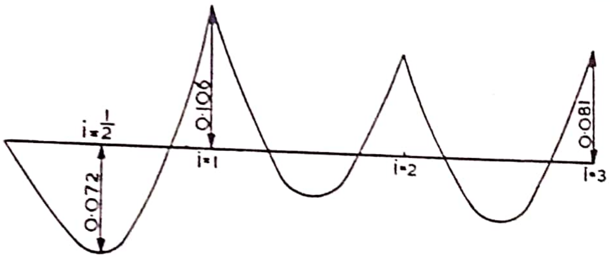

(c) TOTAL B.M. MAXIMUM VALUE MAY OCCUR AT POINTS SUCH AS $i=\frac{1}{2}$, 1, 2, ETC.

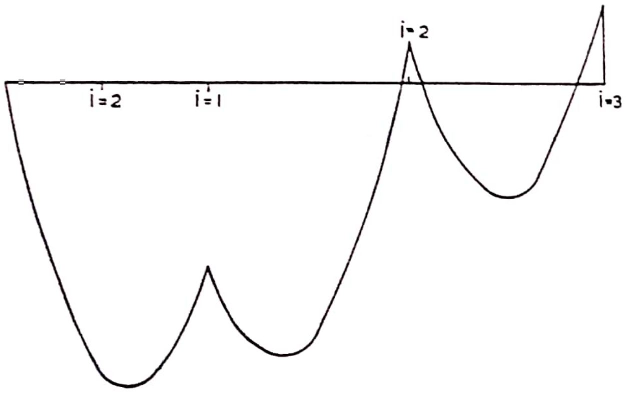

Figure 18.55 Simply Supported Beams: Procedure for Calculating Total Maximum Bending Moment

(a) B.M. DUE TO LOADS AT INTERSECTION

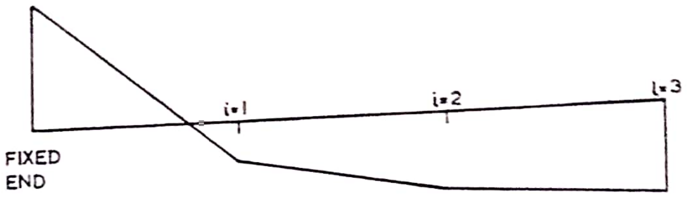

(b) B.M. DUE TO LOCAL BENDING ORDINATES SHOW VALUE OF B.M./$Q_T a^2$ OR B.M./$Q_S b^2$

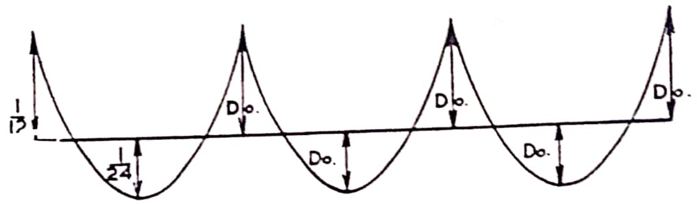

(c) TOTAL B.M. MAXIMUM VALUE ALWAYS OCCURS AT EDGE i=0

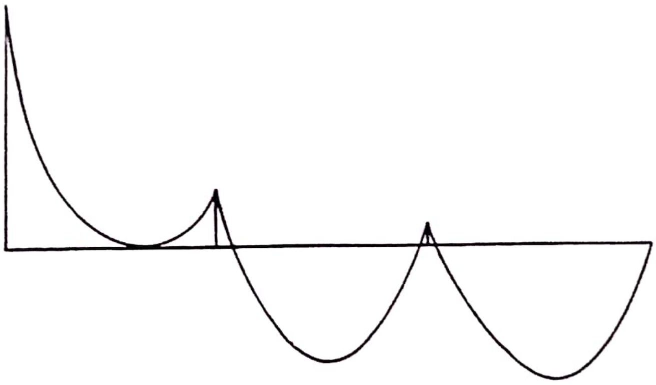

Figure 18.56 Fixed End Beams: Procedure for Calculating Total Maximum Bending Moment

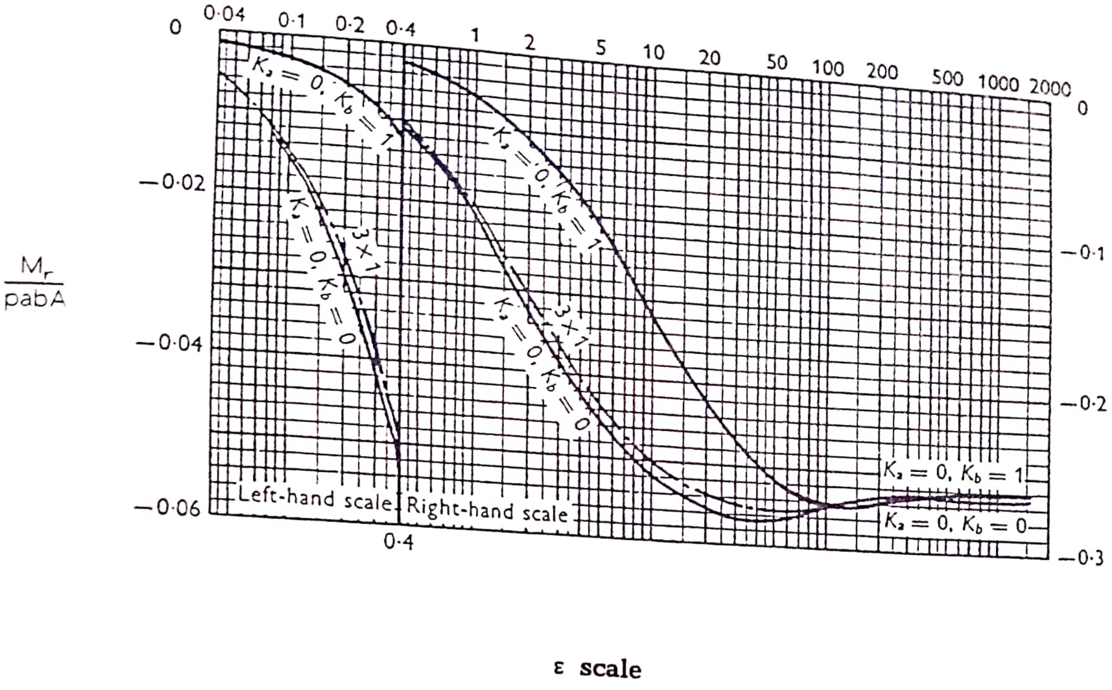

Figure 18.57 r × 1 Grillages, M_r for $K_a = 0$

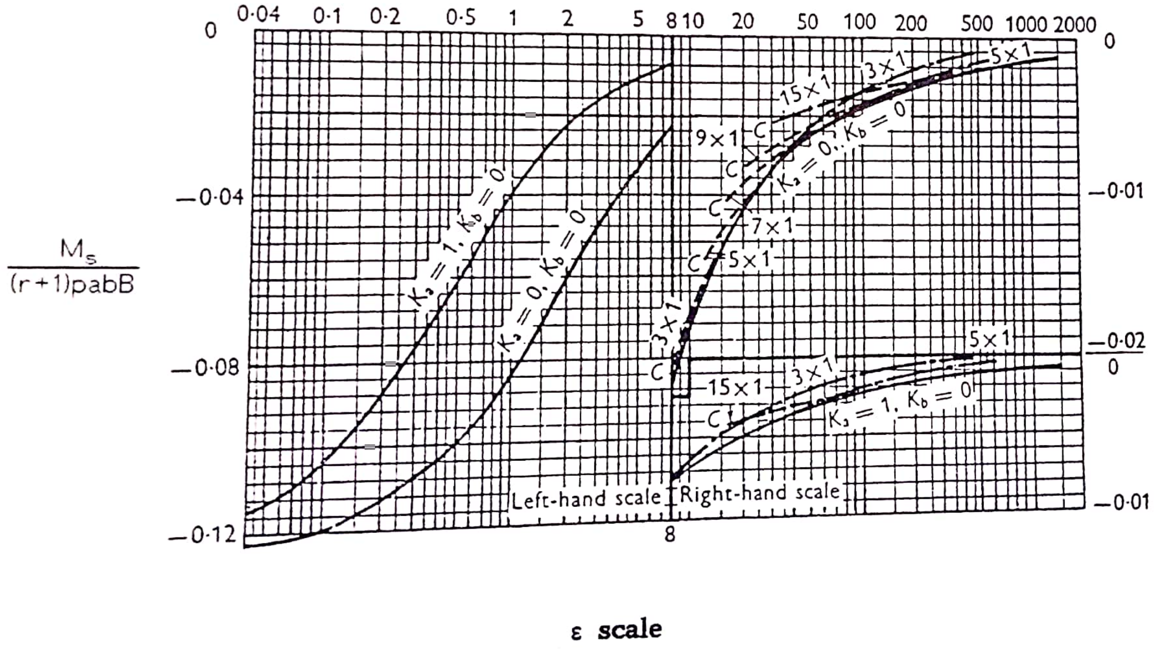

Figure 18.58 r × 1 Grillages, M_s for $K_b = 0$

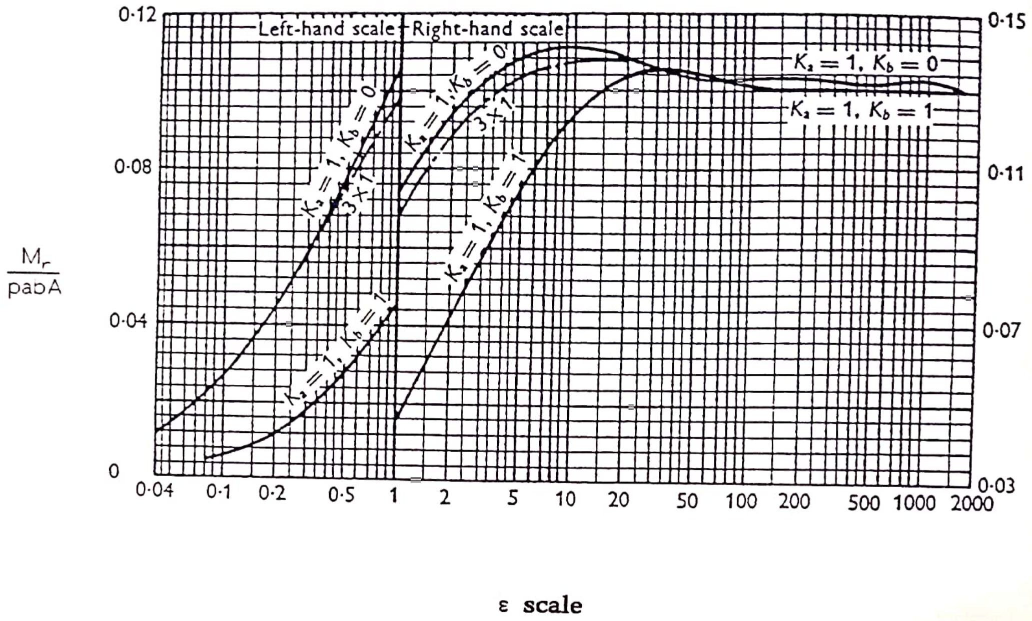

Figure 18.59 r × 1 Grillages, M_r for $K_a = 1$

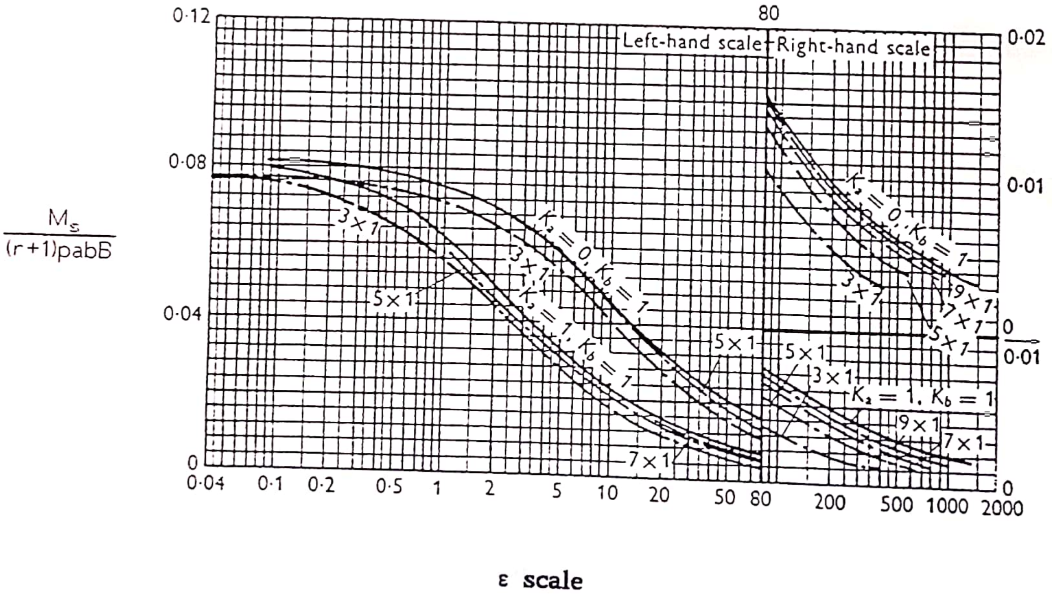

Figure 18.60 r × 1 Grillages, M_s for $K_b = 1$

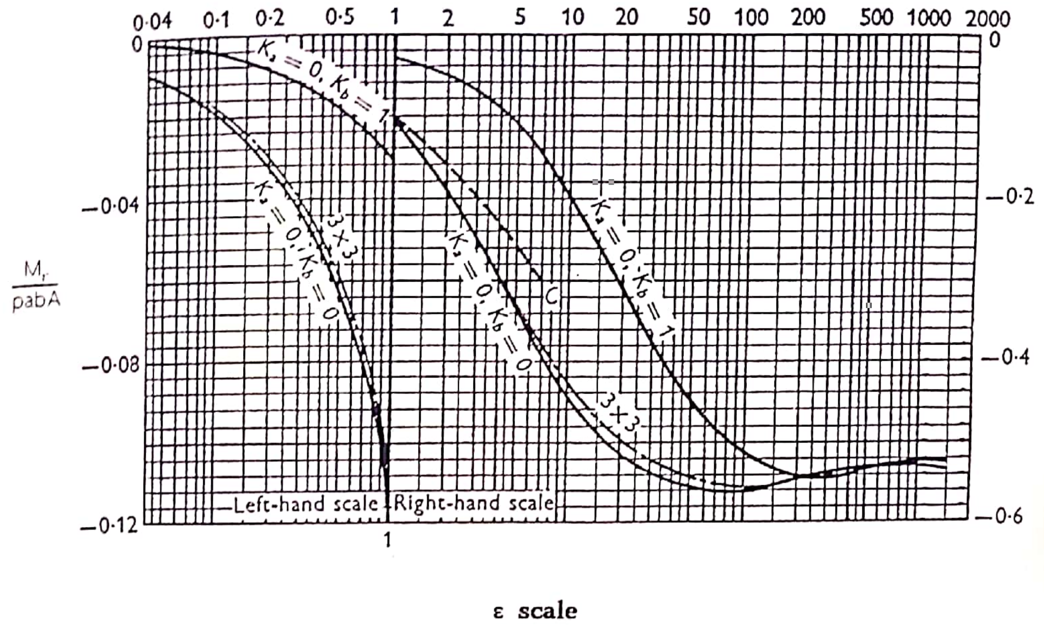

Figure 18.61 r × 3 Grillages, M_r for $K_a = 0$

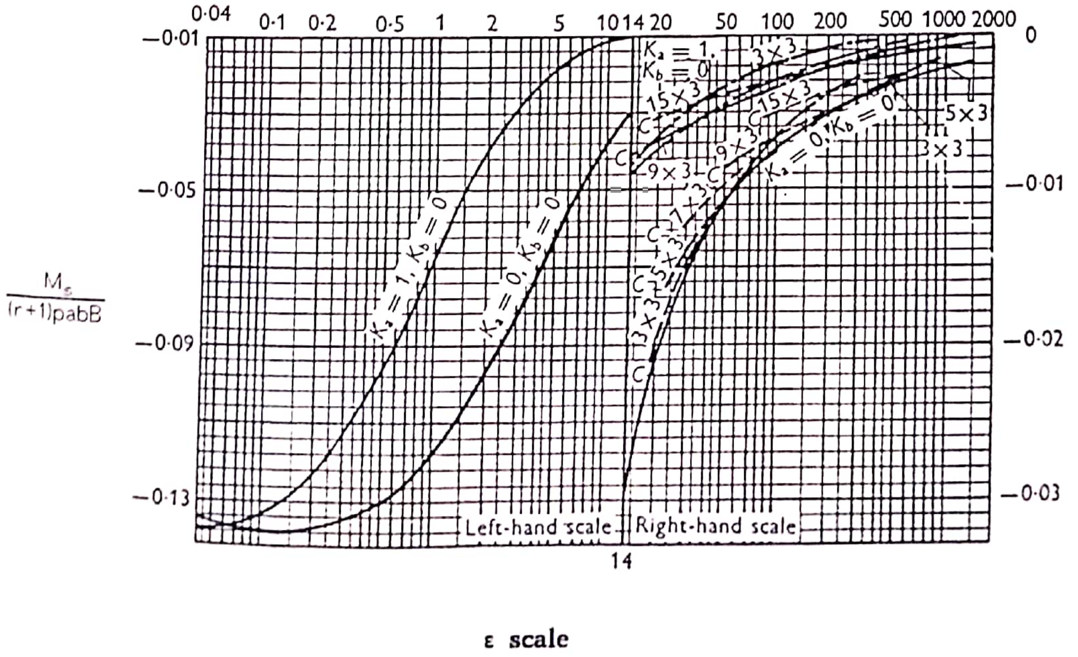

Figure 18.62 r × 3 Grillages, M_s for $K_b = 0$

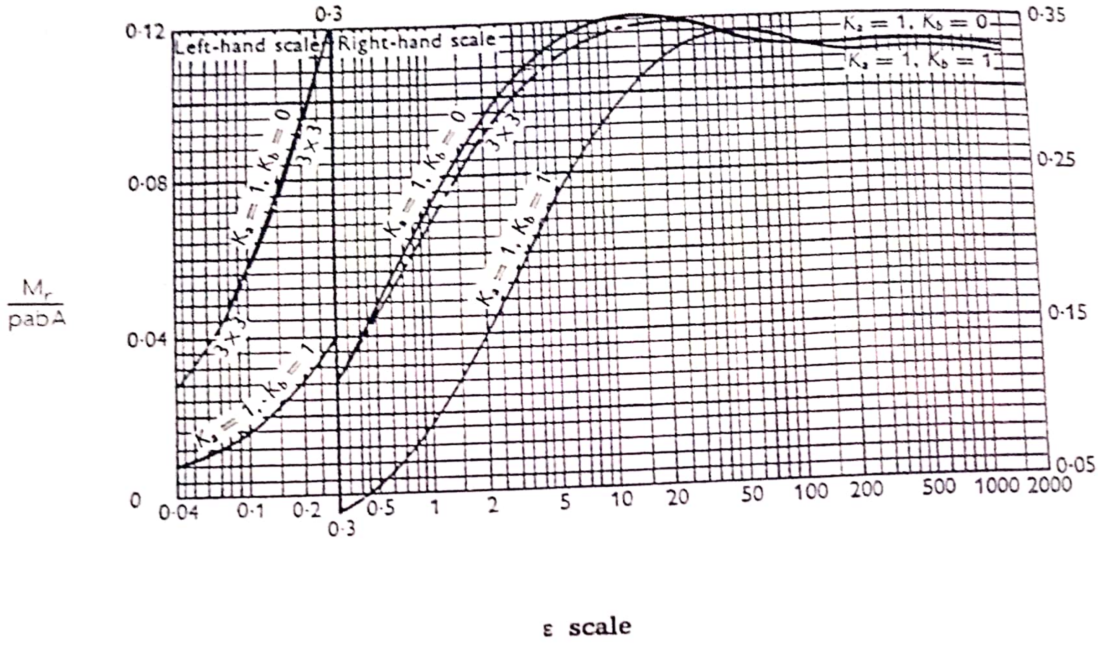

Figure 18.63 r × 3 Grillages, M_r for $K_a = 1$

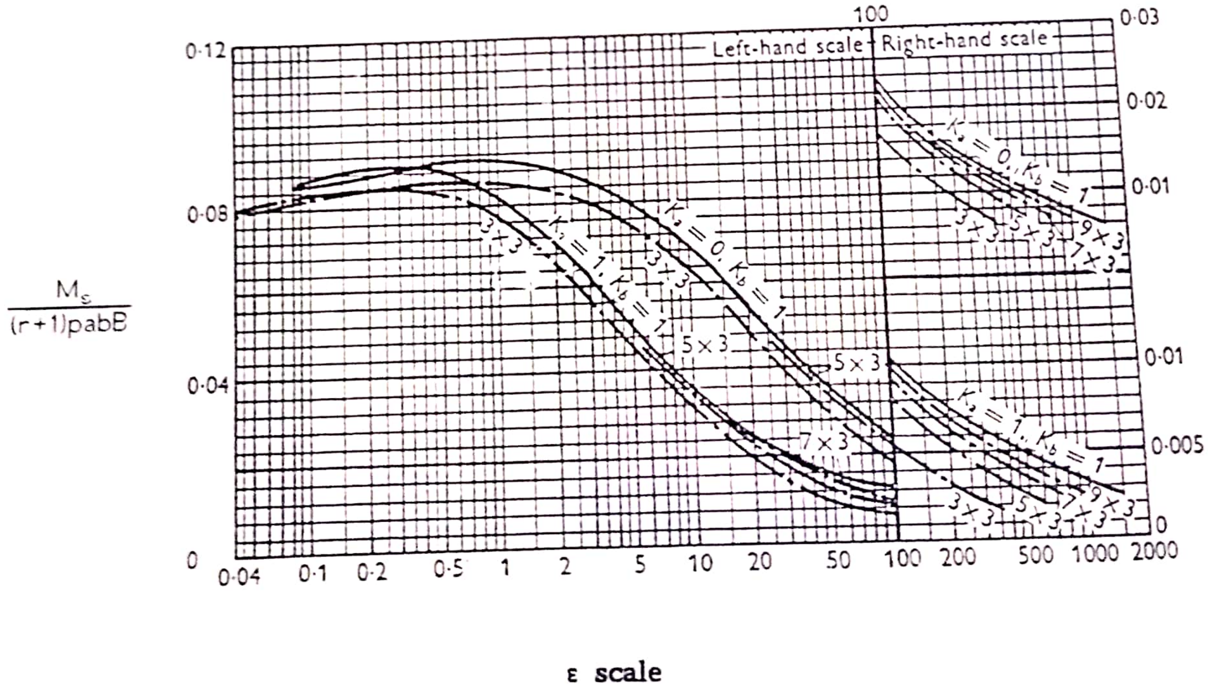

Figure 18.64 r × 3 Grillages, M_s for $K_b = 1$

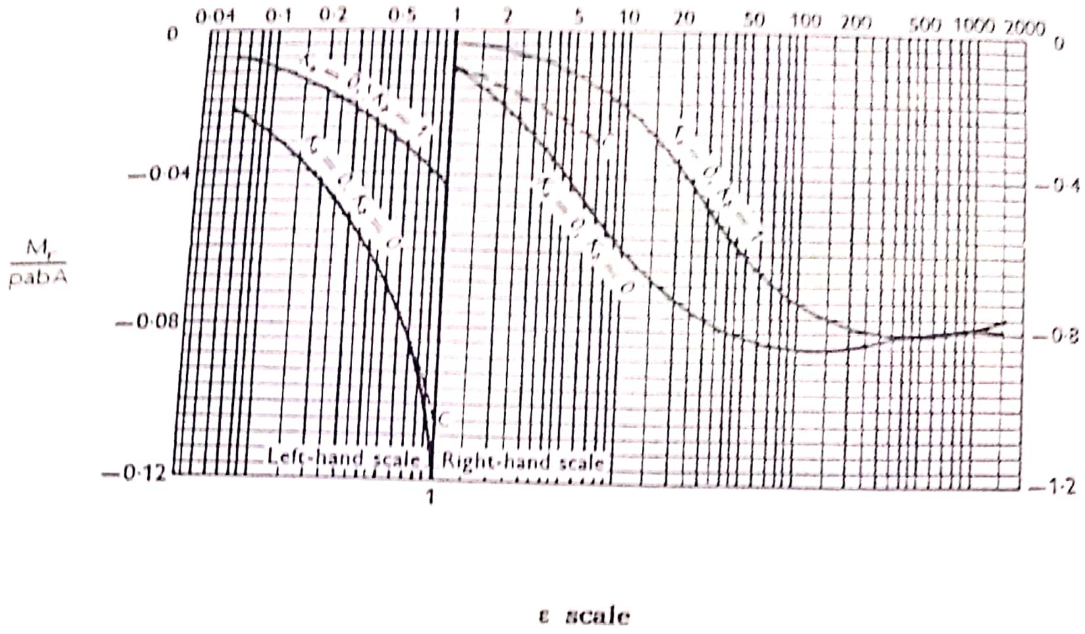

Figure 18.65 r × 5 Grillages, M_r for $K_a = 0$

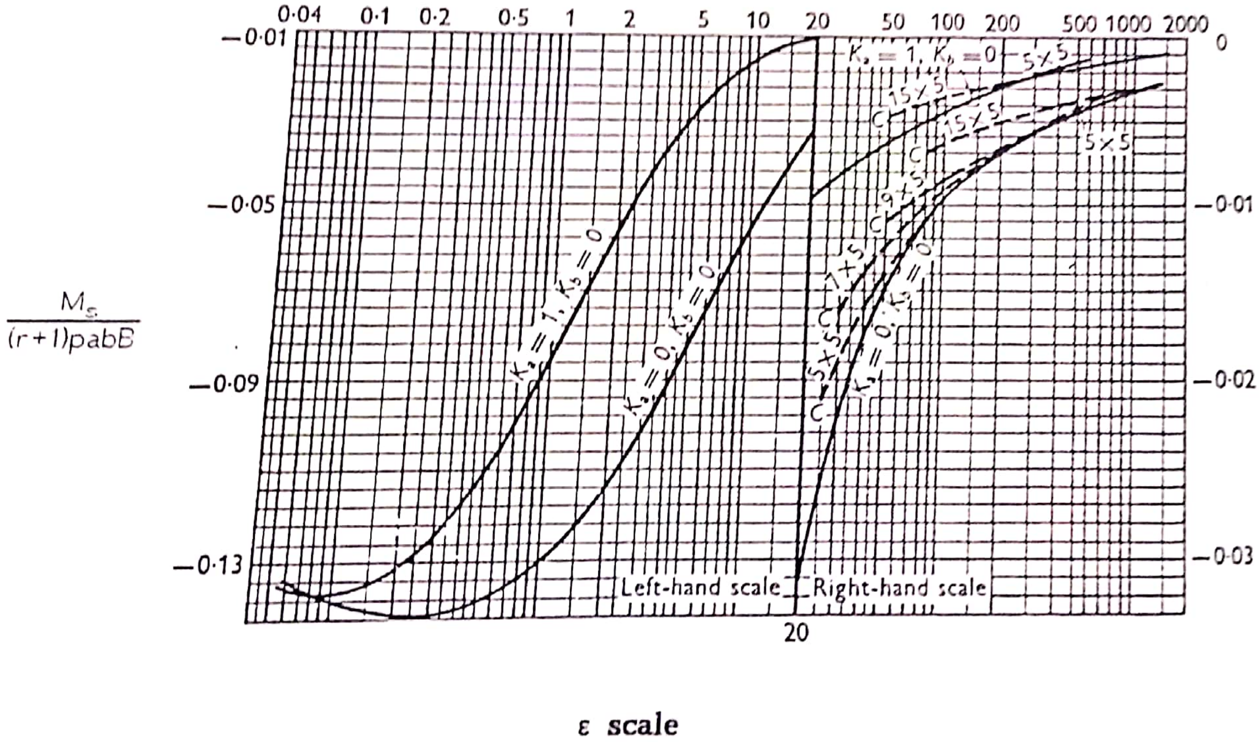

Figure 18.66 r × 5 Grillages, M_s for $K_b = 0$

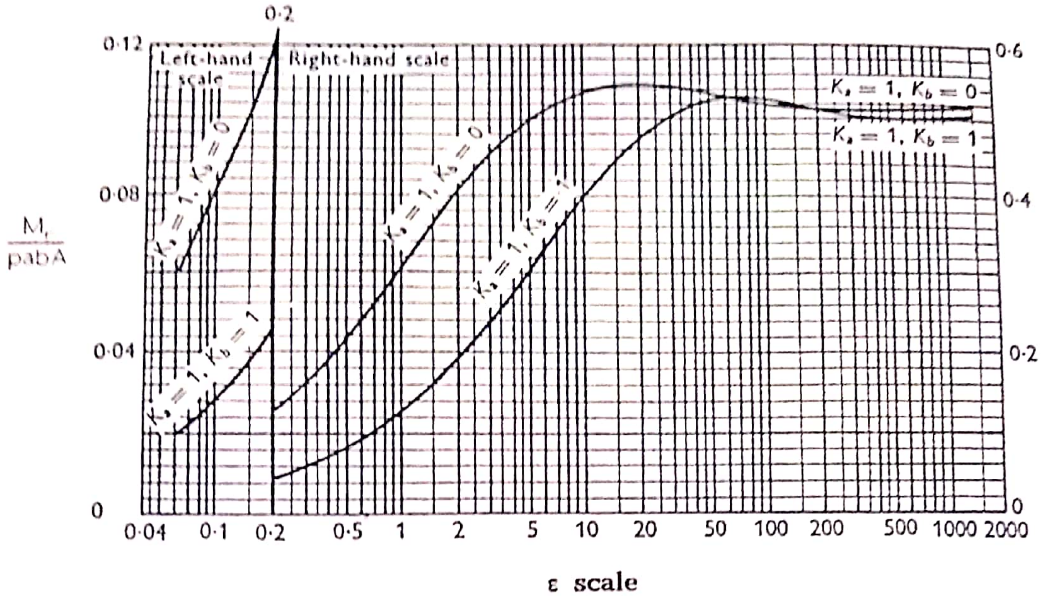

Figure 18.67 r × 5 Grillages, M_r for $K_a = 1$

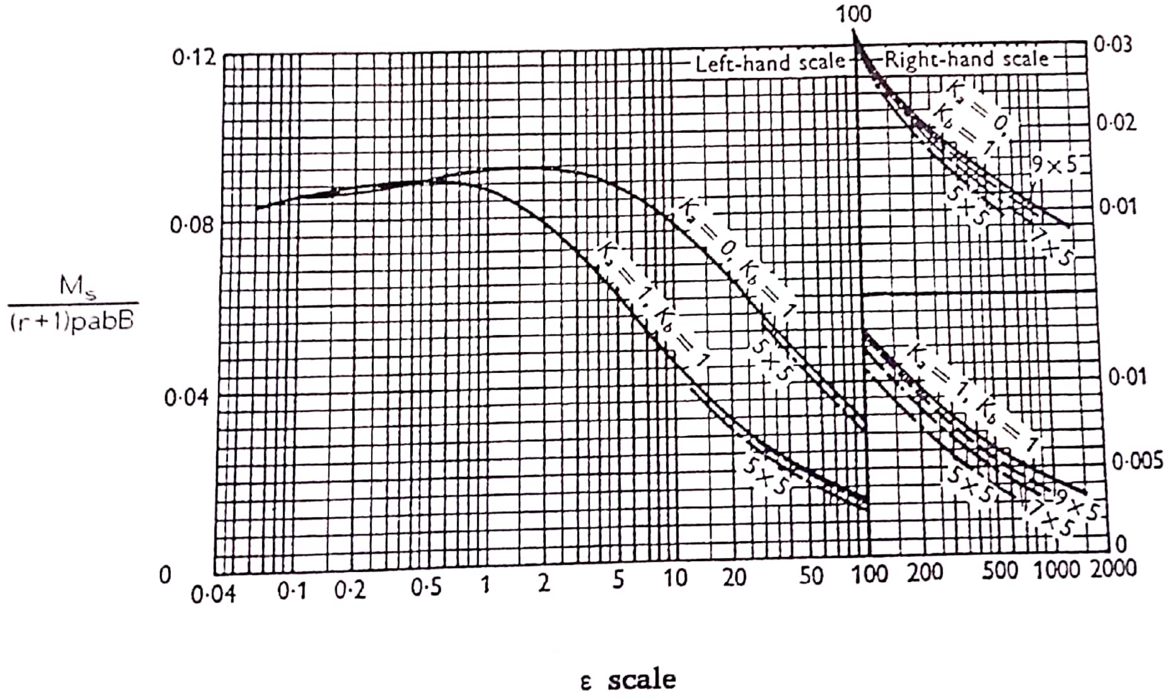

Figure 18.68 r × 5 Grillages, M_s for $K_b = 1$

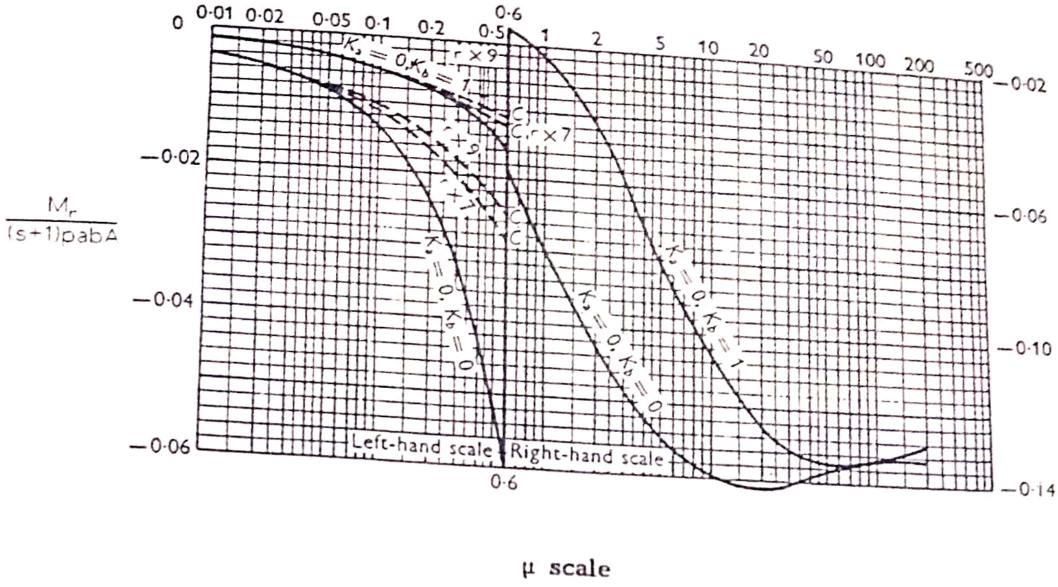

Figure 18.69 r × 7 and r × 9 Grillages, M_r for $K_a = 0$

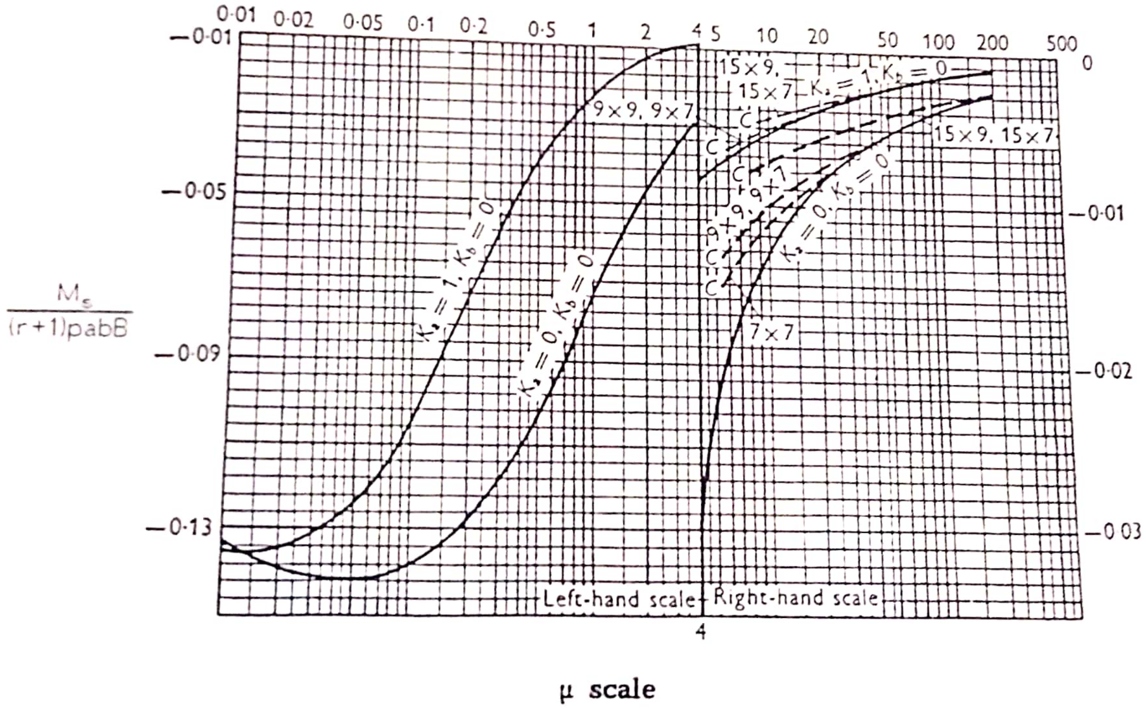

Figure 18.70 r × 7 and r × 9 Grillages, M_s for $K_b = 0$

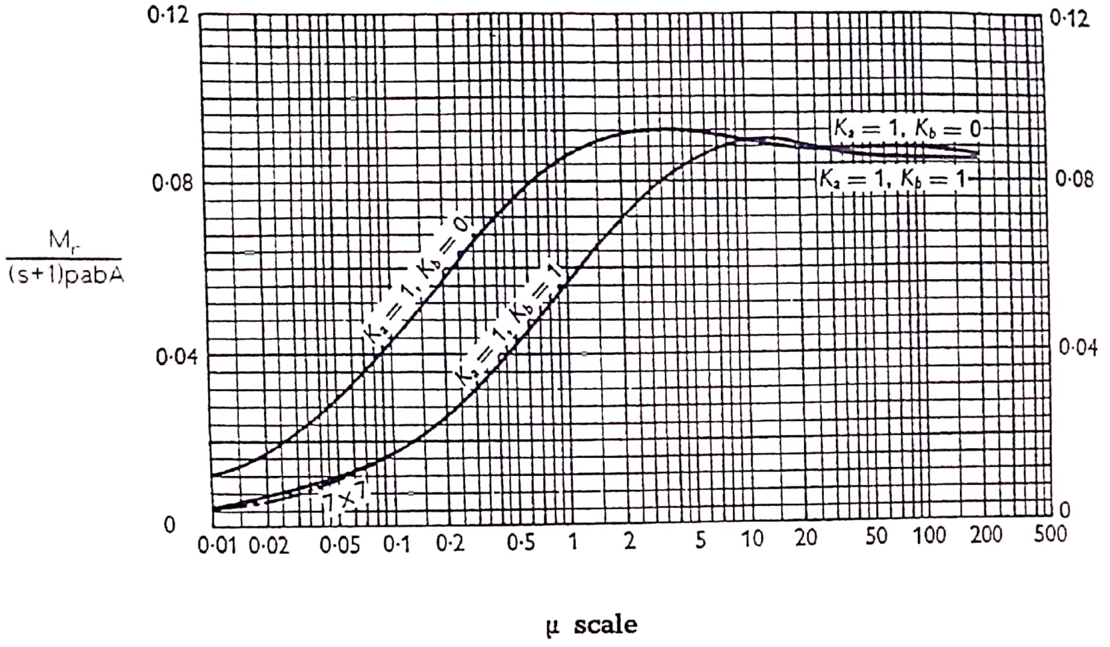

Figure 18.71 r × 7 and r × 9 Grillages, M_r for $K_a = 1$

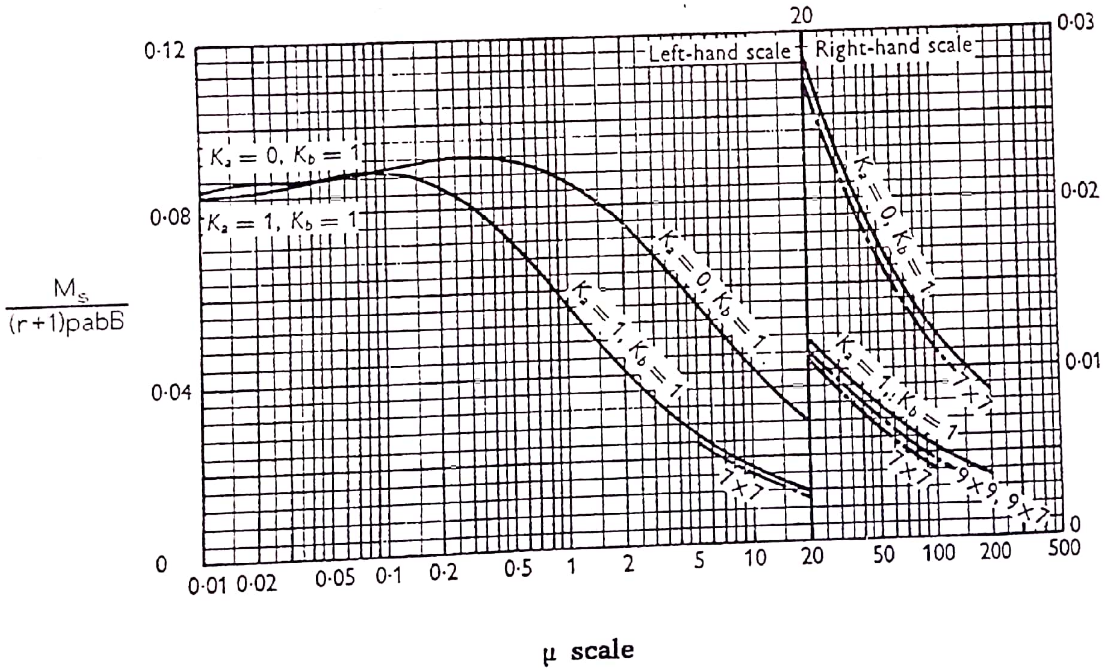

Figure 18.72 r × 7 and r × 9 Grillages, M_s for $K_b = 1$

Calculation of Slamming Pressures

58 The method included here for estimation of equivalent static slamming pressures is empirical and is based on curves which allow for the angle of rise of floor and the draught at the section of the hull in question. The pressure p in kPa is deduced from equation 18.12 as follows:

$$p = 22.6\ F.G.H\ (kPa) \tag{18.12}$$

where F and G are taken from *Figures 18.73* and *18.74* respectively and H is equal to $0.61\sqrt{L}$ with L the waterline length of the ship in metres. Note that T_x in *Figure 18.73* is the draught to the *keel* at the section of the hull at which slamming pressure is to be calculated, and α in *Figure 18.74* is the angle between the tangent to the hull and the horizontal at the *point* at which the pressure is required.

59 Pressures should be calculated between the fore perpendicular (FP) and 40% of the length abaft the FP along several buttock lines at suitably chosen distances from the centreline of the ship. The pressure at the keel may be taken to be that calculated at a distance from the centreline equal to 5% of the beam of the ship at that section. Note that the result is an envelope of maximum static equivalent pressures and does not indicate the pressures that are experienced during any particular slam.

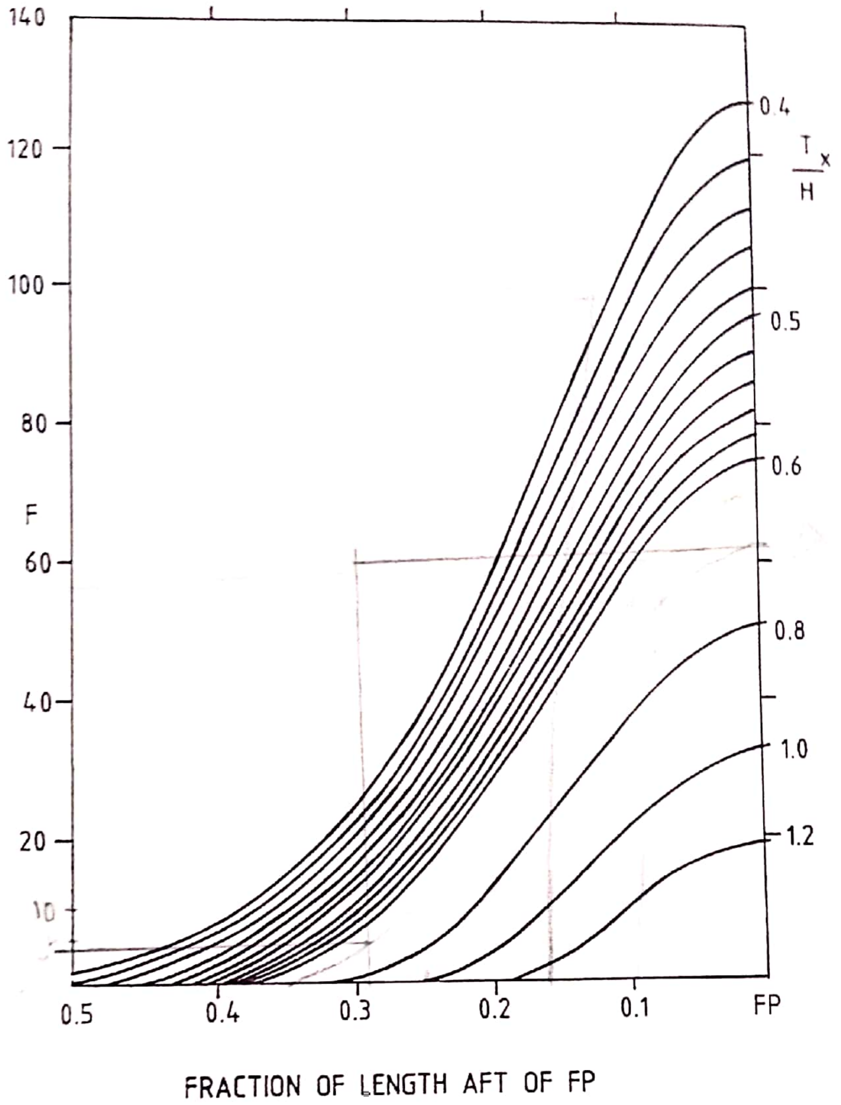

Figure 18.73 Slamming Pressure Factor F

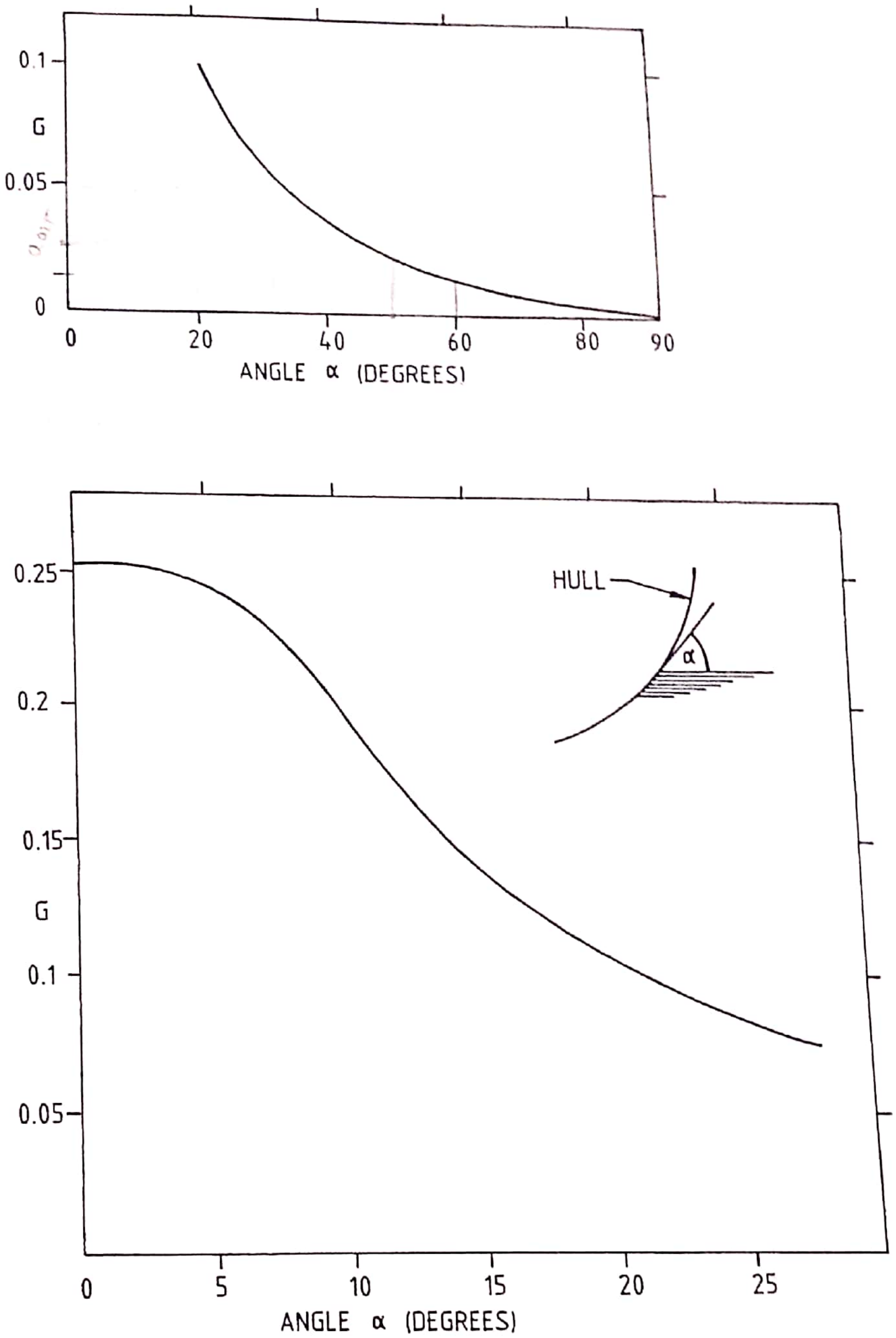

Figure 18.74 Slamming Pressure Factor G

60 *Figures 18.75, 18.76* and *18.77* present the allowable load in the form of a non-dimensional parameter C_p given by equation 18.13 in terms of the plate slenderness ratio ß (=(b/t)$\sqrt{(\sigma_y/E)}$) and the panel width to tyre width ratio b/b_t (assuming that b and b_t are parallel) for three different values of permanent set parameter C_{sp} given by equation 18.14.

(18.13) $C_p = PE/(b^2\,\sigma_y^2)$

(18.14) $C_{sp} = (s_p/b)\,\sqrt{(E/\sigma_y)}$

Note that P is the *load*, not the pressure, b is the *smallest* plate panel dimension between stiffeners and s_p is the allowable permanent set due to application of the load P. For values of C_{sp} between those in the figures interpolation may be used. Further details of how these curves should be used, and in particular how to deal with the case of an aircraft landing at right angles to the main longitudinal deck structure, are given in Chapter 12.

61 When the undercarriage is twin wheeled it may be necessary to derive an equivalent load. The load on the plating may be divided equally between the two wheels if $(b_t + w)/b > 0.6$ where w is the spacing between the wheel centre planes, that is the design value of P is halved, otherwise the load on *one* wheel must be *increased* to allow for the uneven distribution of the load due to landing attitude and also for the wheel spacing relative to plate width. The total applied load should then be *divided* by an 'equivalent load factor' taken from *Figure 18.78* for the particular values of w/b and b/b_t, interpolating as necessary, to obtain the design load P.

62 The load on a stiffener also needs modifying to allow for a twin wheeled undercarriage. *Figure 18.79* gives the equivalent load factor plotted against w/b, but note that in this case the total applied load must be *multiplied* by the load factor to obtain the design load.

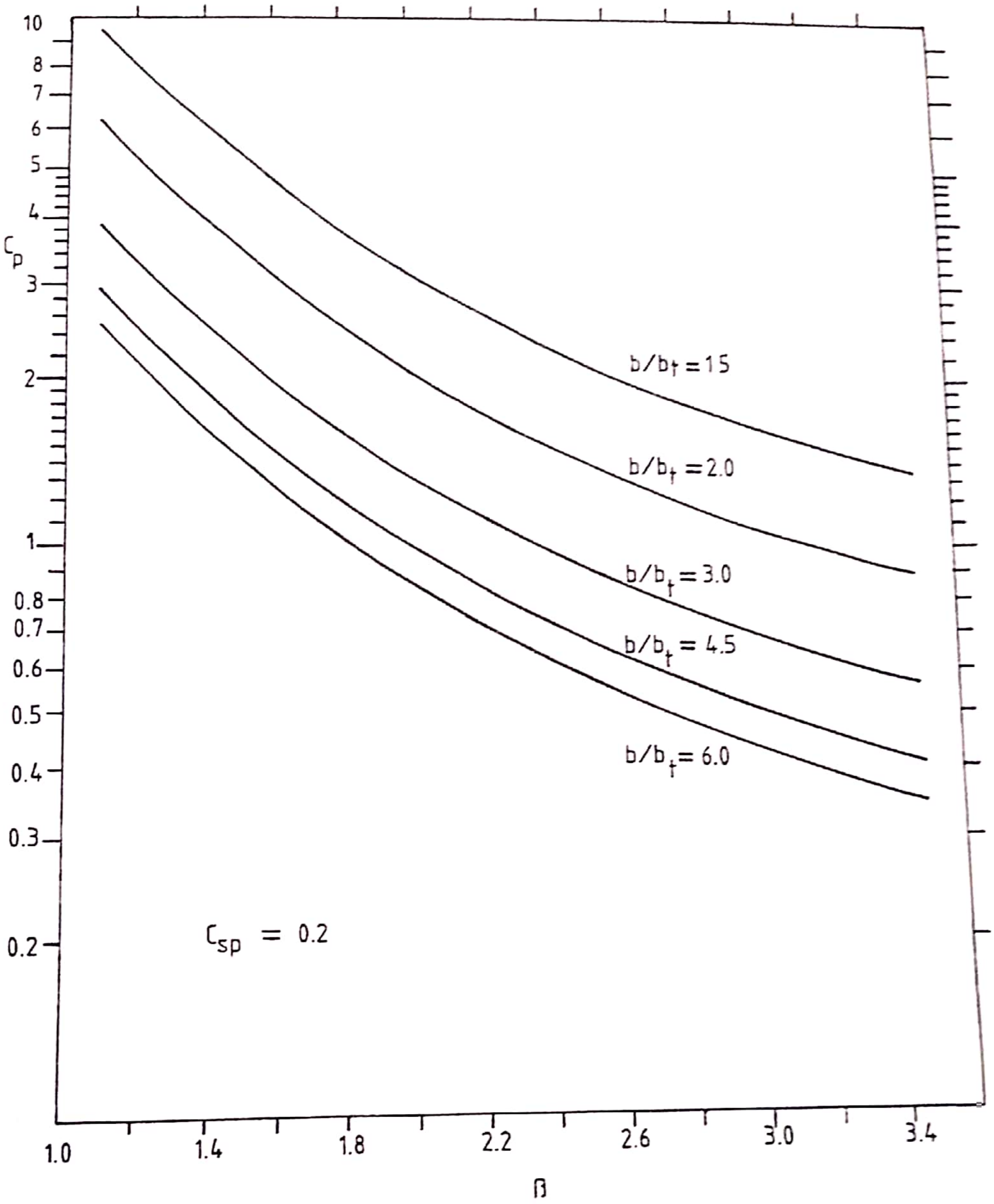

Figure 18.75 Plating Design Curve $C_{sp} = 0.2$

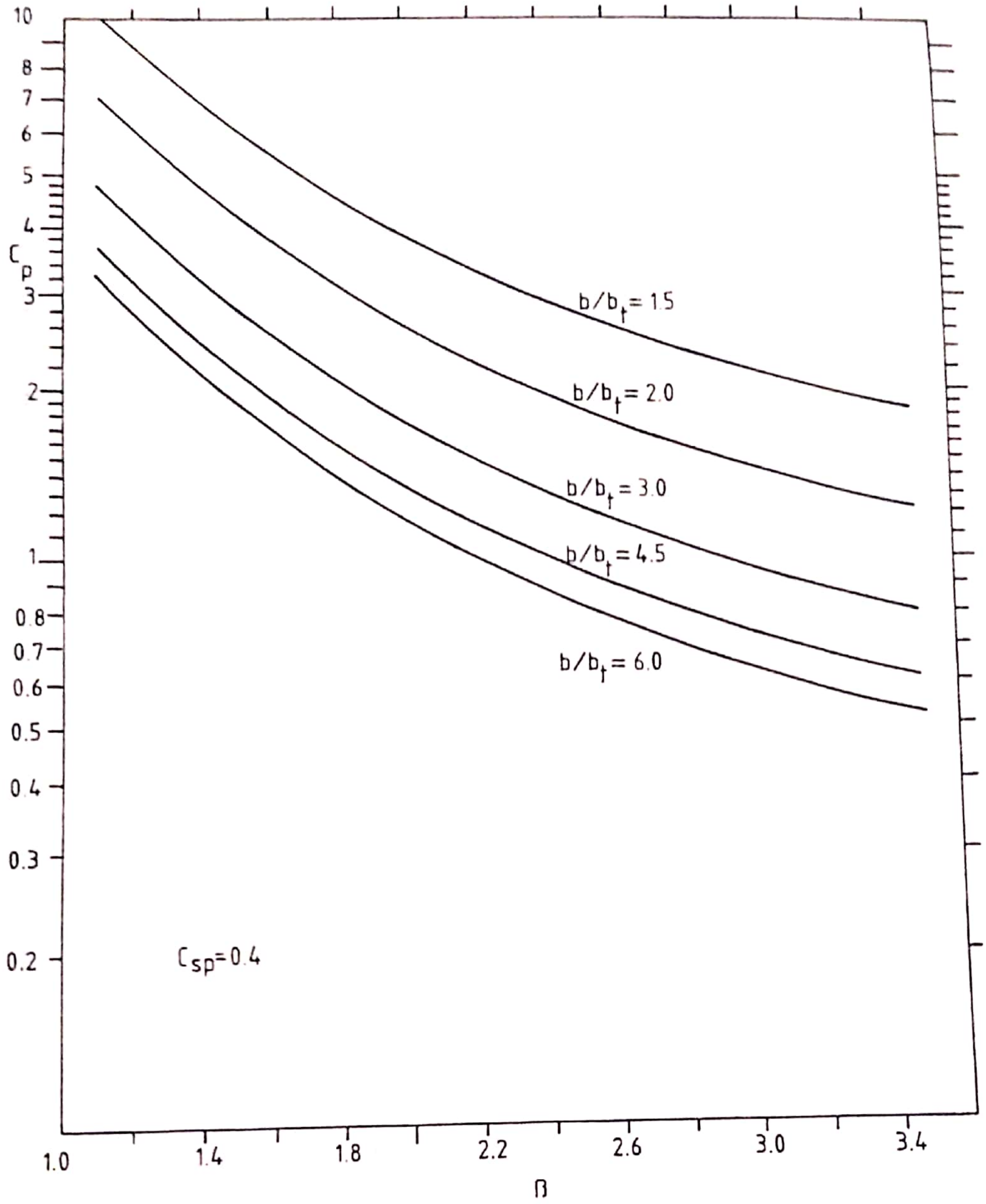

Figure 18.76 Plating Design Curve $C_{sp} = 0.4$

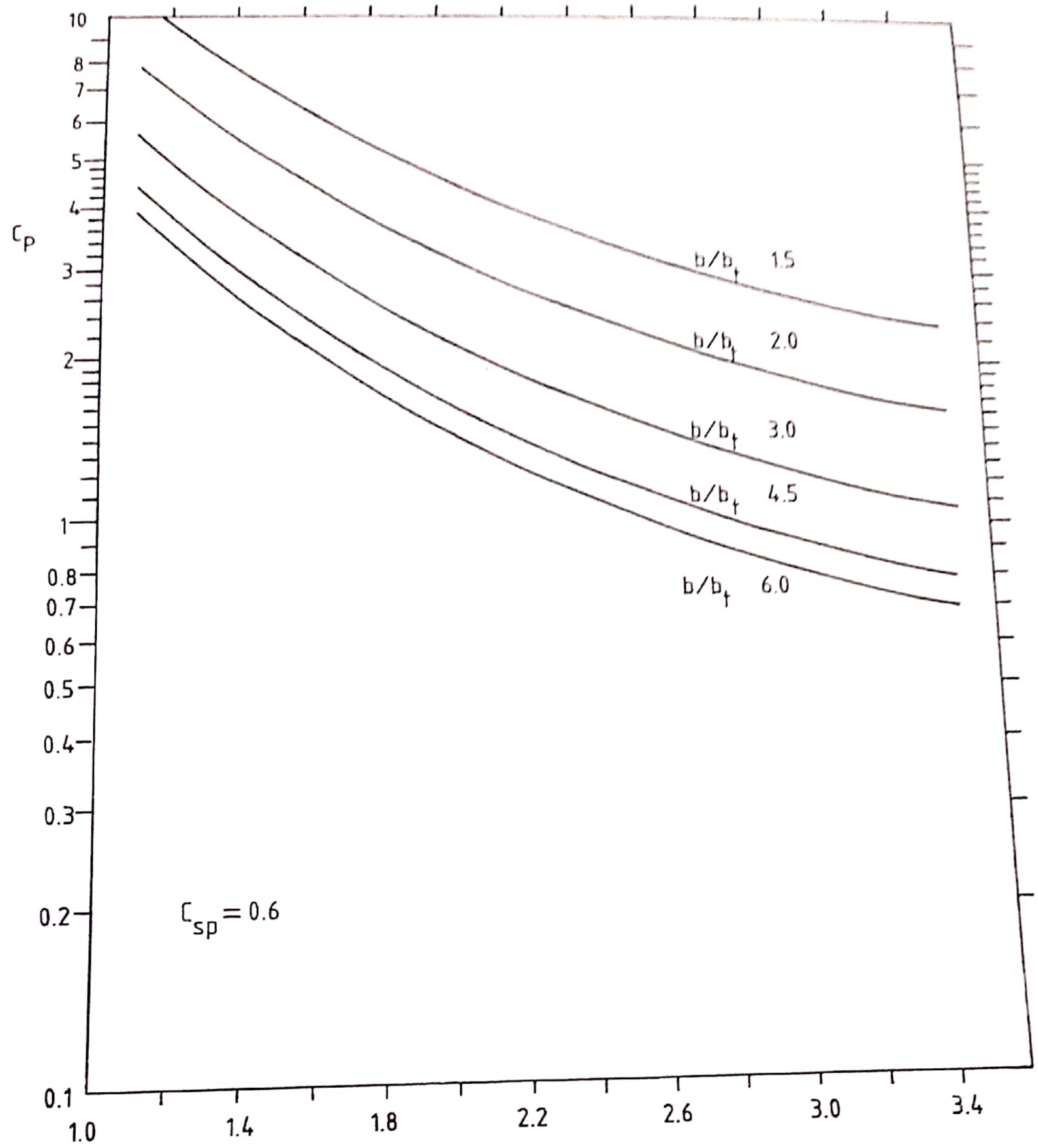

Figure 18.77 Plating Design Curve $C_{sp} = 0.6$

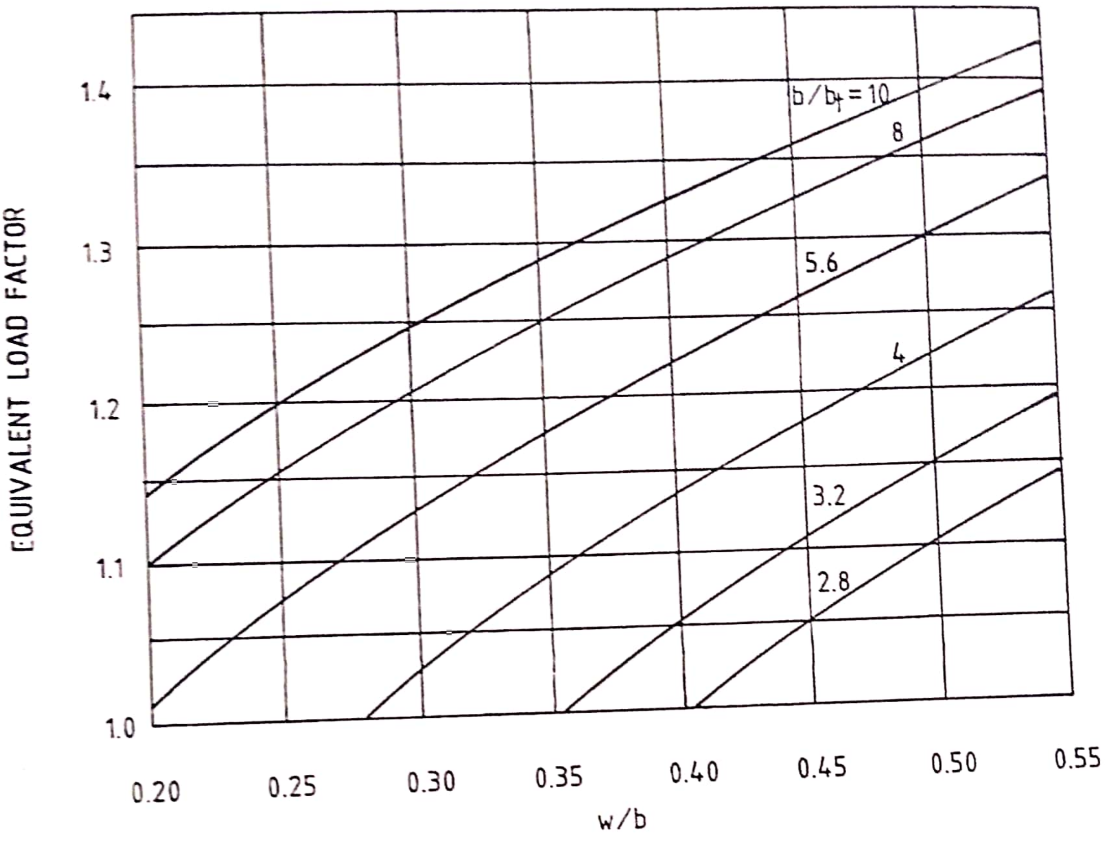

Figure 18.78 Equivalent Load Factor for Plating Design

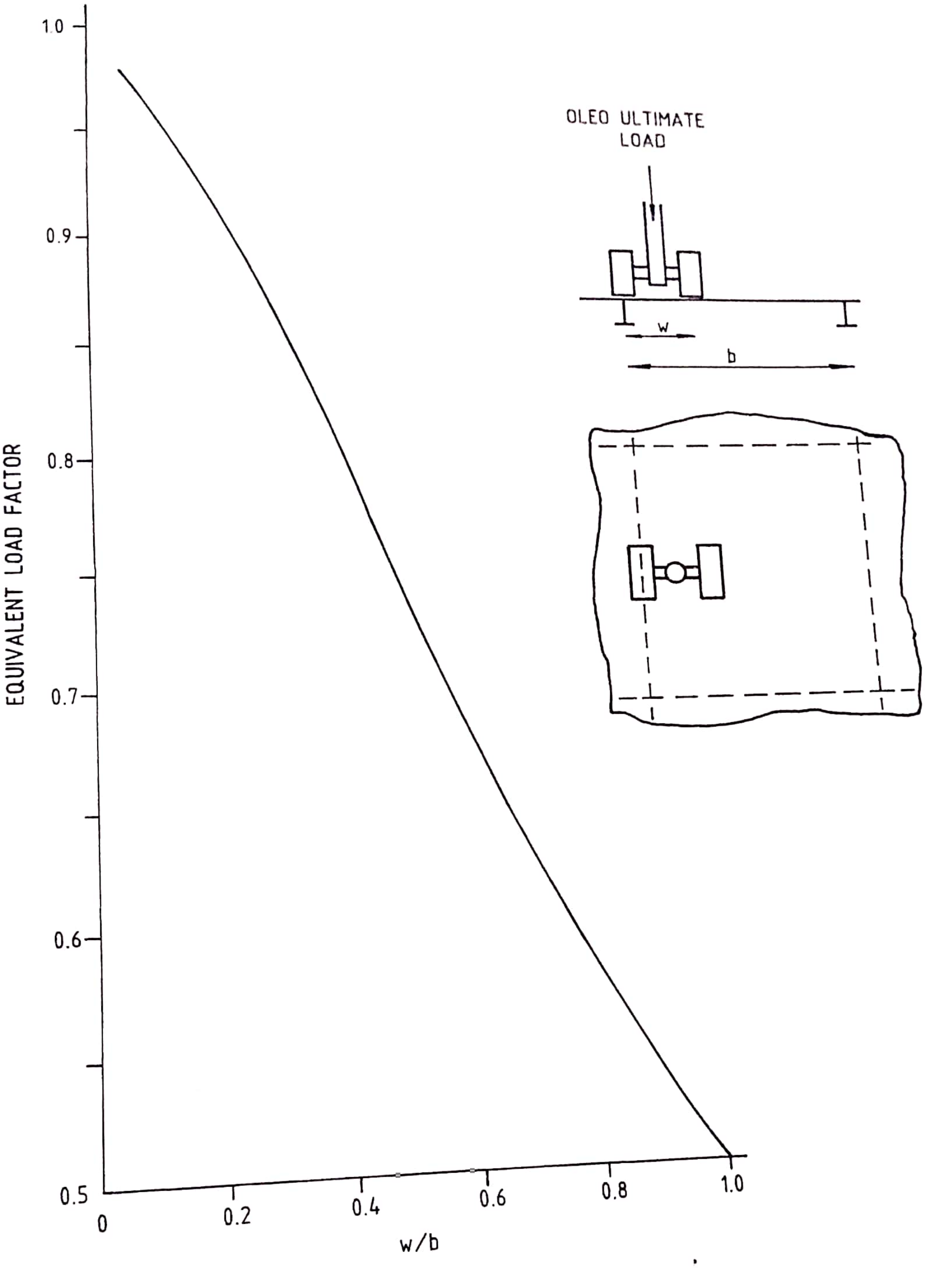

Figure 18.79 Equivalent Load on Stiffener due to Twin Wheels

Efficiency of Short Decks

63 This figure gives an estimate of the percentage of the primary longitudinal bending stress in a short deck as a function if distance X from the free edge and the deck breadth B. To obtain the average stress across a deck near to a free edge, enter *Figure 18.80* with the ratio X/B and read off the efficiency η_d at that section. In calculating the stress at the section the deck may be assumed to be effective but with a Young's modulus reduced by the factor η_d, and in designing the deck the average stress is then the simple beam bending stress also reduced by the factor η_d. Note that as the stress at the edge of the deck must be the same as in the ship's side or other longitudinal structure, and is therefore greater than the average, the stress at the centre will be a little less than the average.

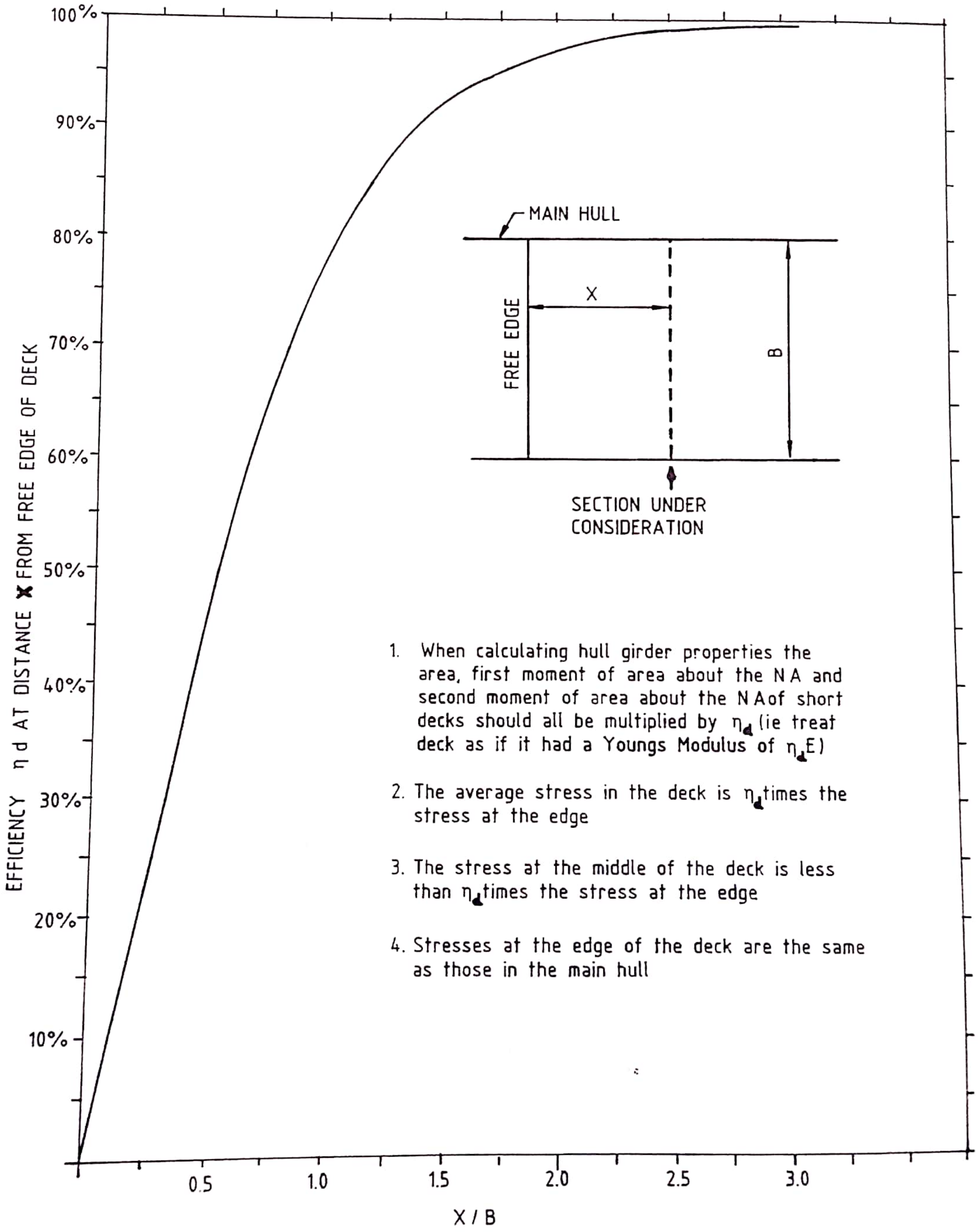

1. When calculating hull girder properties the area, first moment of area about the N A and second moment of area about the N A of short decks should all be multiplied by η_d (ie treat deck as if it had a Youngs Modulus of $\eta_d E$)

2. The average stress in the deck is η_d times the stress at the edge

3. The stress at the middle of the deck is less than η_d times the stress at the edge

4. Stresses at the edge of the deck are the same as those in the main hull

Figure 18.80 Efficiency of Short Decks

Stress Concentration at a Reinforced Circular Hole

64 *Figure 18.81* gives the stress concentration factor around a circular hole which has been reinforced with a local thick insert. Curves are drawn for stress concentration factor (SCF) against t_r/t, where t is the basic place thickness and t_r is the *additional* thickness of the reinforcement. Two sets of curves are included, each for three different values of the ratio of reinforcement diameter to hole diameter; one set is for uniaxial tensile stress σ and the maximum stress at the hole is therefore σ × SCF, and the second set is for pure shear τ so the maximum stress is τ × SCF.

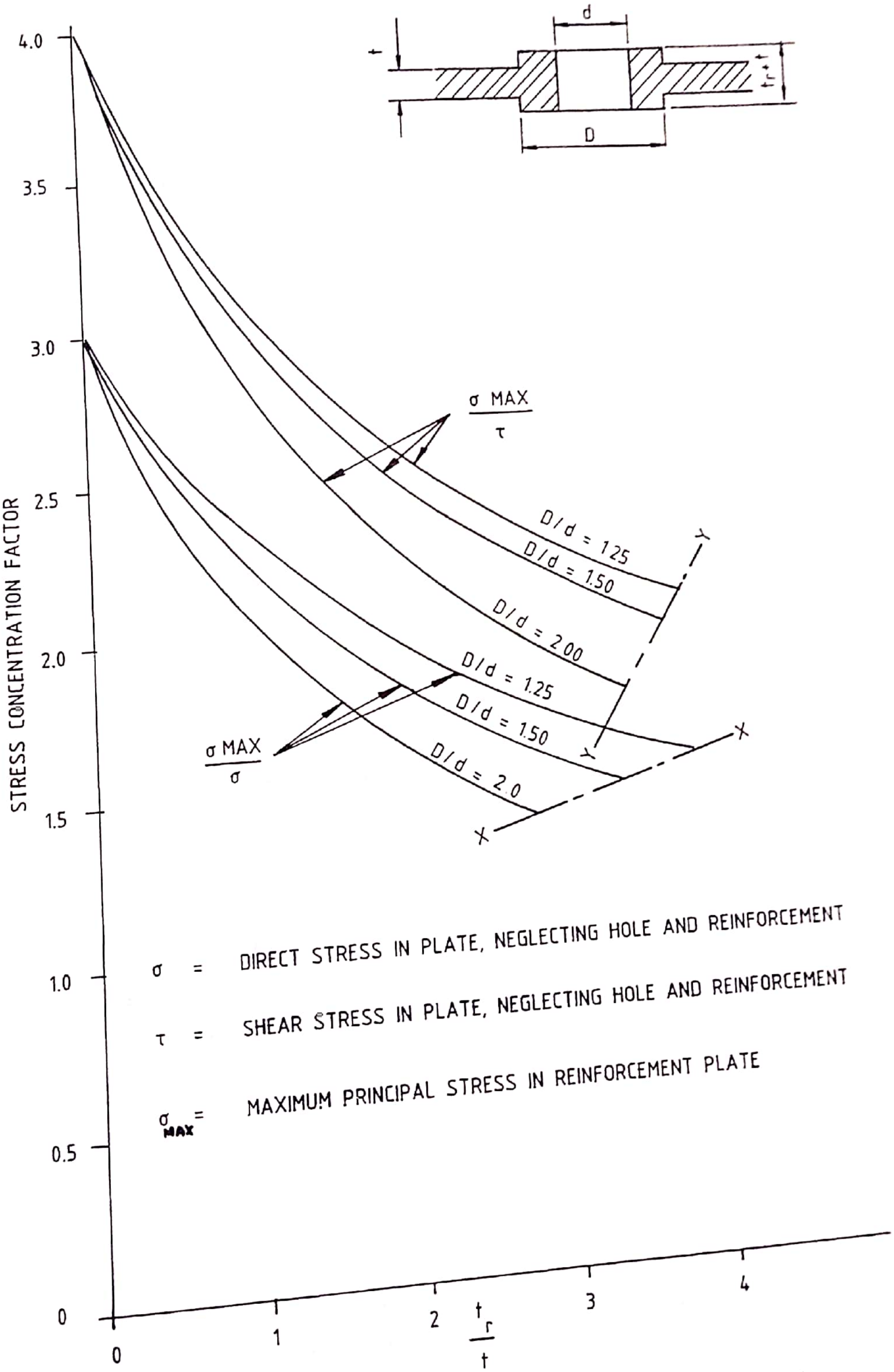

Figure 18.81 Stress Concentration at Reinforced Circular Hole

Maximum Deflection of Panels Normal to a Blast Wave

65 *Figures 18.82* to *18.84* give the maximum deflection of stiffened panels in response to an incident nuclear air blast wave normal to the panel and are based on Kendrick (1963). The output from the curves is in the form of the ratio x_{max}/x_e where x_{max} is the maximum dynamic deflection and x_e is the maximum elastic deformation of the panel given by equation 18.15.

$$x_e = L^2 (5M_{p1} - M_{p2})/48EI \qquad (18.15)$$

where L is the unsupported span of the panel in the direction of the stiffeners, E is the Young's modulus of the material, I is the second moment of area of a stiffener with an effective breadth of plating of 50t and M_{p1} and M_{p2} are the plastic hinge moments for the two ends of the stiffener such that $M_{p1} \leq M_{p2}$. these plastic hinge moments should be for the stiffener alone about its toe, and should relate to whichever is the smaller of the stiffener on the panel or the stiffener to which the panel is attached at the boundary.

66 The inputs to the curves are, unfortunately, in imperial units and it is not practicable to change the curves to metric units. The user will therefore have to convert between the two sets of units and appropriate factors are given below. The first input is the nominal free field overpressure P_{so} and the three data sheets are drawn for three values of this parameter, 5 lb/in^2 (34.5 kPa), 8 lb/in^2 (55.2 kPa) and 10 lb/in^2 (69.0 kPa). Interpolation between the sets of curves or extrapolation downwards is acceptable, but not extrapolations upwards as the limit for use is set at $P_{so} = 70$ kPa.

67 The second input is the static collapse pressure (p_c) of the panel given by equation 18.16. This will also have to be converted to lb/in^2 and the required factor is to multiply kPa by 0.145 to give lb/in^2.

$$p_c = 8\,(M_{p1} + M_{p2})/L^2 s \qquad (18.16)$$

where s is the stiffener spacing on the panel and the other parameters are defined above. Appropriate curves must be chosen to span the calculated value of p_c and again interpolation is acceptable.

68 The third input on the ordinate of the curves is the parameter $t_s/\sqrt{(W_e x_e)}$, where t_s is the duration in seconds of the reflection and diffraction phase of the pressure pulse (defined in Chapter 4) and W_e is a measure of the effective weight of structure being accelerated by the pulse and is given by equation 18.17.

$$W_e = (W_p + W_r/s)/1.5 \qquad (18.17)$$

where W_p is the weight per unit area of the plating and W_r is the weight per unit length of the stiffeners at spacing s. In the curves W_e has units of lb/ft^2 and x_e has units of inches; if units of kg/m^2 and mm are used respectively, then to convert the parameter to imperial units the metric value must be multiplied by 11.14. That is, t_s (seconds)/$\sqrt{(W_e \text{ (lb/ft}^2) \; x_c \text{ (in)})}$ = 11.14 [t_s (seconds)/$\sqrt{(W_e \text{ (kg/m}^2) \; x_c \text{ (mm)})}$]. With these input values and ratio x_{max}/x_e can be read off the curves and so the maximum dynamic deflection x_{max} can be deduced.

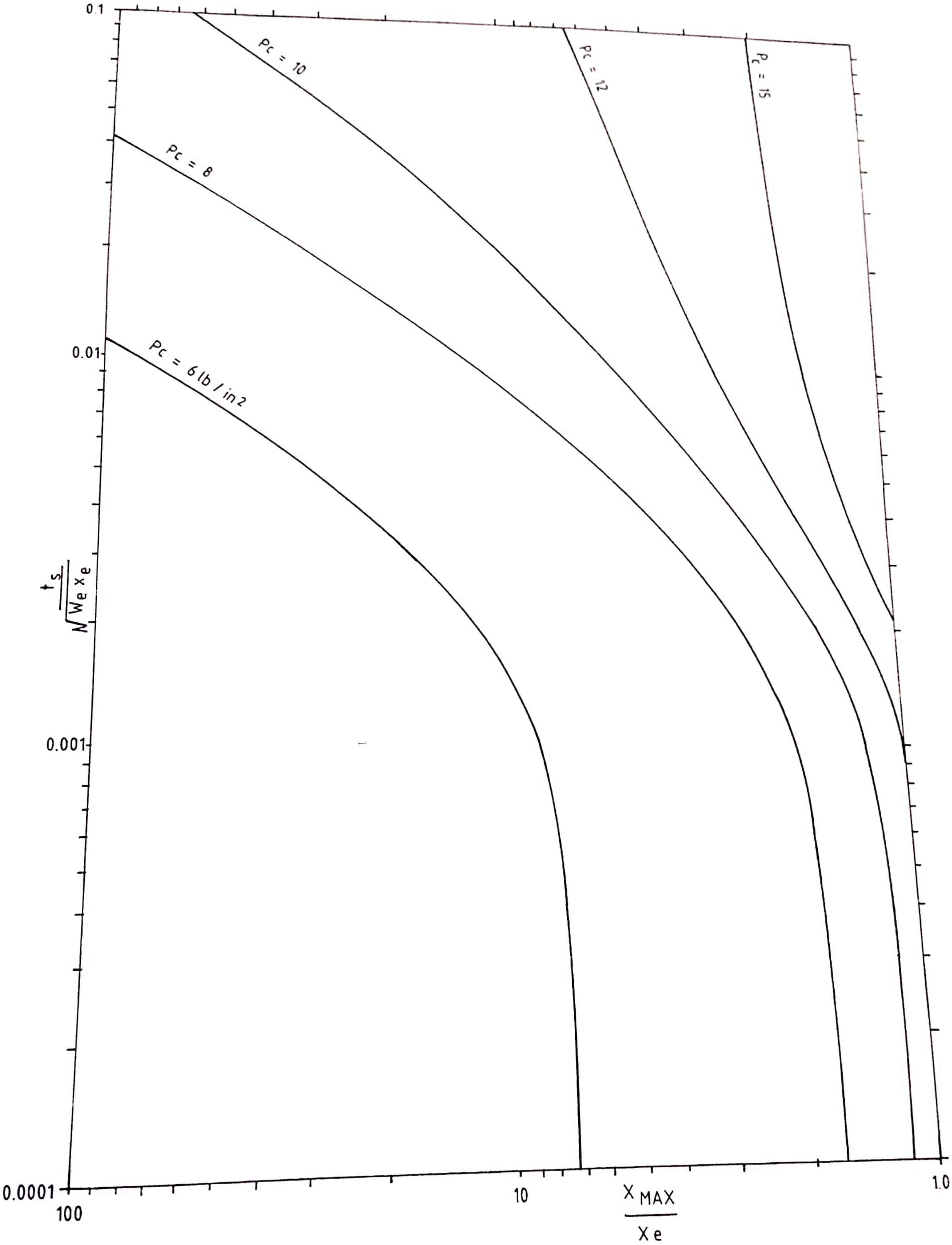

Figure 18.82 Panel Deflection Under Incident Blast Wave Pressure Pso = 5 lb/in^2

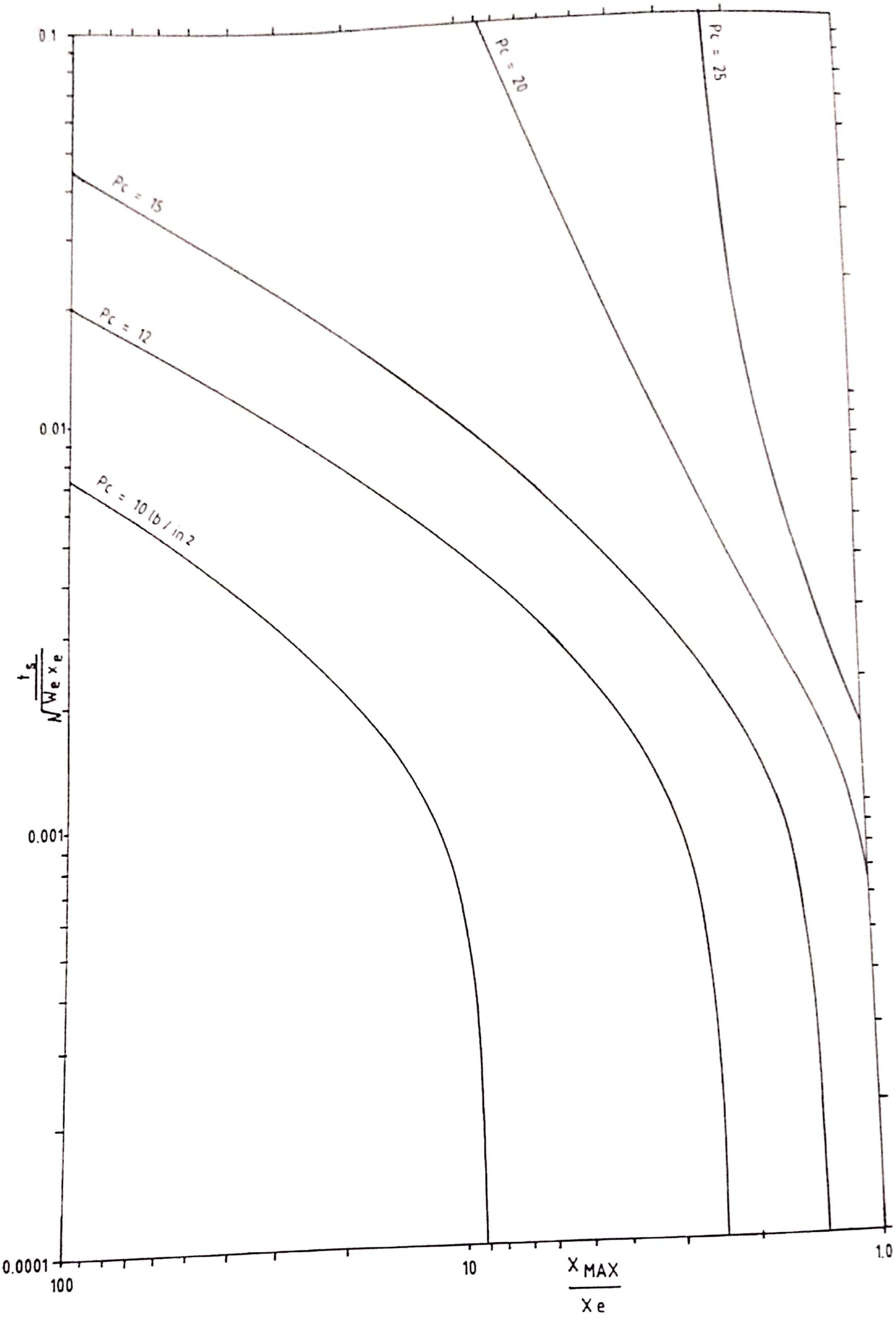

Figure 18.83 Panel Deflection Under Incident Blast Wave Pressure Pso = 8 lb/in^2

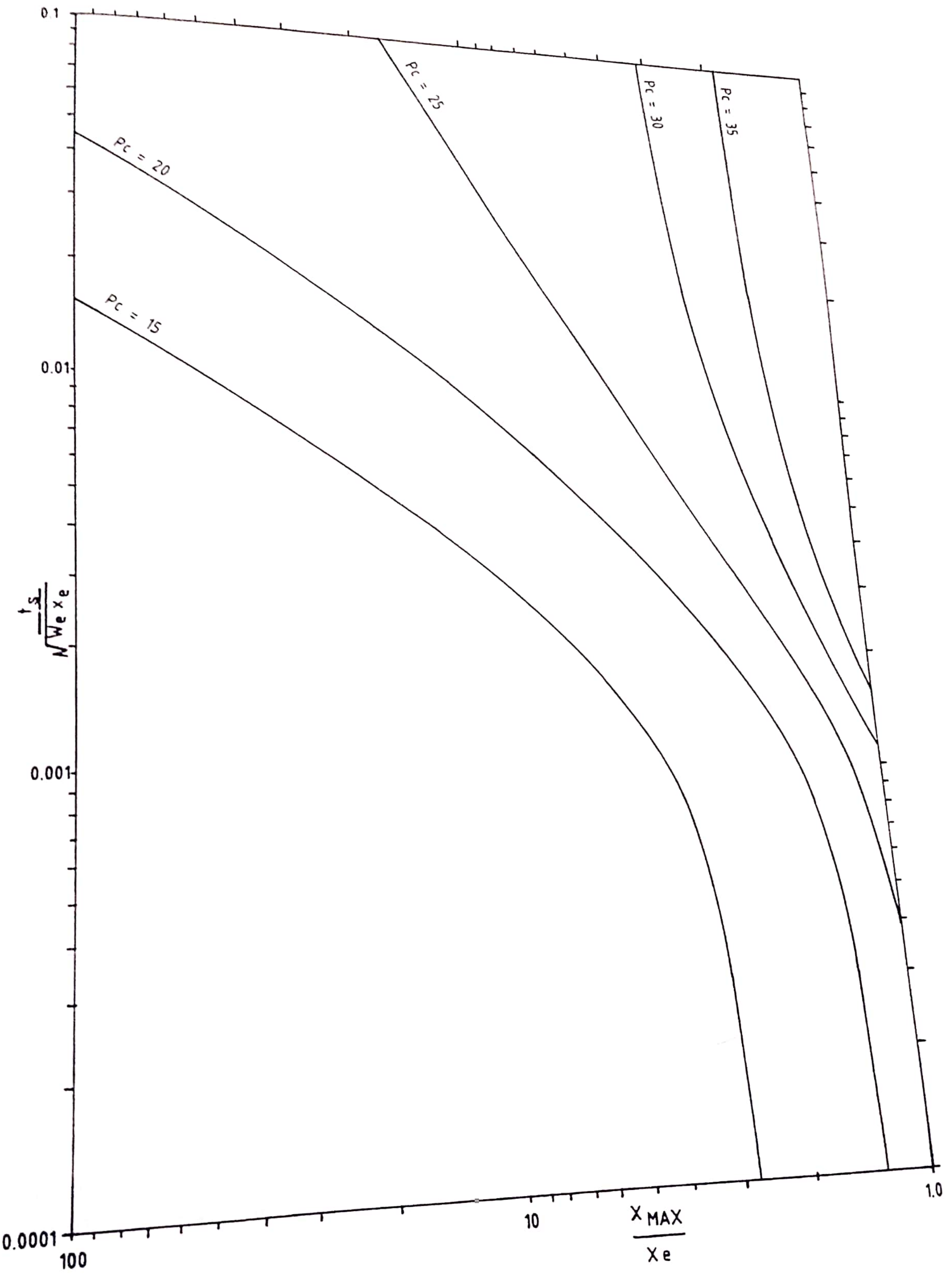

Figure 18.84 Panel Deflection Under Incident Blast Wave Pressure Pso = 10 lb/in^2

Estimation of Vibration Characteristics

Propeller Force on Hull

69 *Figure 18.85* gives an early means of estimating the total vertical force on the hull due to propeller rotation, that is bearing forces and pressure forces combined. The plot is entered with the factor PK/zcD, where P is propeller power in kW, z is the number of blades, c is the tip clearance and D the propeller diameter, both in metres, and K is a factor given on the data sheet relating to the rise of floor. The effective force in kN is read off directly. This figure gives a reasonable first estimate provided that the propeller is of conventional design, without high skew or unusual pitch distribution.

Ship Vibration Data and Estimation of Vertical Hull Resonances

70 A table of merchant ship vibration chracteristics is published in the BSRA Ship Design Manual - Vibration (1981); some warship data also exists but is not openly published. The data is intended to assist the designer in finding a suitable similar ship from which to scale the natural frequencies for new design using factors given in Chapter 14.

71 If it is not possible to identify a similar ship from which to scale, then a graph for estimating the two-mode vertical (2NV) frequency is given in *Figure 18.86* where measured frequencies in cycles/minute for both warships and merchant ships are plotted against the parameter $\sqrt{\{I_v/\delta_{1v}L^3\}}$, where I_v is the vertical second moment of area of the hull amidships, δ_{1v} is the displacement including virtual added mass for vertical vibration (defined in equation 14.11a) and L is the length between perpendiculars (units are in **tonnes** and **metres**).

72 For more detailed analysis of hull vibration it is necessary to use finite beam element models and for these the fluid added mass is required. This is obtained from equation 14.14 which uses, inter alia, the Lewis shape factor. This can be found as a function of immersed area (A), beam (B) and draught (T) in *Figure 18.87.*

Hull Vibration Amplitude Due to Propeller Excitation

73 *Figure 18.88* gives a plot of average mobility against trial displacement derived from trials on a number of ships at frequencies below 600 cycles/min. From this plot, with an estimate of propeller force on the hull, it is possible to make a prediction of the hull vertical vibration amplitude at the stern gland.

74 At a higher level of accuracy, using for example finite analysis, it will be necessary to make an estimate of modal damping. The percentage of critical damping for frequencies up to 1200 cycles/min can be taken from *Figure 18.89* for three different types of merchant ships (there are no equivalent measurements for warships). It is suggested that the lower line, light damping, is probably appropriate for the majority of warships.

Resonant Frequencies of Stiffened Panels

75 *Figure 18.90* contains values of the coefficient α_r for mode r from 1 to 6 for input to equation 14.18. The parameter ξ defines the rotational constraint at the boundaries, $\xi = 0$ being the simply supported case and $\xi = \infty$ being the clamped case.

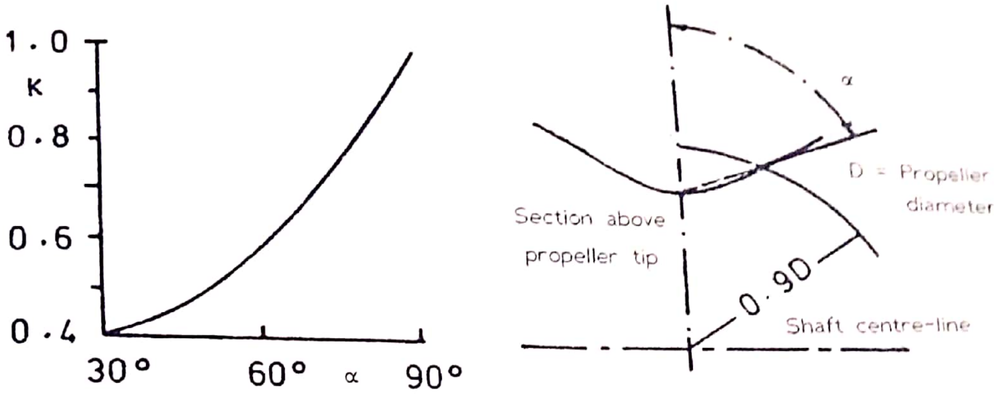

Coefficient K Related to Rise of Floor at Propeller Tip

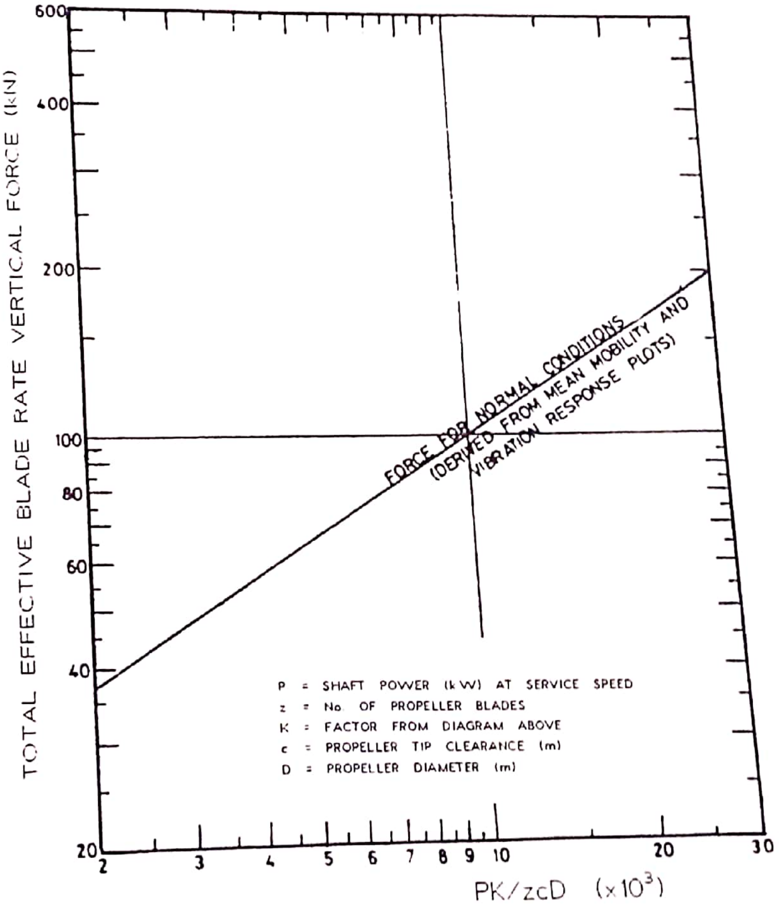

Figure 18.85 Propeller Vertical Force at Blade Rate

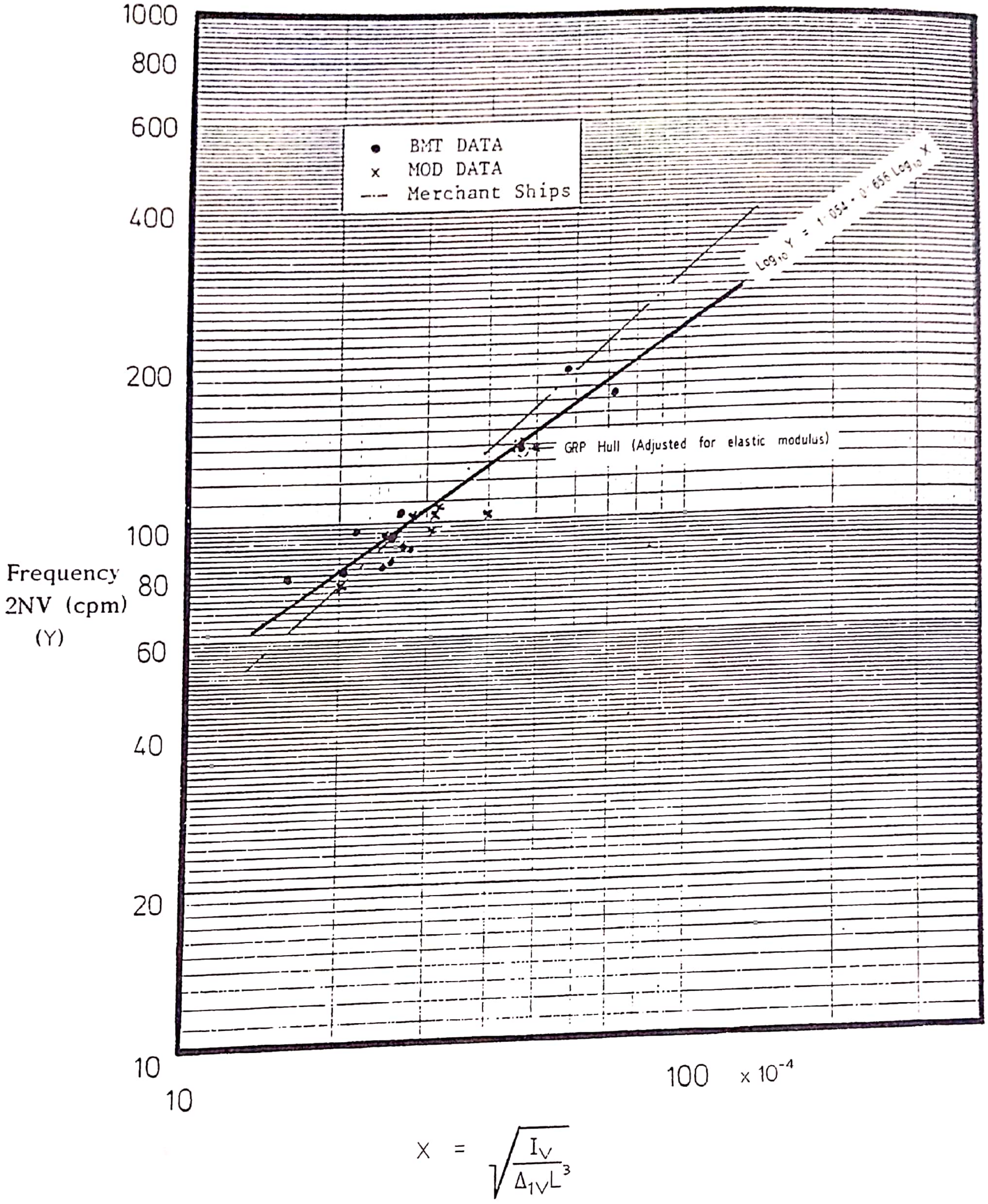

Figure 18.86 Two Node Vertical Hull Natural Frequencies

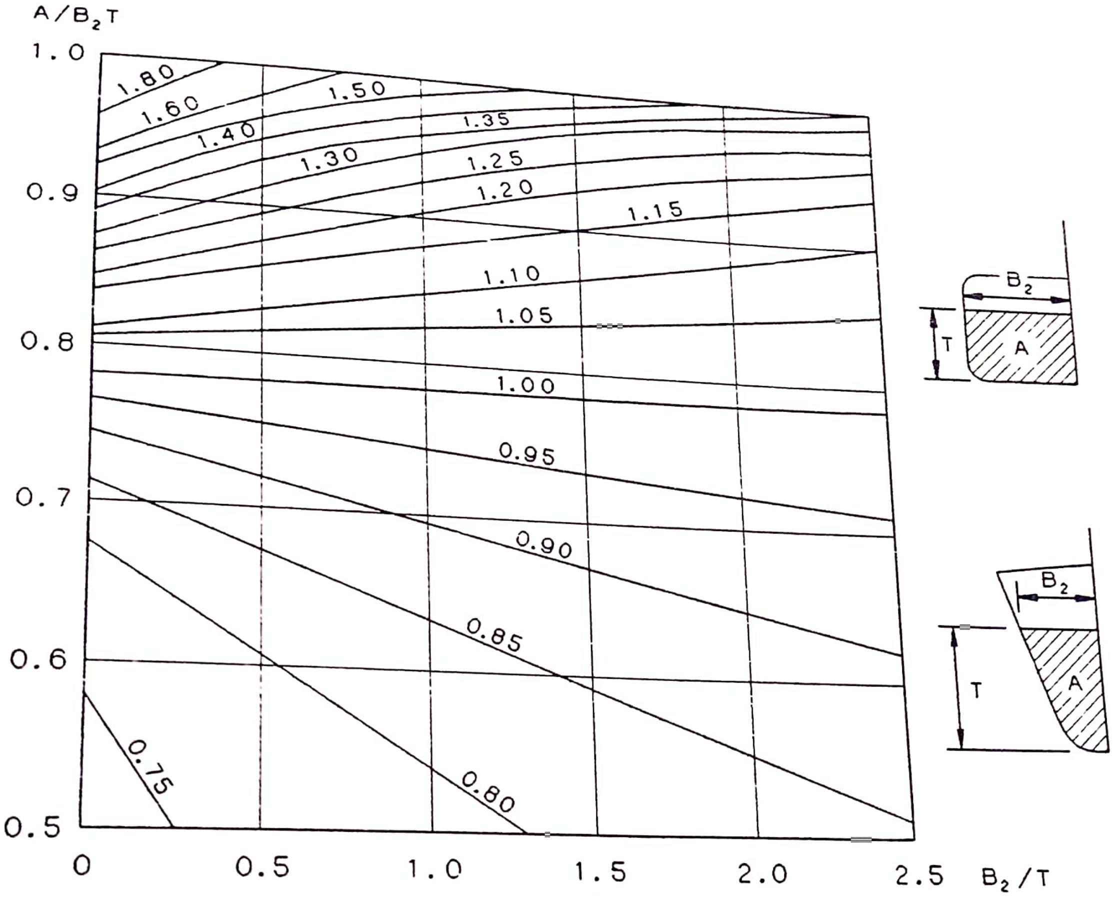

Figure 18.87 Lewis Shape Factor C_V for Added Mass Calculation

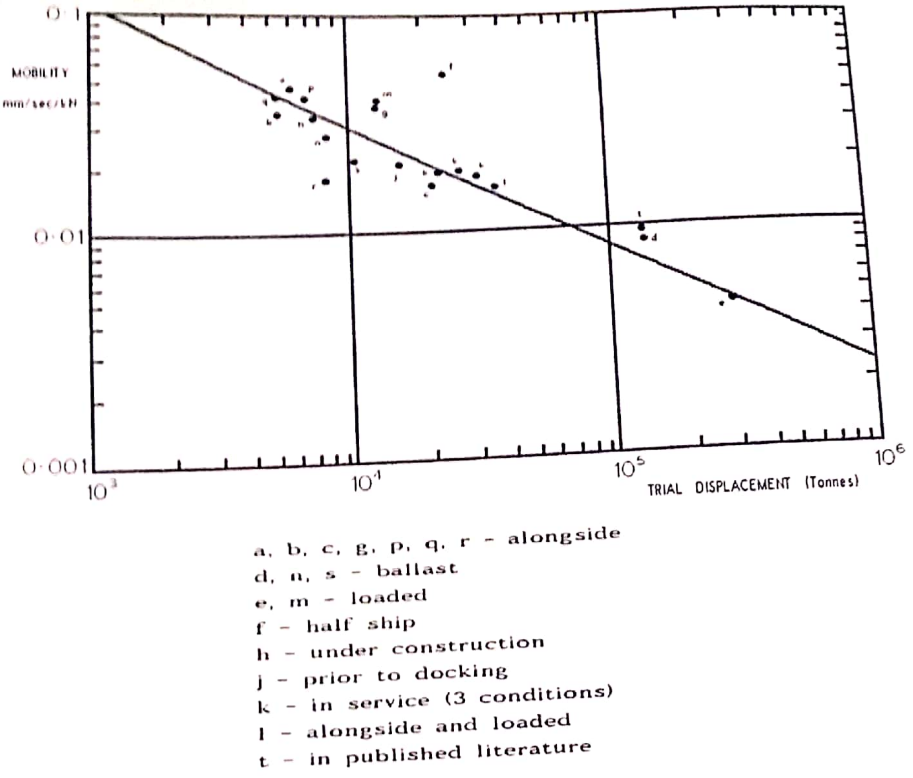

Figure 18.88 Relationship Between the Mean Magnitude of Vertical Mobility at the Stern Gland and the Trial Displacement for a Variety of Ships

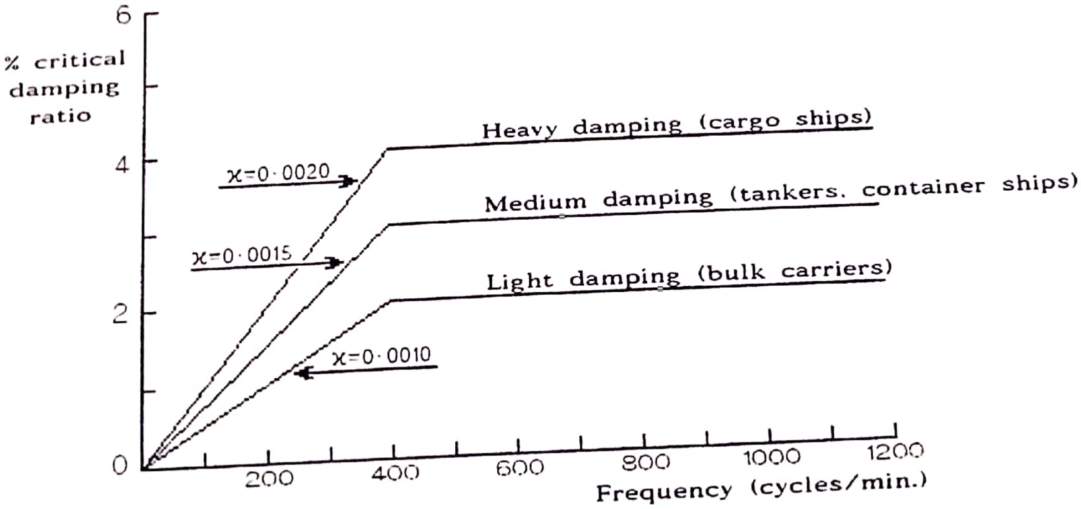

Figure 18.89 Suggested Damping Coefficients to be Applied in Vibration Response Calculations